Titre: Title:	Hydrodynamics and Mass Transfer of Two-Phase and Three-Phase Bubble Column Reactors
Auteur: Author:	El Mahdi Lakhdissi
Date:	2020
Type:	Mémoire ou thèse / Dissertation or Thesis
Référence: Citation:	Lakhdissi, E. M. (2020). Hydrodynamics and Mass Transfer of Two-Phase and Three-Phase Bubble Column Reactors [Thèse de doctorat, Polytechnique Montréal]. PolyPublie. https://publications.polymtl.ca/5338/

POLYTECHNIQUE MONTRÉAL

affiliée à l'Université de Montréal

Hydrodynamics and mass transfer of two-phase and three-phase bubble column reactors

EL MAHDI LAKHDISSI

Département de génie chimique

Thèse présentée en vue de l'obtention du diplôme de *Philosophiæ Doctor*

Génie chimique

Juillet 2020

POLYTECHNIQUE MONTRÉAL

affiliée à l'Université de Montréal

Cette thèse intitulée:

Hydrodynamics and mass transfer of two-phase and three-phase bubble column reactors

présentée par **El Mahdi LAKHDISSI**

en vue de l'obtention du diplôme de *Philosophiæ Doctor*

a été dûment acceptée par le jury d'examen constitué de :

Robert LEGROS, président
Jamal CHAOUKI, membre et directeur de recherche
Christophe GUY, membre et codirecteur de recherche
Bruno BLAIS, membre
Muthanna H. AL-DAHHAN, membre externe

DEDICATION

To my beloved parents Mohammed and Amina

To my beloved sisters Maryam and Asmaa

الحمد لله الذي بنعمته تتم الصالحات،

أود إهداء رسالة الدكتوراه هاته إلى والدي محمد ووالدتي أمينة اللذان لولاهما لما تحقق هذا الحلم.

هذا العمل مُهدىً أيضا إلى أختاي أسماء ومريم، شكرا لكما على دعمكما المستمر واللامشروط.

ACKNOWLEDGEMENTS

I would like to acknowledge and thank all who contributed to the completion of this project. First, I wish to express my sincere gratitude to my advisors Prof. Jamal Chaouki and Prof. Christophe Guy for their patience, motivation, support, as well as providing me with an appropriate atmosphere for conducting my research especially in the difficult moments of the PhD journey. Sharing their knowledge, their experience and their way of solving problems helped me throughout this process. It was a pleasure to work with you professors, you taught me lessons that will help me in all aspects of my life.

I would like to acknowledge Prof. Tijani Bounahmidi who encouraged me to start the PhD journey and was always supporting me during my undergraduate studies.

I would like to acknowledge the members of my committee, Prof. Muthanna H. Al-Dahhan, Prof. Robert Legros, Prof. Bruno Blais, Prof. Lahcen Saydy for taking interest in my work, examining my thesis and providing insightful comments.

I am deeply thankful to Mr. Iman Soleimani, Mr. Afshin Fallahi, Dr Shuli Shu and Dr Amin Esmaeili whose collaboration and friendly attitude in accomplishing important parts of this project were extremely valuable. I am also grateful to Dr. Sherif Farag for his assistance in conducting the experimental work in the HP-HT multiphase reactor unit.

In my daily work I have been blessed with a supportive and qualified group of fellow students and researchers. I am very grateful to all my colleagues in the PEARL research group for their friendly support. I would like to offer my special thanks to, Dr. Jean-Philippe Laviolette, Dr. Mohammed Latifi for their help during the periods they were managing the TOTAL/NSERC industrial chair.

One of the most beautiful outcomes of a PhD project, is the number of people and new friends that we met during the journey. This thesis would not have been accomplished without the constant support of my great friends Kamal, Ayoub, Fadoua, Boukil, Amine, Adrian, Hamed, Afshin, Jaber Said and all those whose company made my stay in Montreal an enjoyable and memorable one.

During the course of my research work, several pieces of equipment needed to be designed and machined. My deepest gratitude goes to the technicians in the Department of Chemical Engineering, particularly Robert Delisle and Sylvain Fleury-Simard. Their help to build my

experimental setup was amazingly valuable. In addition, I wish to thank the secretaries of the Department of Chemical Engineering for the ideal atmosphere they provide to help us to conduct our research work

I also wish to acknowledge the financial support of TOTAL American Services, Inc. and the Natural Sciences and Engineering Research Council of Canada (NSERC) which made this PhD work possible.

And last but not least, I would like to express my deep gratitude to my mother, father, my two sisters Asmaa and Maryam, my two brothers-in-law Driss and Ilyass, Mr Boubker Rachdi and Mrs Hasna Bricha for the support they have provided me throughout this journey, and without whose encouragement I would not have finished this dissertation. I don’t have words to express what I feel in my heart for you.

RÉSUMÉ

Les colonnes à bulles (gaz-liquide) et les colonnes à bulles à suspension (gaz-liquide-solide) sont connues comme l'un des types de réacteurs polyphasiques les plus utilisés dans l'industrie et qui traitent les matières premières renouvelables ainsi que les ressources fossiles conventionnelles. Plusieurs procédés chimiques, pétrochimiques, biochimiques, alimentaires, pharmaceutiques et de capture de dioxyde de carbone sont effectués dans des colonnes à bulles. Ils sont sélectionnés parmi d'autres contacteurs gaz-liquide car ils offrent des avantages uniques, en l'occurrence des faibles coûts de maintenance et d'exploitation, une facilité d'utilisation et des taux de transfert de chaleur et de masse élevés.

Bien que la construction des réacteurs à colonne à bulles soit simple, les phénomènes liés au flux de bulles à l'intérieur de ce contacteur sont très complexes. En général, le comportement des écoulements bullaires est affecté par l'échange d'énergie, de quantité de mouvement et de masse ainsi que par l'angle de contact entre les bulles et le liquide, les forces de tension interfaciales et les caractéristiques de mouillage de la phase liquide sur la paroi du réacteur. Par conséquent, la compréhension de l'hydrodynamique des colonnes à bulles en termes de description physique du comportement des bulles est une tâche difficile. Ainsi, le design de tels réacteurs par une approche de savoir-faire basée sur le développement de modèles phénoménologiques s'avère très complexe. De plus, la plupart des procédés sont effectués à des débits élevés, à pression et température élevées avec et sans particules solides. Le transfert de chaleur et de masse peut alors être modifié négativement si l'effet de ces conditions extrêmes n'est pas bien assimilé et pris en compte dans la procédure de design. Les nouvelles matières premières sont intrinsèquement variables et pourraient avoir une qualité inférieure par rapport aux ressources conventionnelles. Ainsi, le design de nouvelles colonnes à bulles fonctionnant avec ces nouveaux matériaux ne peut pas être réalisé par une approche de savoir-faire basée sur l'empirisme et quelques règles de base.

L'hydrodynamique et le transfert de masse sont des facteurs clés pour le design et la mise à l'échelle des réacteurs à colonnes à bulles biphasées et triphasées. Ces deux aspects importants sont significativement affectés par les propriétés de chacune des trois phases (gaz-liquide-solide). La présence de particules solides dans les réacteurs polyphasiques est très importante car elles sont utilisées comme catalyseurs pour plusieurs réactions chimiques. Par conséquent, lorsqu'ils sont

suspendus dans un milieu gaz-liquide, ils modifient le comportement des bulles ainsi que le transfert de masse gaz-liquide. Cet impact doit être étudié attentivement et assimilé sur la base des phénomènes physiques apportés par les particules. De plus, l'effet de l'augmentation de la pression sur l'hydrodynamique d'un système gaz-liquide fonctionnant avec des liquides de viscosités différentes doit être exploré avant d'étudier l'effet de ces particules solides à ces pressions élevées.

Trois aspects étaient au centre de l'intérêt de ce travail de recherche. Premièrement, toutes les applications du SBCR sont basées sur des réactions catalytiques où des particules solides sont suspendues dans un système gaz-liquide. En général, on rapporte que les particules solides sont mélangées de manière homogène avec la phase liquide et forment ensuite une suspension ou une phase pseudo-homogène. Par conséquent, toutes les théories et tous les modèles développés pour l'hydrodynamique et applicables au système gaz-liquide peuvent être utilisés pour les systèmes triphasés. En considérant cela, de nombreuses propriétés solides telles que la taille, le degré de mouillabilité et la forme sont omises, et les phénomènes liés aux interactions micro-bulles-particules et particules-liquide sont négligés. Par conséquent, il est primordial de considérer l'effet des propriétés solides lors de la mesure des paramètres hydrodynamiques (rétention de gaz, taille des bulles, vitesse de transition, etc.).

Deuxièmement, des réacteurs à colonnes à bulles sont utilisés pour améliorer le transfert de masse gaz-liquide lorsque la vitesse de réaction globale est limitée par le transfert de matière. La présence de particules solides utilisées pour favoriser la cinétique intrinsèque pourrait avoir un effet physique sur le coefficient de transfert de masse volumétrique $k_l a_l$.

Troisièmement, la plupart des processus industriels sont effectués à pression et température élevées. À titre d'exemple, l'hydroconversion des coupes pétrolières lourdes est effectuée à une pression de 100 atm et à une température de 400 ° C par barbotage d'hydrogène gazeux. L'étude de l'hydrodynamique dans des conditions aussi extrêmes est presque impossible. Les fluides de similitude sont des fluides ayant presque les mêmes propriétés que les réactifs gaz-liquide utilisés industriellement mais à une pression et une température relativement plus faibles. Par conséquent, il est très intéressant d'imiter les conditions industrielles extrêmes en utilisant ces fluides de similitude dans une unité à l'échelle pilote pour étudier le comportement des bulles.

Dans la première partie de cette étude, l'effet simultané de la taille et de la concentration des particules sur la rétention totale de gaz des réacteurs à colonne à bulles à suspension a été étudié. La rétention totale de gaz a été mesurée pour les systèmes air-eau-billes de verre. Trois concentrations solides et trois diamètres de particules ont été utilisés. Il a été constaté que l'augmentation de la taille des particules à une concentration en volume constante élevée diminue la rétention de gaz. De plus, l'augmentation de la concentration en solides diminue la rétention de gaz et cet effet décroissant est plus important pour les particules les plus grosses. De plus, les particules solides ont deux effets sur l'hydrodynamique, à savoir le changement de la viscosité et de la densité de la phase liquide ainsi que le fait d'empêcher les bulles de monter dans la colonne par le phénomène de collision. Par conséquent, un nouveau facteur de correction a été introduit pour corriger la rétention de gaz. Cette correction s'avère nécessaire pour prendre en compte l'effet additionnel des particules solide sur la rétention de gaz. Le facteur de correction appelé facteur d'atténuation considère à la fois l'efficacité de collision affectée par la taille des particules ainsi que la concentration en solides. Une nouvelle corrélation a été développée pour prédire les données expérimentales de la rétention de gaz en trois phases.

Dans la deuxième partie de cette étude, l'effet des particules solides sur le coefficient volumique de transfert de matière gaz- liquide $k_l a_l$ dans les réacteurs à colonne à bulles à suspension a été étudié et mesuré pour un système d'air-eau-billes de verre en utilisant la technique d'absorption dynamique de l'oxygène. Trois concentrations solides et deux diamètres de particules ont été utilisés. Les particules solides ont eu un effet négligeable sur le $k_l a_l$ en raison de deux effets opposés. Tout d'abord, une fraction des particules a tendance à se localiser dans la phase liquide, modifiant ainsi sa viscosité. Dans le régime hétérogène, l'augmentation de la concentration en solides favorise la coalescence des bulles, ce qui a entraîné une augmentation de la taille et, par conséquent, une diminution de la surface interfaciale gaz-liquide a_l. Deuxièmement, une autre fraction de particules se déplace vers la surface de la bulle en raison du phénomène de collision et a tendance à s'accumuler dans le film liquide, entraînant une turbulence locale et une augmentation du coefficient de transfert de masse côté liquide k_l. Le mécanisme d'effet hydrodynamique était le mécanisme directeur de l'effet des particules solides sur le transfert de matière gaz-liquide dans la fourchette des conditions de fonctionnement étudiées.

Enfin, dans une colonne à bulles à échelle pilote fonctionnant avec des hydrocarbures de viscosités faible et modérée, l'effet de la pression sur la rétention totale et axiale du gaz, ainsi que la vitesse de transition du régime, ont été étudiés. Des expériences ont été effectuées pour deux systèmes gaz-liquide air-Ketrul D100 et air-Hydroseal G250 HL. Il a été constaté que l'augmentation de la pression augmentait la rétention de gaz dans le régime hétérogène, et cet effet était plus prononcé pour le liquide de faible viscosité. De plus, l'augmentation de la pression stabilisait davantage le régime homogène, et encore une fois, cet effet stabilisant était plus significatif pour le liquide de faible viscosité. De même, en réponse à l'augmentation de la pression, la rétention axiale du gaz est devenue plus uniforme dans le cas du liquide à faible viscosité et moins uniforme dans le cas du liquide à viscosité modérée.

Ces travaux de recherche ont fourni une grande compréhension et une quantité considérable d'informations concernant l'hydrodynamique et le transfert de matière des colonnes à bulles fonctionnant avec et sans la présence de particules solides. Les résultats de cette étude déclencheront un débat scientifique sur l'effet des particules solides sur le comportement des bulles en suspension dans un milieu gaz-liquide. Il a été démontré que le design simplifié et la procédure de mise à l'échelle basés sur la considération de la phase de suspension en tant que phase liquide pseudo homogène doivent être modifiés. Le design pourrait être biaisée si les modèles développés pour prédire les paramètres hydrodynamiques, et applicables aux systèmes gaz-liquide, sont utilisés pour les systèmes triphasés.

ABSTRACT

Bubble columns (gas-liquid) and slurry bubble columns (gas-liquid-solid) are known as one of the most utilized commercially types of multiphase reactors that treat renewable feedstocks as well as conventional fossil resources. Several chemical, petrochemical, biochemical, food, pharmaceutical, and carbon dioxide capture processes are carried out in bubble columns. They are selected among other gas-liquid contactors since they offer some unique advantages such as low maintenance and operating costs, ease of operation and high heat and mass transfer rates.

Although the simple construction of the bubble column reactors, the phenomena related to the bubbly flow inside this contactor are very complex. In general, the behaviour of bubbly flows is affected by the exchange of energy, momentum and mass and also the contact angle between bubbles and liquid, interfacial tension forces and the wetting characteristics of the liquid phase on the reactor wall. Consequently, the understanding of bubble column hydrodynamics in terms of bubble behaviour physical description is a challenging task. Hence, the design of such reactors by a know-why approach based on developing phenomenological models turns out to be very challenging. Moreover, most of the processes are carried out at high flow rates, elevated pressure and temperature with and without solid particles. The heat and mass transfer can then be negatively altered if the effect of these extreme conditions is not well understood and taken into account in the design procedure. The new feedstocks are intrinsically variable and might have lower quality if compared to conventional resources. Thus, the design of new bubble columns operating with these new materials could not be carried out by a know-how approach based on empiricism and rules of thumb.

The hydrodynamics and mass transfer are key factors for the design and scale-up of two-phase and three-phase bubble column reactors. These two important aspects are significantly affected by the properties of each of the three phases (gas-liquid-solid). Solid particles' presence in multiphase reactors is highly important as they are used as catalysts for several chemical reactions. Therefore, when suspended in a gas-liquid medium, they alter the bubble behaviour as well as the gas-liquid mass transfer. This impact should be studied carefully and understood based on the physical phenomena brought by the particles. Moreover, the effect of increasing pressure on the

hydrodynamics of a gas-liquid system operating with liquids of different viscosities should be explored prior to add solid particles at these elevated pressures.

Three aspects were in the center of interest of this research work. First, all applications of SBCR are based on catalytic reactions where solid particles are suspended in a gas-liquid system. In general, it is believed that solid particles are homogeneously mixed with the liquid phase and then form a slurry or pseudo-homogeneous phase. Therefore, all theories and models developed for hydrodynamics and applicable for the gas-liquid system can be used for three-phase systems[1, 2]. By considering this, lots of solid properties such as size, degree of wettability and shape are omitted, and the phenomena related to micro bubble-particle and particle-liquid interactions are neglected. Consequently, it is of prime importance to consider the effect of solid properties when measuring the hydrodynamic parameters (gas holdup, bubble size, regime transition velocity, etc.). Second, bubble columns reactors are utilized to enhance the gas-liquid mass transfer when the overall reaction rate is mass transfer limited. The presence of solid particles used to promote the intrinsic kinetics could have a physical effect on the volumetric mass transfer coefficient $k_l a_l$. Third, most of the industrial processes are carried out at elevated pressure and temperature. As an example, the hydroconversion of heavy oils is conducted at 100 atm pressure and 400˚C temperature by bubbling the hydrogen gas. Investigating the hydrodynamics in such extreme conditions is almost impossible. S*imilitude fluids* are fluids having nearly the same properties as the gas-liquid reactants used industrially but at relatively lower pressure and temperature. Therefore, it is of great interest to mimic the extreme industrial conditions by using those similitude fluids in a pilot-scale unit to study bubble behaviour.

In the first part of this study, the simultaneous effect of particle size and concentration on the total gas holdup of slurry bubble column reactors was investigated. The total gas holdup was measured for air-water-glass beads systems. Three solid concentrations and three particle diameters were used. It was found that increasing particle size at high constant concentration decreases gas holdup. Moreover, increasing solid concentration decreases gas holdup and this decreasing effect is higher for larger particles. Also, solid particles have two effects on hydrodynamics, namely changing the viscosity and density of the liquid phase as well as hindering the bubbles from rising within the column by the collision phenomenon. Therefore, a new correcting factor was introduced to correct the gas holdup correlation to predict the gas holdup in a three-phase slurry bubble column. The

hindering factor considers both the collision efficiency affected by the particle size as well as the solid concentration. A novel correlation was developed to predict the experimental data of the three-phase gas holdup.

In the second part of this study, the effect of solid particles on the volumetric gas liquid mass transfer coefficient $k_l a_l$ in slurry bubble column reactors was investigated. $k_l a_l$ was measured for an air-water-glass bead system using the dynamic oxygen absorption technique. Three solid concentrations and two particle diameters were used. Solid particles had a negligible effect on $k_l a_l$ due to two opposite effects. First, a fraction of the particles tends to locate in the bulk liquid, altering its viscosity. In the heterogeneous regime, increasing the solid concentration enhances bubble coalescence, which led to an increase in size and, as a result, a decrease in the gas-liquid interfacial area a_l. Second, another fraction of particles moves to the bubble surface due to the collision phenomenon and tends to accumulate in the liquid film, resulting in local turbulence and an increase in the liquid-side mass transfer coefficient k_l. The *hydrodynamic effect* mechanism was the governing mechanism of the effect of solid particles on gas-liquid mass transfer within the range of the investigated operating conditions.

Finally, in a pilot-scale bubble column operating with low and moderate viscosity hydrocarbons, the effect of pressure on the total and axial gas holdup, as well as the regime transition velocity, was investigated. Experiments were performed for two air-Ketrul D100 and air-Hydroseal G250 HL gas-liquid hydrocarbon systems. It was found that increasing pressure increased gas holdup at the heterogeneous regime, and this effect was more pronounced for the low-viscosity liquid. Moreover, increasing pressure stabilized more the homogeneous regime, and again, this stabilizing effect was more significant for the low-viscosity liquid. Also, as a response to the increasing pressure, the axial gas holdup became more uniform in the case of the low-viscosity liquid and less uniform in the case of the moderate-viscosity liquid.

This research work provides great insight and a considerable amount of information regarding the hydrodynamics and mass transfer of bubble column reactors operating with and without the presence of solid particles. The findings of this study will instigate a scientific debate on the effect of solid particles on bubble behavior when suspended in a gas-liquid medium. It was demonstrated that the simplified design and scale-up procedure based on considering the slurry phase as a pseudo homogeneous liquid phase must be amended. The design could be biased if the models developed

to predict hydrodynamic parameters, and applicable for gas-liquid systems, are utilized for three-phase systems.

TABLE OF CONTENTS

LIST OF TABLES

LIST OF FIGURES

LIST OF SYMBOLS AND ABBREVIATIONS

BCR Bubble column reactors

SBCR Slurry bubble column reactors

CHAPTER 1 INTRODUCTION

The growth of the world population, as well as our society's needs, is putting more pressure on establishing an innovative supply chain for the production of fuels, energy, materials, and high-value chemicals. Indeed, a more pronounced chemical processing and then a growing shortage of non-renewable resources (coal, petroleum, minerals, etc.) is resulting from this century's economical and societal constraints. Therefore, it is critical to shift toward green processes in order to reduce energy consumption and meet environmental considerations. The European Commission set in 2006 a new policy to support the creation of high societal and economical value markets. Several steps were proposed to reach this goal, among which we can cite the use of expendable and renewable resources, decreasing the dependency on the limited, expensive fossil resources, developing sustainable industrial processes, improve the community health and reduce greenhouse gas emissions[3]. Improving the production and environmental performance could be complex and limited if the focus is only on the production stage of the life cycle. In addition to this stage, a product's life cycle includes the raw material used, the product delivery and also the end-use and disposal upstream and downstream steps. Consequently, using renewable feedstocks could offer more freedom and flexibility for companies to satisfy the requirements of sustainable supply chains. It is worth mentioning that sustainability is based on three pillars, namely economical development, environmental protection and social progress.

Research is ongoing to explore the feasibility of using new alternative molecules derived from renewable resources. Another driver is the effect of the currently produced chemicals on humans and the environment. Pfaltzgraff and Clark[3] reported that the polybrominated compounds in flame retardants and the volatile chlorinated compounds used in dry cleaning could be harmful, and new replacement molecules should be explored. The integration of safe and clean processing technologies are then required to treat these new feedstocks. Therefore, it becomes of extreme importance to design and optimize processes that ensure maximum reactant conversion, minimum waste production, and renewable materials use. As an example, the challenge of biorefineries is to take into account the lignocellulosic biomass complex nature to develop a cost-effective competing bioprocess.

90% of industrial chemicals are manufactured by catalytic processes involving multiphase systems[4]. Some of those processes are based on homogeneous catalysis, where the reactants are present in two phases. Examples of these processes are carbonylation, oxidation and hydroformylation. However, the most widely used category is heterogeneous catalysis based processes. Fischer-Tropsch synthesis, hydro-desulfurization, alkylation and hydrogenation are among of the three-phase reactions that involve the contacting of gas-liquid-solid (catalyst) phases. Fixed bed, sparged and stirred contactors are the most used reactors to handle those reactions. The interest given to the research works on catalysis to develop selective processes should be as important as the interest given to these reactors, considered as the 'hardware' of multiphase reactions[4]. In summary, developing sustainable processes is dependent first on catalysis to reach a high selective green raw material transformation and second on selecting the appropriate multiphase contacting device.

Multiphase systems are characterized by at least one free interface: bubble, droplet, liquid film. This interface can coalesce and break in a continuous process when being placed in a turbulent field. Hence, the size of this bubble or droplet might be affected by the turbulent shear stress, flow patterns and the coalescing or no coalescing nature of the medium. Besides, the turbulence parameters also affect the transport of mass from and to the surrounding liquid. The flow rate of the dispersed phase (either gas or liquid) determines the mass and heat transport characteristics. Several criteria were proposed for the multiphase reactor selection for a specific process. First, kinetics should be compared to the mass transfer rates[5]. If a reaction has intrinsic fast kinetics, it might become mass transfer limited if it is held in a multiphase reactor with poor mass transfer characteristics. It should be mentioned that the intrinsic kinetics is invariant with respect to the type and size of the multiphase reactor. Pangarkar reported that for the fast catalytic hydrogenation reactions, noble metal catalysts (Pd/Pt) tend to form complexes with the liquid-organic reactant when there is no sufficient hydrogen conveyed to the catalyst surface. This can cause a 40% catalyst loss. Thus, using gas-dispersed reactors (sparged, stirred or venturi loop) that offer high mass transfer rates could be an appropriate option. Other criteria for multiphase reactors selection are the ability to add and remove heat, different phases flow patterns, the ability to handle solids, the safety regarding the pressure and temperature operating conditions and the material of construction.

Bubble columns (gas-liquid) and slurry bubble columns (gas-liquid-solid) are known as one of the most utilized types of multiphase reactors. As 25% of all chemical reactions are between gas and liquid reactants[6], the importance of these gas-liquid contactors is justified. They are characterized by *bubbly flows* in which a gas or a mixture of gas flows in a continuous liquid in the form of bubbles dispersed phase. Besides, they are used in several chemical, biochemical and petrochemical processes and are usually selected when the overall reaction rate is mass transfer limited. They also have great potential to be used in carbon dioxide capture processes such as CO_2 absorption by different amine solutions (monoethanolamine (MEA)-diethylethanolamine/2-ethoxyethyl acetate (DEEA/EEA)- methyl diethanolamine (MDEA))[7-9]

Although the simple construction of the bubble column reactors, the phenomena related to the bubbly flow inside this contactor are very complex. In general, the behaviour of bubbly flows is affected by the exchange of energy, momentum and mass and also the contact angle between bubbles and liquid, interfacial tension forces and the wetting characteristics of the liquid phase on the reactor wall[10]. Consequently, the understanding of bubble column hydrodynamics in terms of bubble behaviour physical description is a challenging task. Hence, the design of such reactors by a know-why approach based on developing phenomenological models turns out to be very challenging. Moreover, most of the processes are carried out at high flow rates, elevated pressure and temperature with and without solid particles. The heat and mass transfer can then be negatively altered if the effect of these extreme conditions is not well understood and taken into account in the design procedure. The new feedstocks are intrinsically variable and might have lower quality if compared to conventional resources. Thus, the design of new bubble columns operating with these new materials could not be carried out by a know-how approach based on empiricism and rules of thumb.

The starting point of a successful design is to classify the parameters and variables affecting the performance and efficiency of bubble columns. The first category is the design parameters (reactor size, internals, gas distributor characteristics, etc.). The second is the operating variables (operating pressure and temperature, gas and liquid flow rates, and catalyst concentration). The third is the different phase properties (liquid viscosity, particles' wettability, gas density, etc.). The effect of each parameter on bubble behaviour (pressure, for example) and the significance of this effect in

the presence or absence of other parameters effect (solid concentration) is the key to estimate the optimum reactor geometry and the optimal operating conditions.

Hydrodynamics and mass transfer characteristics in bubble columns and slurry bubble columns have been explored over the last few decades. Several experimental and numerical research works have been carried out to elucidate the phenomena occurring within those complex reactors. However, the general approach adopted by most of the previous works is to explore the effect of several parameters at the same time and within a wide range of variability on the bubble behaviour. As an example, by investigating the impact of the sparger orifice diameter, the operating pressure, the gas flow rate and solid concentration at the same time, several physical phenomena could be omitted. Therefore, it is critical to narrow the number and the range of the studied parameters and to link each one of them to the appropriate physical phenomenon. The final goal is to develop reliable phenomenological models for the know-why design approach.

In light of this new approach, three aspects were in the center of interest of this research work. First, all applications of SBCR are based on catalytic reactions where solid particles are suspended in a gas-liquid system. In general, it is believed that solid particles are homogeneously mixed with the liquid phase and then form a slurry or pseudo-homogeneous phase. Therefore, all theories and models developed for hydrodynamics and applicable for the gas-liquid system can be used for three-phase systems[1, 2]. By considering this, lots of solid properties such as size, degree of wettability and shape are omitted, and the phenomena related to micro bubble-particle and particle-liquid interactions are neglected. Consequently, it is of prime importance to consider the effect of solid properties when measuring the hydrodynamic parameters (gas holdup, bubble size, regime transition velocity, etc.). Second, bubble columns reactors are utilized to enhance the gas-liquid mass transfer when the overall reaction rate is mass transfer limited. The presence of solid particles used to promote the intrinsic kinetics could have a physical effect on the volumetric mass transfer coefficient $k_l a_l$. Third, most of the industrial processes are carried out at elevated pressure and temperature. As an example, the hydroconversion of heavy oils is conducted at 100 atm pressure and 400˚C temperature by bubbling the hydrogen gas. Investigating the hydrodynamics in such extreme conditions is almost impossible. S*imilitude fluids* are fluids having nearly the same properties as the gas-liquid reactants used industrially but at relatively lower pressure and

temperature. Therefore, it is of great interest to mimic the extreme industrial conditions by using those similitude fluids in a pilot-scale unit to study bubble behaviour.

CHAPTER 2 LITERATURE REVIEW

2.1 Slurry bubble column reactors (SBCR)

Bubble columns are reactors where two or three phases are brought into contact with each other. They are used in several industries as strippers, absorbers and multiphase chemical reactors. The main feature of these reactors is their simple construction in which the different phases (gas, liquid and solid) are directly contacted without the need for mechanical stirring equipment. The simple design of bubble columns consists of a cylindrical vessel where a gas phase is sparged into a liquid or liquid-solids medium. Usually located at the bottom of the reactor, gas distributors are utilized to feed the gas phase into the column in the form of discrete ascending bubbles. Depending on the specific need of the process, several geometric configurations can be considered for gas distribution, namely, porous plates, jet nozzles, perforated pipes, ring-type distributors and perforated plate spargers[11]. For continuous operation, the liquid phase can either flow co-currently or counter-currently with respect to the gas phase flow direction and is recycled to the feed vessel after leaving the column[12]. The liquid superficial velocity should be lower than the superficial gas velocity by, at least, an order of magnitude. Generally, bubble columns operate with superficial gas velocities in the order of 1 to 30 cm/s and liquid velocities in the order of 0 to 2 cm/s. Gas-lift reactors are different from bubble column reactors in terms of that gas, and liquid superficial velocities are of the same order of magnitude[13]. Semi-batch operation in which the liquid doesn’t flow can also be considered. Solid particles can be suspended within the liquid medium and act as a chemical reactant or catalyst to promote the chemical reaction. Bubble columns operating with small particles of terminal settling velocities in the liquid phase less than 7cm/s are called slurry bubble column reactors SBCR[13]. If large particles of terminal settling velocity larger than 50cm/s are used, the reactor is called a three-phase fluidized bed[14]. The solid phase, like the liquid phase, can flow either in the continuous or semi-batch modes. The aspect ratio or length-to-diameter ratio for industrial bubble columns is at least 5[12]. For biochemical processes, this ratio is between 2 and 5. Operating with large gas throughputs dictates the use of large diameter reactors, whereas obtaining significant conversion levels requires considerable reactor heights. However, it is necessary to optimize this ratio to maintain the ease of operation.

Bubble column reactors have been used for several types of processes, namely pharmaceutical, chemical, petrochemical, biochemical and food industries. A summary of the industrial applications of bubble columns is given in Table 2.1 (Cui et al. [15], Gunjal et al. [16], Basha et al. [17], Shaikh et al. [18]). As most of the industrial applications of bubble columns are related to complex and cumbersome feedstocks treatment, most of the processes are held at high pressure and high temperature

Table 2.1 Summary of industrial applications of bubble column reactors

Industry	**Application**	**P (atm)**	**T (˚C)**
Chemical and petrochemical	• Oxidation of p-xylene to dimethyl terephthalate	P_{atm}	T_{amb}
	• Partial oxidation of ethylene to acetaldehyde	4-10	150-180
	• Low-temperature Fischer-Tropsch (LTFT) for wax, diesel and Naphta production	1-30	200-250
	• Synthesis of methanol from syngas conversion	50-150	275-350
	• Oxidation of ethylene to acetaldehyde	9-12	125-175
	• Oxidation of acetaldehyde to acetic acid	5-12	50-80
	• Ozonisation of wastewater	P_{atm}	T_{amb}

	• Hydroxylamine formation by hydrogenation	25-30	50-60
	• Hydroformylation processes	50-100	160-200
	• Residuum hydrotreating	55-210	300-425
	• Benzene hydrogenation	50	180
	• Methanation	68	350
	• Coal gasification	30	980
	• Methanol synthesis: 1- BASF 2- Eastman Chemicals, Air-Product, DOE	250-350 50-100	350-400 220-250
	• Hydrogenation of maleic acid (MAC)	P_{atm}	T_{amb}
Biochemical, food and pharmaceutical	• Fermentation (production of ethanol and mammalian cells) • Biological wastewater treatment • Cultivation of mold fungi • Production of single-cell protein	P_{atm}	T_{amb}

	• Animal cell and bacteria cultivation • Treatment of sewage		

Bubble column reactors provide several advantages if compared with other contactors such as packed-bed and stirred-tank reactors. The most appealing characteristics of bubble columns are as follows (Esmaeili et al. [19], Ferreira et al. [20], Deckwer and Schumpe[21]):

- Low capital cost and simple construction
- Low maintenance cost due to the absence of moving parts
- High heat and mass transfer rates per unit volume with a low energy input
- High overall mass transfer coefficients and interfacial areas
- High liquid residence time, which enables the performing of slow reactions
- High liquid or slurry phase fraction to allow the occurring of the reaction
- Temperature is easily controlled and has a uniform distribution
- Ability to operate with very fine particles (≤ 100 μm) which increases the surface area per unit volume and enhances the mass transfer between the liquid and solid phases
- Ability to add and remove the catalyst particles continuously without attrition or plugging problems and most importantly without reactor shutdown
- Low to moderate mixing intensity induced by the gas flow
- Ability to reach a wide range of residence time values

In contrast, bubble columns have some drawbacks that affect their performance significantly and that should be taken into consideration to optimize their design (Esmaeili et al. [19], Ferreira et al. [20], Deckwer and Schumpe[21]):

- The high static head of the liquid causes a high gas pressure drop
- The gas-liquid interfacial area is significantly decreased by the bubble coalescence phenomenon especially in the heterogeneous regime

- The back-mixing is substantial in both the continuous liquid (or slurry) and dispersed gas phases and may result in unfavourable selectivity and lower conversion
- The high shear in the region close to the gas distributor can cause catalyst attrition and deactivation
- The high liquid fraction results in a considerable amount of side products
- Scaling up difficulties

Bubble columns can be built and modified in different configurations compared to their classical design to meet a specific requirement of an industrial process such as circulation of solids, redistribution of bubbles and also to overcome one of the abovementioned drawbacks. For instance, using bubble columns with static mixers or sectionalized reactors like multichannel or multistage vessels with baffles can suppress the axial back-mixing and improve the mass transfer rate (Deckwer and Schumpe[21] and Gunjal et al.[16]). Moreover, the easy operating of these reactors allows them to safely handle extreme operating conditions such as high pressure and high temperature as well as aggressive media. Bubble columns can be equipped with vertical or horizontal internal heating or cooling coils for temperature controlling and effective heat management. Figure 2.1 shows some of the possible configurations of bubble column reactors.

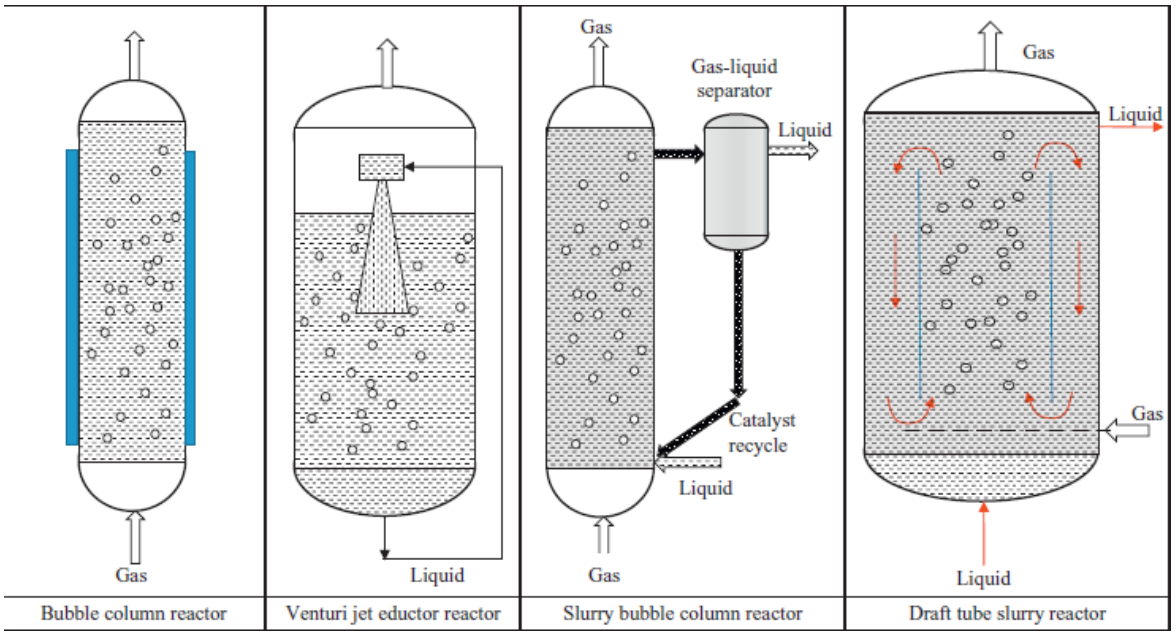

Figure 2.1 Configurations of gas-liquid and gas-liquid-solid bubble column reactors. Taken from reference [16]

Bubble column reactors design and scale-up are based on the quantification of three main aspects: mixing characteristics and hydrodynamics, heat and mass transfer characteristics and chemical reaction kinetics. The difficulty to scale up this type of reactor is that heat and mass transfer properties, as well as fluid dynamic phenomena such as turbulence, back-mixing and dead zones, are scale-dependent. In chemical and biotechnological industries, there are three types of scale-up methods. The first one is a know-how method based on empiricism and rules of thumb. The design procedures are based on several pilot plant experiments by using equipment of different sizes, which is time and money consuming. The second one is based on dimensional analysis and dynamic similitude. The third and most reliable method is the know-why approach based on regime analysis and the development of phenomenological models that clearly describe the complex hydrodynamics[12]. The fourth approach is the use of simulation and high-performance computing. In other words, a deep understanding and accurate determining of the following hydrodynamic parameters are required: Sauter mean bubble diameter, gas holdup, gas, liquid and solid axial dispersion coefficients, overall mass and heat transfer coefficients between different phases, specific gas-liquid interfacial area…The aim is to come up with large scale-up factors. In the following parts of the literature review, the main hydrodynamic aspects of slurry bubble column reactors, as well as the fundamentals of bubble-particle interaction, are described.

2.2 Fundamentals of bubble - particle interaction in slurry bubble column reactors

To elucidate the effect of adding solid to the gas-liquid bubble column system, it is of prime importance to understand the impact of particle presence on bubbles and liquid behaviour and vice-versa. In this context, this part of the literature review describes bubbles as well as particle behaviours in terms of dynamics and exerted forces by the surrounding medium in slurry bubble columns.

2.2.1 Bubble behaviour in slurry bubble columns

Bubble dynamics is a critical factor in the design and scale-up of slurry bubble column reactors. Indeed, dynamic parameters such as bubble rise velocity, bubble frequency, bubble size distribution, bubble shape and bubble motion affect directly the gas-liquid interfacial area as well

as the residence time of bubbles within the column[22]. Consequently, the overall rate of reactions held in industrial, commercial reactors is tributary to bubble dynamics. Besides, bubble dynamics is closely related to the laminar or turbulent nature of the flow characterizing the bubble wake[23]. In slurry bubble column reactors, describing the dynamics of an individual rising bubble is very complex due to its interaction with neighbouring bubbles as well as with the liquid and solid phases. Hence, this interaction can be quantified by the several forces governing in the column, which characterize the flow behavior of bubbles, liquid and solid particles. Also, it is worth mentioning that those forces are affected by the properties of each phase and by the conditions prevailing in the column.

Understanding bubble dynamics is then related to determining the forces that affect bubble behaviour in each of the two subsequent stages that bubbles pass through, namely the bubble formation and the bubble rising stages.

2.2.1.1 Bubble formation stage:

Luo et al.[24] reported the forces responsible for a single bubble formation in liquid-solid suspension. The most used model to characterize bubble formation in the gas distributor is the two-stage spherical bubble formation model developed by Ramakrishan et al.[25]. In this model, bubbles are assumed to form in two stages. The first is the expansion stage, where the bubble grows, and its base is maintained in contact with the nozzle. The second stage is bubble detachment, in which the base moves away from the nozzle, but the bubble is kept connected to it through the neck. Also, the model is based on two assumptions: The bubble keeps its spherical shape during the two stages, and a liquid film is formed around the bubble and trap the particles that collide with it. When the bubble grows and rises, the liquid and particles around are set in motion. The two-stage spherical bubble formation model determines the initial bubble size that will further affect the dynamics of rising bubbles. If the gas velocity through the orifice is known, bubble size at the end of the first stage and during the second stage can be determined by the following force balance:

$$(F_B)_{buoyancy} + (F_M)_{Gas\ momentum} = (F_D)_{liquid\ drag} + (F_\sigma)_{surface\ tension} + (F_{BA})_{Basset} + \left(F_{I,g}\right)_{bubble\ inertia} + (F_C)_{bubble-particle\ collision} + \left(F_{I,m}\right)_{suspension\ inertia} \quad (2.1)$$

The same forces are applied to the bubble in the two stages with some differences in the force

expression. The magnitudes of the abovementioned forces were reported by Luo et al.[24] as follows:

The upward effective buoyancy force: $(F_B)_{buoyancy} = \frac{\pi}{6} {d_B}^3 (\rho_l - \rho_g) g$ (2.2)

The upward gas momentum force: $(F_M)_{Gas\ momentum} = \frac{\pi}{4} {D_o}^2 \rho_g {u_0}^2$ (2.3)

The downward surface tension force: $(F_\sigma)_{surface\ tension} = \pi D_0 \sigma \cos\gamma$ (2.4)

With γ is the measured contact angle between bubble and liquid.

The downward liquid drag force: $(F_D)_{liquid\ drag} = \frac{1}{2} C_D \rho_l \frac{\pi}{4} {d_b}^2 {u_b}^2$ (2.5)

With $C_D = \frac{24}{Re}$ is the drag coefficient, and Re is the Reynolds number based on density and viscosity of liquid and bubble size. u_b is the bubble center rise velocity.

In the expansion stage, u_b is the bubble expansion velocity $u_e = \frac{dr_b}{dt}$ and r_b is the bubble radius. In the detachment stage, u_b is the sum of the expansion velocity u_e and the bubble base rise velocity u. Also, the bubble volume V_b is the sum of bubble volume at the end of the expansion stage V_E and Qt_2 with t_2 as the time spent in the second stage. Q is the volumetric gas flow rate.

The downward bubble inertial force $\left(F_{I,g}\right)_{bubble\ inertia}$ induced by the acceleration of the bubble can be expressed by:

$$F_{I,g} = \frac{d(u_b V_b \rho_g)}{dt} = \rho_g V_b \frac{du_b}{dt} + \rho_g u_b \frac{dV_b}{dt} \quad (2.6)$$

By substituting u_b and V_b by their appropriate expression, we obtain the following expressions for the bubble inertial force:

For the expansion stage: $F_{I,g} = \frac{\rho_g Q^2 {V_b}^{-\frac{2}{3}}}{12\pi\left(\frac{3}{4}\pi\right)^{\frac{2}{3}}}$ (2.7)

For the detachment stage: $F_{I,g} = \rho_g V_b \frac{du}{dt} + \rho_g Q u \frac{\rho_g Q^2 {V_b}^{-\frac{2}{3}}}{12\pi\left(\frac{3}{4}\pi\right)^{\frac{2}{3}}}$ (2.8)

The downward Basset force $(F_{BA})_{Basset}$ which describes an additional resistance to bubble motion due to the development of a boundary layer around the bubble that results from bubble acceleration.

In the expansion stage, the bubble acceleration is negligible, and then Basset force is neglected. In the detachment stage, Luo et al.[24] proposed the following expression:

$$(F_{BA})_{Basset} = \frac{3}{2} {d_b}^2 \sqrt{\pi \rho_l \mu_l} \int_0^t \frac{{du}/{dt}}{\sqrt{t-\tau}} d\tau \tag{2.9}$$

The downward bubble-particle collision force $(F_C)_{bubble-particle\ collision}$: This force is induced by the presence of solid particles and presents an additional resistance to bubble growth. The collision force can be quantified by considering the rate of change of particle momentum before and after the collision. It has different expressions in expansion and detachment stages.

In the expansion stage, radial expansion velocity of bubble surface dominates bubble vertical velocity, and Luo et al.[24] proposed the following expression:

$$F_C = \frac{\pi}{4} {D_0}^2 \rho_p (1+e) \varepsilon_S {u_e}^2 \tag{2.10}$$

Where ε_S is the solid concentration and e is the collision coefficient defined as $e = \frac{u_{particle\ rebound\ speed}}{u_{particle\ incoming\ speed}}$ is equal to 0 or 1 for inelastic or elastic collision, respectively[26].

In the detachment stage, Luo et al.[24] proposed the following expression for the magnitude of the bubble-particle collision force : $F_C = \frac{\pi}{4} {d_b}^2 \varepsilon_S \rho_S u^2$ (2.11)

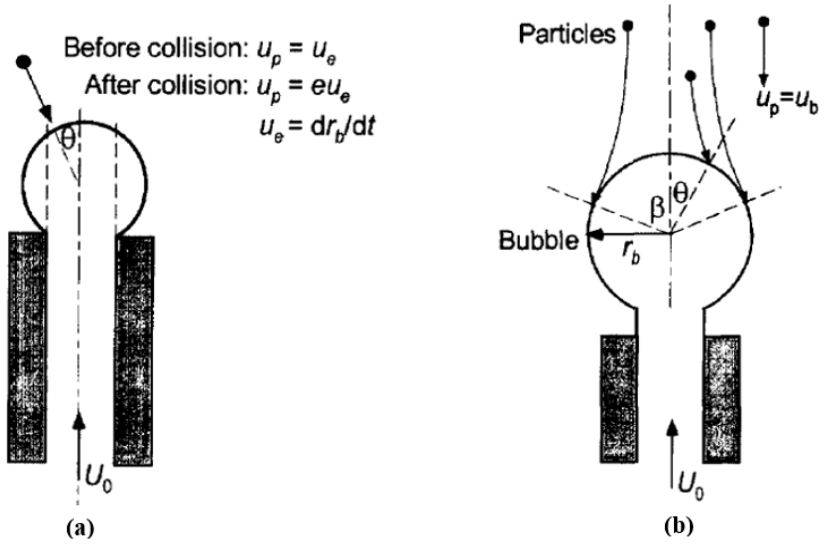

Figure 2.2 Particle-bubble collision forces in the : (a) expansion stage (b) detachment stage adapted from Luo et al.[24]

The downward suspension inertial force $\left(F_{I,m}\right)_{suspension\ inertia}$ **:** It is a resistance induced by the acceleration of the surrounding liquid and particles. It is assumed that the slip velocity between liquid and solid particles is negligible and then liquid and solid inertial force can be approximated to the suspension inertial force $F_{I,m}$. This later is based on the rate of momentum change of suspension with respect to time:

$$F_{I,m} = \frac{d(\int\int\int \rho_m u_m \delta V)}{dt} \tag{2.12}$$

Where ρ_m is the suspension apparent density. Also, the force has the same expression in the expansion and detachment stages.

2.2.1.2 Bubble rise stage

A rising bubble can be characterized by its shape, rise velocity and motion[23]. However, it is of prime importance to distinguish between two types of forces describing bubble dynamics. The first type is the global forces that control the occurring of bubble coalescence and bubble breakage phenomena. As a result of those forces, a specific bubble size distribution is developed within the

column. The second type is the local forces that tend to maintain the bubbles in a particular shape and to control its rise velocity. Those forces are a function of the bubble size (controlled by global forces) and physical properties of the bubble surrounding medium.

a- Local forces:

When a single bubble is rising in a Newtonian liquid, three forces are present, namely surface tension, viscous and buoyancy forces[23]. However, an individual rising bubble is different from an isolated rising bubble in a liquid medium by its interaction with the neighbouring bubbles. Hence, this interaction gives rise to additional forces that are applied to the rising bubble. The most simplified case used in literature is the case of two bubbles rising in line in which a trailing bubble is accelerated due to its attraction with the wake of a leading bubble[27]. Therefore, it is not only surface tension, viscous and buoyancy forces that dominate, but forces such as inertia, pressure gradient, Basset forces and added mass should be considered. For small bubble size (d_b < 1mm), the dominant forces are surface tension forces and viscous forces, and the bubble shape is spherical. For intermediate bubble size, surface tension and buoyancy forces dominate, bubble wake is formed, and the bubble has an ellipsoidal shape. For large bubbles, the buoyancy force is dominant, and the bubbles have a spherical cap shape[23]. In general, the balance of forces applied to an interactive rising bubble is written as follows:

$$F_{inertia} = F_B - F_D - F_P - F_A - F_{Basset} \tag{2.13}$$

The magnitudes of the abovementioned forces were reported by Luo et al.[24] as follows:

Inertia force: $F_{inertia} = \frac{1}{6}\pi {d_b}^3 \rho_g \frac{du_b}{dt}$ (2.14)

The effective buoyancy force: $F_B = \frac{1}{6}\pi {d_b}^3 (\rho_l - \rho_b) g$ (2.15)

The drag force: $F_D = C_D \frac{\pi}{8} \rho_l {d_b}^2 (\bar{u} - u_b)^2$ (2.16)

This force is based on the relative velocity between the trailing bubble and the local wake velocity of the leading bubble. $\bar{u}$ is the radial average wake velocity over the trailing bubble frontal area.

The pressure gradient force: $F_P = \frac{\pi}{6} {d_b}^3 \Delta P$ (2.17)

ΔP is the difference of liquid static pressure between the trailing bubble and the wake of the leading bubble.

The added mass force or virtual mass force due to trailing bubble acceleration: $F_A = \frac{\pi}{12} {d_b}^3 \rho_l \frac{du_b}{dt}$ (2.18)

Basset force: $F_{Basset} = {d_b}^2 \sqrt{\pi \rho_l \mu} \int_0^t \frac{{du_b}/{dt}}{\sqrt{t-\tau}} d\tau$ (2.19)

In the presence of solid particles, there are three approaches in the literature to determine the forces applied to a rising bubble. The first one is the homogeneous approach that assumes that adding solid particles alters liquid density and viscosity. Therefore, the medium in which bubble rises has a higher apparent viscosity and then solid particles modify viscous forces. The second approach is the non-Newtonian approach that considers that the liquid-solid mixture exhibits non-Newtonian behaviour, and then additional forces such as elasticity force should be considered. Also, the drag coefficient should be corrected in function of the nature of the non-Newtonian mixture[28]. The third approach is the heterogeneous approach that considers the forces induced by the interaction of the bubble with an individual particle. The additional force due to bubble-particle collision is the impaction force that is equal to the impacting particles' momentum rate of change[26].

b- Global forces:

- **Bubble coalescence:**

Bubble coalescence results from the specific forces controlling bubbles collision. Prince and Blanch[29] developed a phenomenological model in which the bubble coalescence rate is the product of the collision frequency multiplied by the collision efficiency. It is worth mentioning that collision efficiency is a function of both coalescence time and contact time and determines whether a collision between two bubbles will lead to their coalescence or no. On the other hand, three forces contribute to the collision frequency:

- *The turbulence force* in which the fluctuating turbulent velocity of gas bubbles causes bubble collisions[29]. The turbulent eddy velocity $\overline{u_b}$ should have the same magnitude as the length scale of the bubble so as to cause the relative motion between bubbles. Indeed, small eddies

don’t contain the necessary energy to affect bubble motion, while large eddies transport a group of bubbles and don’t lead to considerable relative motion.

- *The buoyancy force* is a force resulting from the rise velocity difference between bubbles of different sizes.
- *The laminar shear force* is present more specifically in the heterogeneous regime at high gas flow rates. Hence, large bubbles rise at high velocities and preferentially through the center of the column. Thus, a gross liquid circulation pattern is created. An upward liquid velocity prevails in the center of the column, and a downward liquid velocity prevails in the region near the wall. This circulation pattern results in a liquid radial velocity distribution. As a consequence, a bubble situated in an area of high liquid velocity can overtake another bubble of the same size and same rise velocity[29].

- **Bubble breakup:**

Bubble breakup can result from a bubble-particle collision or bubble surface instability[23].

- **Bubble breakup induced by bubble-particle collision:**

When colliding with a bubble, the particle can be ejected from the surface or can penetrate it. In the latter case, the particle can lead to bubble breakage or just adhere to the bubble surface. Chen and Fan [30] determined the following conditions for the penetration of a descending particle in an ascending bubble surface. They stated that penetration would occur if only one of these three criteria is satisfied: The particle acceleration is downward, or the velocity of the particle relative to the bubble is downward, or the penetration depth of the particle is higher than the deformed bubble height.

Moreover, particle dynamics after the collision is related to particle size and density. If a particle is light or/and small, none of the three criteria mentioned above is satisfied. Then, the particle doesn’t penetrate the bubble and is ejected after the collision. However, small particles can cause bubble breakup if many of them collide with the same bubble and then result in its surface instability. On the other hand, if the particle is large or/and heavy enough to satisfy one of the three criteria, bubble penetration occurs. The forces applied to a particle after its penetration through a bubble are given in detail in **part 2.2.2**. Once penetrated, the bubble is deformed to a doughnut-

shape[30], as depicted in **Figure 2.3**. Bubble breakage will occur if the particle diameter is larger than the height of the doughnut[23, 30] : $d_p > H_d$

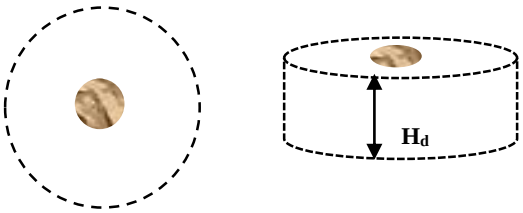

Figure 2.3 Bubble deformed to doughnut-shape after being penetrated by a particle

Clift et al. [31] indicated that three forces control the breakage of bubbles if a particle penetrates the surface: First, the shear stress related to the velocity gradient in the continuous liquid phase and also to the relative bubble-particle impact speed tending to break the bubble. Second, the surface tension force that stabilizes the bubble and returns it to its original shape. Third, the viscous force that slows down the growth rate of surface perturbation. Bubble breakage occurs when shear stress overcomes surface tension and viscous forces.[23]

- **Bubble breakup induced by bubble surface instability:**

A bubble is unstable and subject to breakage when it reaches its maximum stable bubble size $d_{b,max}$[23]. Many mechanisms have been suggested to explain the occurring of bubble breakup. In this part, we will discuss two mechanisms that involve the forces governing in a bubble column. The first mechanism is the one proposed by Hinze [32]. It states that the bubble surface becomes unstable when the hydrodynamic forces in the liquid are more significant than the surface tension force. The hydrodynamic forces are described by the homogeneous isotropic turbulence, where the turbulent eddies result in velocity fluctuations exerting dynamic pressures on gas bubbles and then lead to their breakage. Turbulent eddies should be smaller than gas bubbles since large eddies entrain bubbles and cannot lead to their breakage. The liquid Weber number quantifies this condition. Indeed, when the Weber number is larger than a critical value We_C, bubble breakup will occur: $We_c = \frac{\rho_l \bar{U}^2 d_{b,max}}{\sigma_l}$ (2.20) where $\bar{U}$ is the average value of square of turbulence velocity difference[22].

The second mechanism is the one proposed by Fan et al.[33] and in which the internal circulation of gas inside the bubble creates a centrifugal force pointing outwards of the bubble surface. This force is believed to have the same magnitude as the bubble rise velocity and then increases with bubble size. The authors stated that bubble breakage would occur when the centrifugal force is larger than the surface tension force.

2.2.2 Particles behaviour in slurry bubble columns

Particle dynamics is determined according to two cases. The first one is when the particle doesn't encounter a gas bubble and is moving in the liquid phase. In this case, Newton's second law of motion governs particle acceleration in the liquid phase:

$$m_p \frac{dv_p}{dt} = F_D + F_{AM} + F_{G/B} + F_{Basset} + F_{IP} \quad (2.21)$$

F_D is the drag force, F_{AM} is the added mass force, $F_{G/B}$ is the effective buoyancy force, F_{Basset} is the Basset force and F_{IP} are the interparticle forces represented by the electrostatic repulsion resulting from the overlap of electrical double layers and the attractive Van der Waals forces between particles.

The second case is when a particle encounters a rising bubble. We already described above the effect of a particle on the bubble. Now, we will explain the impact of a bubble on the particle.

Four successive conditions have to be satisfied to achieve bubble-particle attachment in a slurry bubble column [34]: First, the particle has to collide with an encountered bubble. Second, after the bubble-particle collision, the particle has to adhere to the bubble. Third, a three-phase contact line (TPC) has to be built when particles adhere to bubbles. Fourth, a particle-bubble aggregate should be stable against external forces to avoid being cut off in high turbulent regions, which are numerous in slurry bubble columns (e.g., gas distributor region or column operating in the heterogeneous regime). The satisfaction of the above conditions is expressed in terms of probabilities (P_c, P_a, P_{TPC}, P_{stab}) in which hydrodynamic forces and interface forces play a critical role[34, 35].

2.2.2.1 Particle-bubble collision

The collision of particle and bubbles depends on the Stokes number St representing the ratio between particle inertia force and bubbles viscous drag force: $St = \frac{\rho_p {d_p}^2 v_b}{9\mu d_b}$ (2.22) where ρ_p is the density of the particle, μ is the liquid dynamic viscosity and v_b is the bubble rise velocity. If St <0.1, particle motion is not influenced by their inertia. Therefore, particles will be carried by liquid streamlines and slip freely. If 0.1<St <1, inertia forces can affect the attachment. The trajectory of the particle deviates from liquid streamlines and can collide with the bubble. If St >1, the particle will have a straight-line path and will collide with the bubble.

2.2.2.2 Bubble-particle adhesion

When the collision occurs, two kinds of particle-bubble interactions can be distinguished: First, the sliding process in which the surface of the bubble colliding with the particle undergoes a weak deformation. Second, the impact process in which the bubble surface is deformed and a thin liquid film of thickness h_f is formed between the bubble and the particle.

Schulze et al.[34] stated that collision is predominantly occurring by an impact process in which heavy particles encounter the bubble. For the impact process, bubble-particle adhesion can only be reached if the collision time is high enough to permit to the thin liquid film between bubble and particle to drain and then to rupture when it reaches its critical thickness of rupture. Collision time should be higher than the drainage time. Schulze et al.[34] reported that collision time depends on the particle mass, the liquid-gas interface surface tension and the deformation depth. In contrast, the drainage or induction time depends on the thin film critical thickness of rupture, which in its turn depends on the particle surface degree of hydrophobicity.

2.2.2.3 Three-phase contact line expansion

The three-phase contact line TPC is the boundary between the advancing gas phase and the receding liquid phase. Right after bubble rupture, a minimal TPC line has to be formed quickly to enable the bubble-particle aggregate to counteract external forces and avoid detachment. Tsabet et al.[35] reported that the critical TPC line radius depends on the equilibrium contact angle and the critical film thickness. Afterwards, TPC line should have sufficient time τ_{TPC} to expand to a large

radius to ensure that a high force of attachment will be established and will prevent bubble-particle detachment. The radius of TPC is shown in this figure modified from reference [35]:

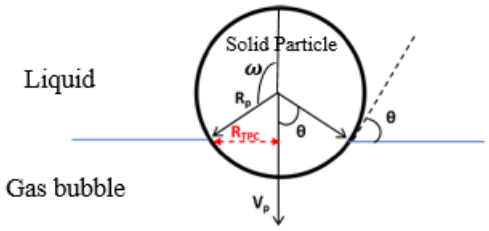

Figure 2.4 Radius of three-phase contact line TPC modified from reference [35]

2.2.2.4 Bubble-particle stability

Bubble-particle stability against detachment is closely related to the attachment and detachment forces exerted on a particle. We consider the following force balance on a spherical particle placed in the gas-liquid interface: $F_b + F_{ca} = F_g + F_\sigma + F_{hyd}$ (2.23)

The magnitudes of the different forces are expressed as follows:

F_g is the force of gravity: $F_g = \frac{4}{3}\pi {R_p}^3 \rho_p g$ (2.24)

F_b is the static buoyancy force of the immersed part of the particle:

$F_b = \frac{\pi}{3}{R_p}^3 \rho_l g(1-\cos\omega)^2(2+\cos\omega)$ (2.25)

and ω is the center angle between the TPC projection area on the attached particle sphere and the rear part of the sphere: $\omega = (\pi - \frac{\theta}{2})$.

F_{ca} is the capillary force acting on the TPC line: $F_{ca} = -2\pi\sigma R_p \sin\omega \sin(\omega+\theta)$ (2.26)

F_σ is the Laplace pressure force corrected by the liquid head due to penetration:

$\mathrm{F_\sigma} = \pi {\mathrm{R_p}}^2(\sin^2\omega)\left(\frac{2\sigma}{\mathrm{R_b}} - 2\mathrm{R_b}\rho_\mathrm{l}\mathrm{g}\right)$ (2.27)

F_{hyd} is the additional hydrodynamic detaching forces that can be presented by the product of the external field flow acceleration and the particle mass: $\mathrm{F_{hyd}} = \frac{4}{3}\pi {\mathrm{R_p}}^3 \rho_\mathrm{p} a$ (2.28)

In which a is the additional acceleration caused by the external flow field. Schulze et al.[34] reported that a depends on the intensity and structure of the flow field and then on the local energy dissipation ε in a given region of the reactor : $a = \frac{1.9\varepsilon^{2/3}}{(R_B+R_p)^3}$ (2.29)

Therefore, the total force of detachment $F_{detach} = F_g - F_b + F_{hyd} + F_\sigma$ and the total force of attachment is $F_{attach} = F_{ca}$. Comparing F_{detach} to F_{attach} determines the stability of particle in the bubble surface.

2.3 Hydrodynamic and mass transfer aspects of slurry bubble column reactors

Bubble columns performance is a complex function of several parameters, which renders its design and scale-up a tedious task[19] as they are mainly related, in addition to kinetics, to three main aspects, namely hydrodynamics, mass transfer and heat transfer as illustrated in **Figure 2.5.**

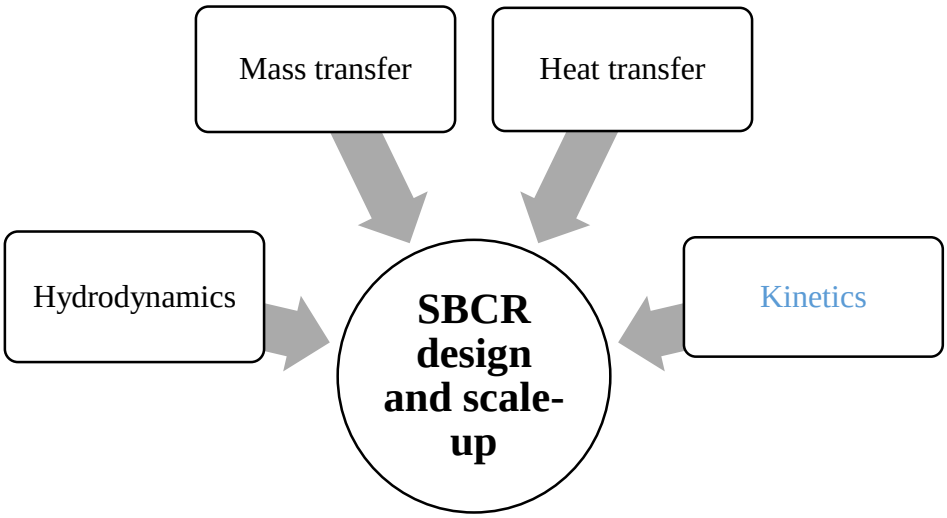

Figure 2.5 Aspects that affect the design and scale-up of slurry bubble column reactors

Several parameters can express these three aspects [36] :

- Gas holdup distribution
- Bubble formation and rise velocity

- Bubbles breakup and coalescence phenomena
- Bubbles growth, dispersion and size distribution
- Flow regimes
- Liquid recirculation, back mixing and turbulence
- Gas-liquid interfacial area
- Gas-liquid or liquid-solid mass transfer
- Solid concentration profile, attrition, agglomeration and recirculation
- Heat transfer

All these parameters are affected by three main categories[36]:

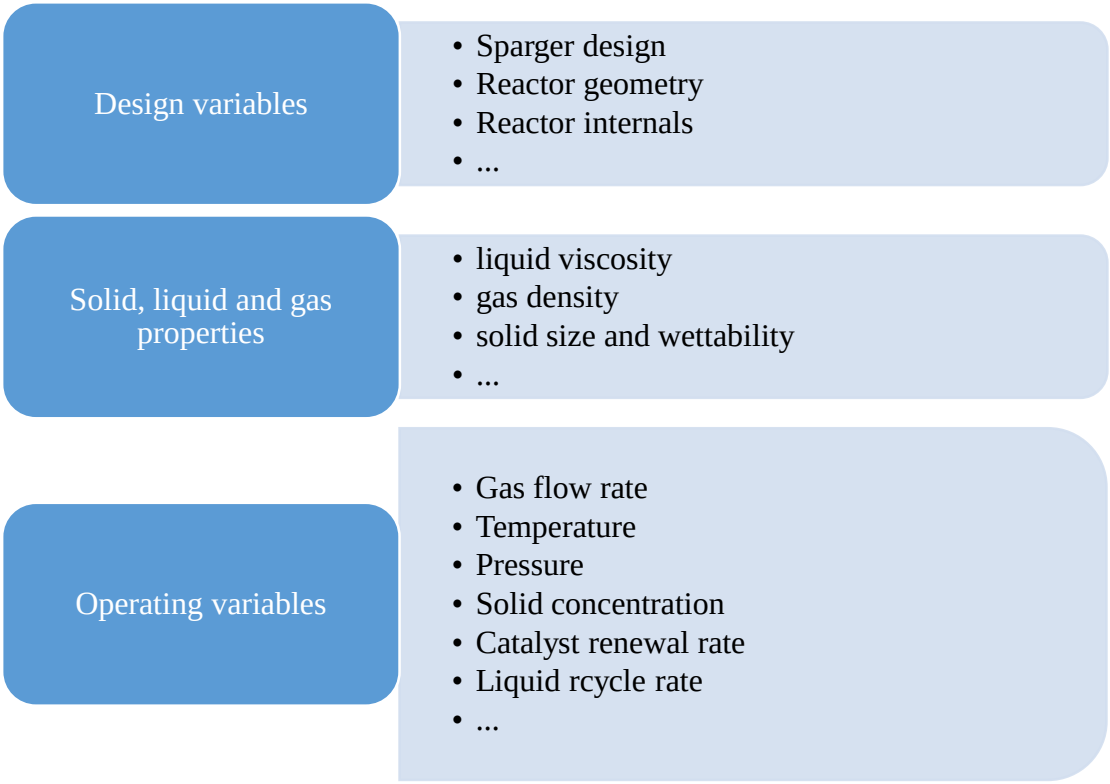

2.3.1 Gas holdup

Hydrodynamic parameters depend inherently on each other[19]. Gas holdup ε_g is defined as the volume fraction of gas in a gas-liquid or gas-liquid-solid medium. It's a key parameter of bubble columns design as it determines the total volume of the reactor required for the process.

2.3.2 Flow regimes in SBCR

Slurry bubble column reactors can operate in four different flow regimes (Figure 2.6):

- *The homogeneous regime or bubbly flow* prevails at low superficial gas velocities. The generated bubbles are small, spherical, monodisperse and rise vertically. The phenomena of bubbles breakup and coalescence are absent, and there is no significant liquid circulation [37].
- *The transition regime:* When increasing gas velocity, the stability of the system decreases and the first large bubbles are formed due to bubbles clustering. The appearance of different bubble classes characterizes this regime.
- *The heterogeneous regime or churn-turbulent regime*: It prevails when the superficial gas velocity is very high or when the orifices of the distributor generate large bubbles. It is characterized by an intense interaction between gas bubbles, which gives rise to coalescence and breakup phenomena. Consequently, bubbles have a large size distribution. Also, a gas holdup parabolic radial profile, as well as a large macro-scale liquid circulation, are observed.[37, 38]
- *The slug flow regime* occurs in case of small diameter columns or at very high superficial gas velocities. Large diameter slugs are formed due to intense bubble coalescence[18].

The most interesting flow regime that ensures high volumetric productivity is the churn-turbulent heterogeneous regime[36]

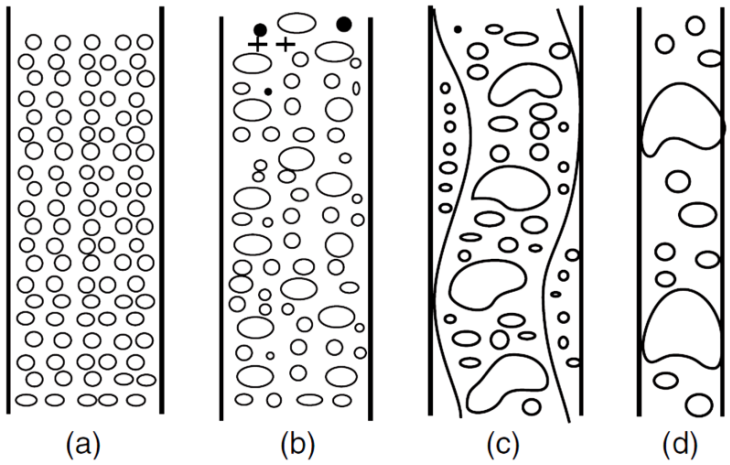

Figure 2.6 Various flow regimes in bubble column reactors. (a) Homogeneous regime. (b)Transition regime. (c) Heterogeneous regime (d) Slug flow regime[39]

These regimes can be identified by plotting the gas holdup versus superficial gas velocity. In typical systems, gas holdup increases with superficial gas velocity following a convex curve in the homogeneous regime. In contrast, it follows a concave curve in the heterogeneous regime, as illustrated in Figure 2.7.

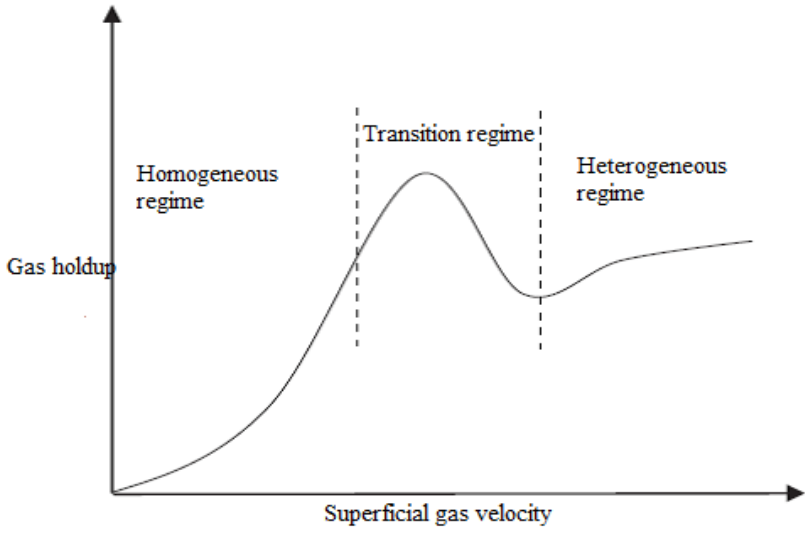

Figure 2.7 Typical graph of gas holdup versus superficial gas velocity. Modified from reference[38]

2.3.3 Regime transition determination

As mentioned above, regime transition is detected by the change of slope of the gas holdup vs superficial gas velocity curve[18]. However, in some cases, the visualization of the slope change is difficult. Another direct method is the drift flux method used by many researchers[40, 41] and proposed by Wallis[42]. It is based on plotting the drift flux velocity $j_e = U_g(1 - \varepsilon_g)$ against the gas holdup ε_g. A change in the slope of this curve means the onset of the heterogeneous regime. Generally, the change in the drift flux method is sharper than the change in gas holdup vs superficial gas velocity.

2.3.4 Effects of solid particles on the hydrodynamics of SBCR

- **Effect of solid intrinsic properties**

Solid particles used as catalysts alter the hydrodynamics and mass transfer of SBCR. This effect can be either due to the increase of slurry viscosity at high solid concentrations or the changing of bubble coalescence behaviour due to the wetting properties in the liquid phase[43]. In literature, the most investigated hydrodynamic parameters are gas holdup and flow regime transition [38, 43-46]. This is justified because each flow regime has different hydrodynamic behaviour, and then transport phenomena properties (momentum, heat and mass) are dissimilar[38]. It is worth mentioning that from literature, several physical mechanisms underlying the effect of solid particles on the hydrodynamics of SBCR were reported:

- **Mechanism 1: Density effect [38, 45]**

This mechanism was reported by various authors [38, 45]. The presence of solid particles can affect the density of the medium in which the bubble is rising. The concept of apparent density quantifies the density effect:

$$\rho_{app} = (1 - C_v)\rho + C_v\rho_p \qquad (2.30)$$

Consequently, the medium in which bubbles rise has an apparent density that is different from the liquid density. This difference has the same magnitude as the solid-liquid density difference. Consequently, the single bubble rise velocity due to buoyancy alteration is affected.

Moreover, the density effect can be considered if the bubble size is much larger than the size of the dispersed solid particles. This condition should be verified by the following inequality [38]:

$$d_B > \frac{d_p}{C_v^{\frac{1}{3}}}$$

It is worth mentioning that the density effect is noticeable for systems with high solid loads and with the great difference between the liquid density and solid density.

- **Mechanism 2: Viscosity effect**

It was generally reported that the presence of solid particles increases the viscosity of the slurry phase (liquid-solid)[43, 45]. The following statement can explain this effect: the presence of each solid particle gives rise to a new no-slip boundary condition and makes the liquid velocity equal to zero. Consequently, more velocity gradients are created within the slurry, and viscous dissipation is increased.

The viscosity effect is quantified by the concept of apparent viscosity μ_{app} which is larger than the liquid phase viscosity. μ_{app} increases with solid particles concentration C_v, particle size and particle density [38, 47, 48].

However, it appears that the viscosity effect on gas holdup and regime transition in literature is contradictory. Indeed, viscosity has two opposing effects. The first one, which is the common belief, is that highly viscous media enhances bubble coalescence and hinder bubble breakage. Schafer et al.[49] stated that with increasing viscosity, turbulence in the liquid phase decreases and then liquid eddies receive less energy to cause bubble breakage. Hence, bubbles become larger and faster. Consequently, gas holdup decreases and the homogeneous regime is destabilized [38, 41]. The other opposing effect is that the bubble rise velocity decreases due to the capability of the flow to absorb the energy motion liberated by the bubble. Therefore, the gas holdup increases for the same gas velocity and the homogeneous regime is stabilized.

- **Mechanism 3: Primary bubble size**

The two-stage spherical bubble formation model widely describes the primary bubble size. The bubble in the orifice is formed in two stages: the expansion stage in which bubbles grow in size but are connected to the orifice and the detachment stage in which bubbles move away from the

distributor[24]. Solid particles can affect gas holdup and regime transition velocity by affecting bubble formation in each of these two stages[38, 43].

In the expansion stage, settling particles apply two downward forces on the growing bubble, namely, the particle-bubble collision force F_c and the suspension inertial force $F_{l,m}$. The bubble size was found to increase due to those two forces. However, this effect is negligible if the particles used have low inertia. The bubble size just before detachment (end of expansion stage) is obtained with a force balance at the orifice[24].

For the detachment stage, bubble size is affected by two parameters. The first one is the injection gas velocity. We can distinguish between three regimes that depend on this velocity[50]. If we increase the gas flow, we can observe successively: separate bubble formation regime, chain bubbling regime and jet regime (Figure 2.8[51]).

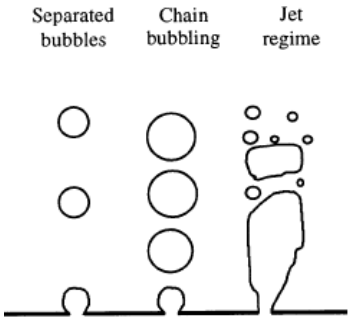

Figure 2.8 Bubble formation regimes[51]

The second parameter is the media properties such as liquid surface tension and viscosity or solid particles presence that affect the coalescence behaviour of bubbles and the bubble size at the detachment.

When the gas is injected at a certain velocity, the frequency of the bubble passing through the orifice is increased. Trailing bubbles collide with leading bubbles. Depending on media properties and, more specifically, solid particles' physical properties that prevent coalescence, the two bubbles can’t coalesce. This can be explained by the fact that certain types of particles increase the coalescence time, and then the two bubbles will not have enough time to coalesce as they are rising and getting far from each other within the column (Figure 2.9 [43]). On the other hand, if solid

particles promote coalescence, the two bubbles coalesce instantly to form one larger bubble that rises faster (Figure 2.9[43]).

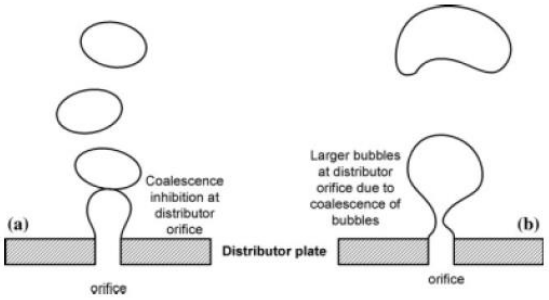

Figure 2.9 Formation of gas bubbles at the orifice in case of coalescing and non-coalescing media[43]

- **Mechanism 4: Effect of bubble-particle interaction on bubble rise velocity:**

Interaction between bubble and particles can also influence bubble rise velocity. It was generally reported that the solid particles hinder bubble motion and then decrease bubble rise velocity due to hydrodynamic forces and mutual collisions [52].

Moreover, solid particles enhance the lateral movement of bubbles due to collision. Hence, the bubble deviates from the vertical trajectory, and a horizontal velocity component is added. Before the collision, the buoyant potential energy corresponds only to the vertical velocity component. However, after the collision, this energy will be shared between the two components of velocity. Therefore, the mean bubble rise velocity will decrease. Mena et al. [38] visualized this effect in their research work (Figure 2.10). They reported that at low solid concentrations (up to $C_v = 3\%$) this mechanism can explain the stabilization of the homogeneous regime.

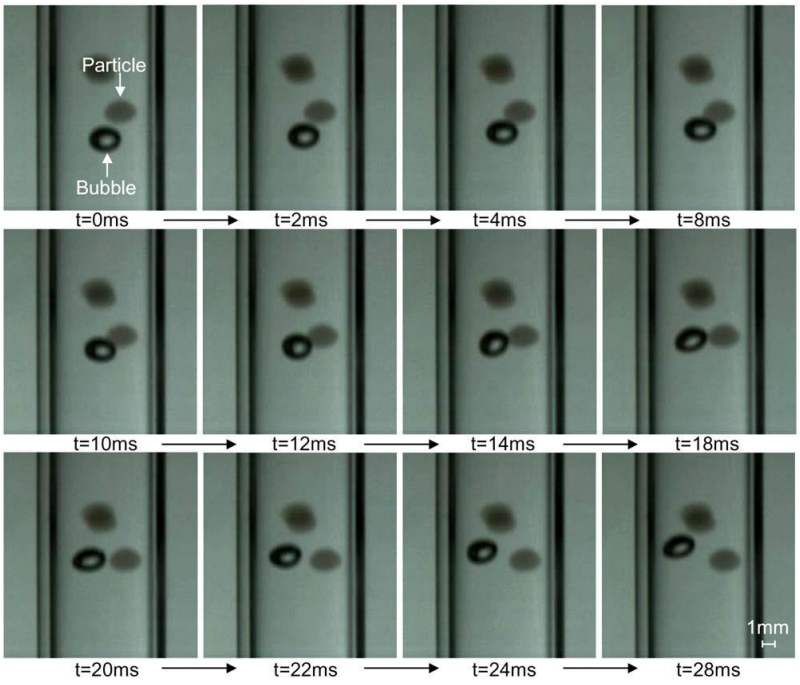

Figure 2.10 Bubble deviation after collision with solid particles[38]

- **Mechanism 5: Bubble coalescence in suspension**

The lyophobicity/lyophilicity solid intrinsic property is reported to affect the coalescence behaviour of bubbles. However, the effect of this property on bubble coalescence is contradictory in literature.

Coalescence inhibition by lyophobic particles is stated by Chilekar et al.[43]. As generally known, the bubble coalescence process includes three steps after bubbles collision: film formation, film drainage and film rupture[43, 53].

The authors mentioned that the film drainage step is the limiting step for bubble coalescence. Hence, a considerable amount of lyophobic particles migrate from the bulk liquid to the gas-liquid interface (Figure 2.11[43]). Consequently, they prevent the draining of the thin liquid film formed by rigidifying the gas-liquid interface. This causes a decrease in the coalescence rate, and then the number of small bubbles is higher, and the gas holdup is increased. However, lyophilic particles have an opposite effect as they tend to be placed on the bulk liquid. Also, the negligible amount of solids placed in the gas-liquid interface tries to reach the bulk fluid and then drag some liquid from the interface. This accelerates the draining of the liquid film.

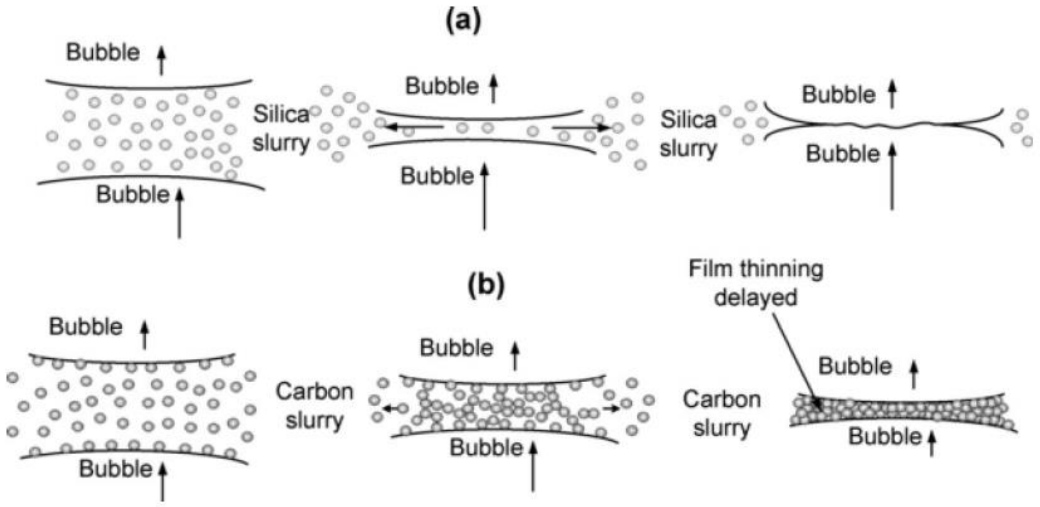

Figure 2.11 Effect of solid particles on two bubbles coalescence. (a)lyophilic particles and (b)lyophobic particles[43]

In contrast, Jamialahmadi et al.[54] reported that lyophilic particles inhibit coalescence by decreasing the rate of bubble coalescence. They repel the gas interface and maintain adjacent bubbles far from each other.

Following the same trend, Van der Zon et al.[53] stated that lyophobic solid particles promote bubble coalescence: Particles contribute to film thinning acceleration by increasing capillary pressure that leads to partial or complete particle dewetting which causes film rupture. However, their speculation stems from foaming flotation systems in which static bubbles are present, and particles are inevitably placed at the gas-liquid interface. Differently from Chilekar et al.[43], they stated that the presence of solid particles affects the film rupture last step of coalescence rather than the film drainage step.

- **Mechanism 6: Non-uniform spatial distribution of solid particles**

Another phenomenon is that the destabilization of the homogenous regime in the slurry bubble column can be caused by spatial nonuniformity induced either in solid-phase or gas phase (The two dispersed phases)[38]. A solid-phase pronounced radial profile can cause flow regime transition even if bubbles are equally distributed in the column cross-section. However, if the solid particles are uniformly distributed, they can prevent bubbles from getting near each other (clustering tendency [38]) and then enable the stabilization of the system.

Generally believed, a random formation of buoyant clusters can cause the introduction of large scale circulations by advection and later the onset of spatial nonuniformity. Therefore, this spatial nonuniformity determines the further clustering tendency of the solid or gas phase and then the destabilization of the flow regime.

It is essential to decide on which phase clusters generate higher buoyant energy and then induce first the spatial non-uniformity. This can be quantified by comparing the density difference between solid and liquid on one part and between gas and liquid on the other part. In the following, we present some findings on the effect of solid particles.

Mena et al. [38] investigated experimentally in a 0.14m diameter column the impact of completely wettable solid particles on the homogeneous regime stability and flow regime transition. They used air as gas phase, distilled water as liquid phase and alginate beads (2.1mm, 1023 kg/m^3) at concentrations c=0-30%(vol). The experimental results showed that the transition velocity increased with solid concentration up to 3% and decreased for concentrations higher than 3%, as depicted in Figure 2.12[38]. This was explained by a dual effect of solid particles on gas holdup. At low concentrations, particles' presence increases gas holdup and stabilizes the homogeneous regime while at high concentrations, particles decrease gas holdup and shift the transition to lower velocities. The mechanism by which they explain this effect is that at low concentrations, bubble-particle interactions reduce bubble rise velocity. However, they couldn't identify a mechanism at high concentrations.

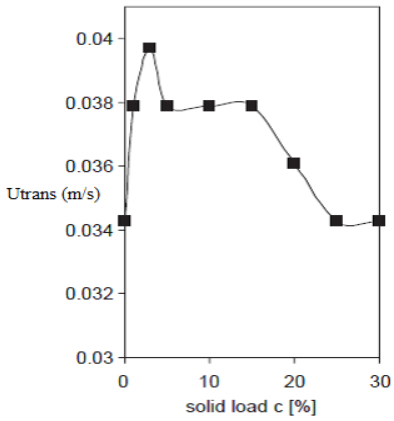

Figure 2.12 Effect of wettable solid particles on flow regime transition[38]

Recently, Mota et al[44] investigated experimentally also the effect of wettable spent grains on flow regime transition in a 0.142m cylindrical Plexiglas bubble column with air as the gas phase and water as the liquid phase and solid concentrations between 0 and 20%. They noticed the same effect of solids as Mena et al. [38] for low solid fractions but found that this effect is verified up to 8% vol concentration, which gives rise to the question of quantifying low solid concentrations in SBCR.

In another study, Chilekar et al.[43] investigated the effect of surface lyophobicity of solid particles on many hydrodynamic parameters such as gas holdup, flow regime transition, average large bubble size and centerline liquid velocity. It was observed that lyophilic particles had a negligible effect on gas holdup and regime transition velocity. In contrast, lyophobic particles increased gas holdup, shifted regime transition velocity to larger gas velocities and also induced foam in the column. The mechanism is depicted in Figure 2.8[43]. Incomprehensibly, this statement contradicts many other authors who observed that lyophobic particles decreased gas holdup by promoting bubble coalescence [45, 53, 54]. Another finding is that adding lyophobic solid carbon particles had no effect on gas holdup in the homogeneous regime, while the effect was clearly noticeable in the churn turbulent regime[43]. This effect can be expected since the coalescence phenomenon is only pronounced in the churn turbulent regime.

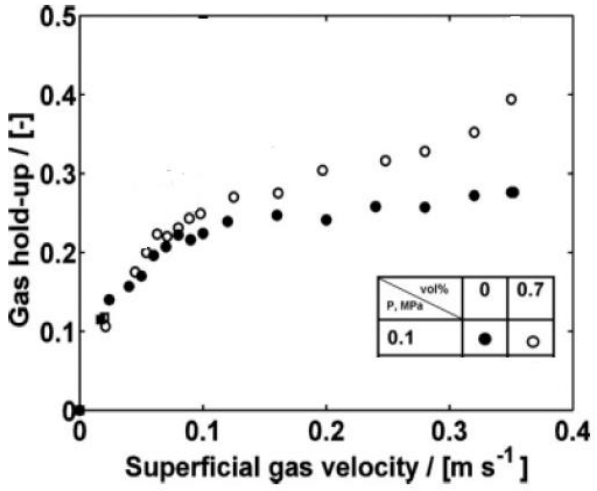

Figure 2.13 Effect of lyophobic particles on gas holdup. Modified from[43]

Kluytmans et al.[45] investigated the effect of hydrophilic carbon particles on gas holdup in a 2D-slurry bubble column operating with nitrogen and distilled water. In the same trend, they were interested in studying the effect of low solid concentrations on hydrodynamics without changing the bulk liquid properties. They found that the addition of hydrophilic carbon particles increases gas holdup and then delays the flow regime transition, which is different from the weak effect of lyophilic particles found by Chilekar et al.[43]. Also, they reported that solid particles influence was present in both homogeneous and heterogeneous regimes (Figure **2.14**[45]) which contradicts Chilekar et al.[43]

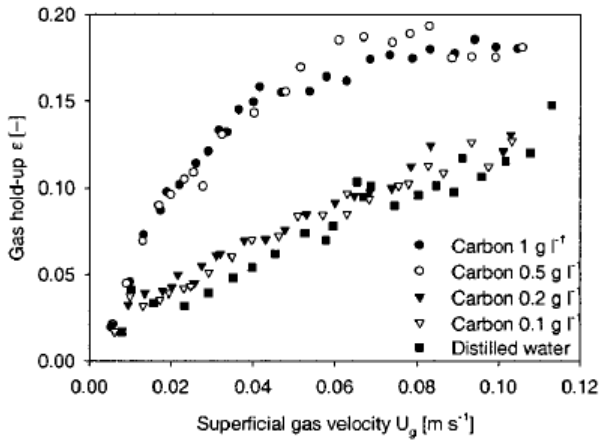

Figure 2.14 Effect of hydrophilic carbon particles on gas holdup[45]

In the homogeneous regime, the density of the layer surrounding the gas bubble is increased by the presence of solid particles. Then bubble motion is reduced, which causes the increase of gas holdup.

In another study, Bukur et al.[55] used silica particles and iron oxides at a concentration up to 30 % wt. They found that between 0 to 20%wt., gas holdup increased with solid concentration and between 20% and 30%wt., gas holdup followed the common trend of decreasing due to particles' presence. They attributed this effect to the poor wettability of silica particles, which adhere to small gas bubbles interface and inhibit coalescence. The impact of poorly wettable particles on gas holdup is in agreement with Chilekar et al.[43] but contradicts other authors.[46, 53]

Van der Zon et al[53] studied the effect of solid particles' hydrophobicity and concentration on gas holdup and bubble size distribution. They stated that hydrophobic particles tend to separate from

the liquid phase. They can either form agglomerates in the liquid phase by particle-particle cohesion or tend to migrate to the gas-liquid interface by particle-bubble adhesion. They found that by increasing solid concentration from 1 vol.%, hydrophobic carbon particles decreased gas holdup and small bubbles fraction if compared with more hydrophilic carbon particles. The authors attributed this effect to the promotion of bubble coalescence by particles' adhesion to bubbles. Hence, as hydrophobicity increases, the three-phase contact angle increases and a stronger adhesion and penetration of particles into the bubble are reached. Consequently, the energy barrier for film rupture is decreased, and then coalescence is promoted.

The effect of low concentration particles (up to 4%) on gas holdup and regime transition was also studied by Ruthiya et al.[46]. They stated that studying bubble-particle adhesion without affecting slurry viscosity can be done for a solid concentration lower than 10%vol. Also, they found that the presence of solid particles decreased the gas holdup. However, their explanation gives rise to the contradictions that govern this field: First, they stated that, in both regimes (homogeneous and heterogeneous), coalescence is promoted to the same extent with solid particles' presence. Second, they found that particles lyophobicity did not affect hydrodynamics.

Omota el al.[56] investigated the effect of particles' hydrophilicity on bubble coalescence. He found that both hydrophilic and hydrophobic particles didn't affect bubble coalescence if solid particles are static, whereas they promote coalescence by causing film rupture in dynamic conditions. More recently, Ojima et al.[57] studied the effect of 100 μm hydrophilic silica particles on the homogeneous regime at a high range of solid concentrations (0-40%). The novelty of their study is the measurement of bubble frequency and local gas holdup as local hydrodynamic parameters. They found that local gas holdup and bubble frequency decreased with solid concentrations. They justified their findings by the coalescence promotion due to the particles' presence. However, when they wanted to identify the effect of solids on particles on the contact time t_c between two colliding bubbles before film rupture, they only compared the lowest and highest concentrations (0% and 40%) (Figure 10[57]). In this way, the intrinsic effect of solid particles was overshadowed by the high concentrations that alter slurry properties. Also, they investigated the effect in the homogeneous regime and didn't consider the churn-turbulent regime that prevails in industrial applications.

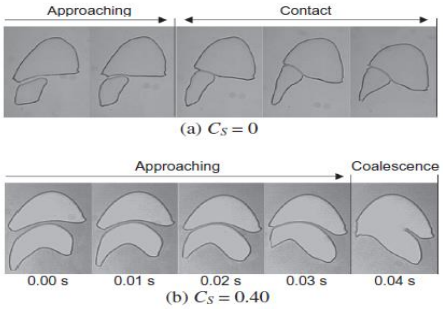

Figure 2.15 Bubble collision and coalescence (a): Long contact time. (b): No contact time and instantaneous coalescence[57]

Overall, the physical understanding of the effect of particles' presence and intrinsic properties on bubble behaviour and then on hydrodynamics is far from satisfactory.

- **Effect of particle size:**

In comparison with the effect of solid concentration and solid surface properties, the effect of particle diameter on SBCR hydrodynamic is scarce[58].

In a recent study, Ojima et al.[58] reported that the decrease of particles' diameter promoted coalescence by decreasing the contact time t_c before film rupture. Also, they found that the effect of particles' diameter vanished at high concentrations (40%) (Figure 2.16[58]). Interestingly, they reported that due to particles' presence, the liquid film between two colliding bubbles takes a porous shape, and then liquid elements in this structure are fragile. By decreasing particle diameter, particle number density increases and then the fragility of liquid elements between the particle and the bubble is increased. This causes to increase in the critical film thickness before the film rupture.

However, from their finding (Figure 2.16), it is clear that the effect of particle diameter also vanished at low concentrations which gives rise to the question of which solid property affects hydrodynamics at low solid loadings (<10%).

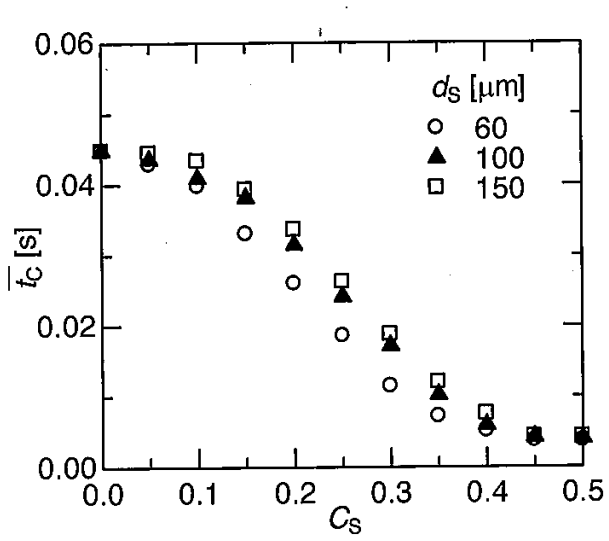

Figure 2.16 Effect of particle diameter and solid concentration on contact time before film rupture[58]

In another study, Chilekar et al.[43] stated that the effect of particle diameter on particle size distribution, in general, prevails when using lyophobic particles. In a non-stationary system as SBCR, particles are affected by the turbulence surrounding the bubble and by the liquid flow. Small lyophobic particles have a long residence time in the gas-liquid interface and stay in the wake of the rising bubbles. In contrast, large particles or agglomerates remain in the bulk of the liquid phase and are not present in the gas-liquid interface. For the coalescence process, trailing bubbles generally collide with leading bubbles. This happens in the wake of the leading bubble where lyophobic particles are present. Hence, particles of this type have the same effect on coalescence inhibition as for a stationary system[43].

For lyophilic particles, they are not present in the liquid-gas interface and then their size distribution (or their diameter) doesn't affect the coalescence behaviour of bubbles. This is in agreement with Ojima et al.[58] findings because the effect of hydrophilic particles vanished at low concentrations. Also, Mena et al.[38] reported that the effect of lyophobic particles is present in the case of small particles.

2.3.5 Effect of solid particles on mass transfer of SBCR

In literature, only a few studies were interested in studying the effect of solid particles' properties (lyophobicity/lyophilicity, diameter, density, shape) on the volumetric liquid-side mass transfer coefficient (k_la_l).

This coefficient depends on two parameters:

- Gas-liquid interfacial area (a_l) that depends on bubble diameter (d_b) and gas holdup (ε_g)
- Liquid side mass transfer coefficient (k_l) that depends on bubble diameter (d_b) and the slip velocity between gas and liquid (u_{slip}).

In agreement with other literature findings, Ruthiya et al.[46] found that k_la_l increased with superficial gas velocity. This increase was related principally to the k_l increase. The latter can be explained by several theories such as that high velocities increase the frequency of gas-liquid film renewal due to the high rate of coalescence and breakup and results in high gas exchange between bubbles [59]. Another theory is that high velocities cause liquid film thickness to decrease[60].

About the effect of particles, the authors reported that k_la_l was not influenced by solid concentration up to 5g/l and decreased at high slurry concentration 20g/l. They related this decrease to the decrease of the interfacial area due to particle presence. Indeed, the interfacial area can be correlated to gas-holdup that they found decreasing by particles' presence. Also, they observed that particles didn't affect k_l. However, from their findings (Figure 2.17[46]: k_la_l vs U_g), it is clear that particles' lyophobicity had a clear impact on mass transfer, especially at high velocities (comparison between 2g/l lyophilic silica and 2g/l modified lyophobic silica). The authors did not highlight this finding, which gives rise to the impact of solid properties on mass transfer.

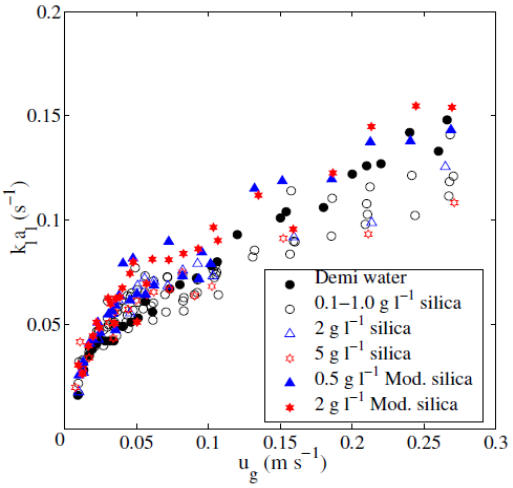

(b) Silica particles

Figure 2.17 Volumetric mass transfer coefficient vs superficial gas velocity for silica particles[46]

It should be mentioned that the mass transfer coefficient k_l depends on fluid dynamics and is estimated by empirical or semi-empirical correlations. Those correlations are generally expressed by the Sherwood number Sh that is correlated to other dimensionless numbers such as Reynolds number Re, Schmidt number Sc or Bond number Bo.

The Sherwood number has the following expression:

$$Sh = \frac{k_l d_b}{D} \tag{2.31}$$

with D is the diffusivity of gas in the liquid.

In literature, many correlations are proposed for Sherwood number calculation:

Table 2.2 Sherwood number model proposed by different authors

Author	**Correlation**	**Description**
Bird et al.[61]	$Sh = 1.13\sqrt{u_{slip} d_b D^{-1}}/2$	Solution of Higbie's model theory
Calderbank and Moo-Young[62]	$Sh = 0.42\left(\frac{g\mu_l}{\rho_l}\right)^{0.33}\left(\frac{D\rho_l}{\mu_l}\right)^{0.5}\frac{d_b}{D}$	$d_b > 2.5mm$

Hughmark[63]	$Sh = 2 + 0.0610Re^{0.78}Sc^{0.55}\left(\frac{gd_b{}^3}{D^2}\right)^{0.039}$	Isolated bubbles
Hughmark[63]	$Sh = 2 + 0.0187Re^{0.78}Sc^{0.55}\left(\frac{gd_b{}^3}{D^2}\right)^{0.039}$	Swarms of bubbles
Akita and Yoshida[64]	$Sh = 0.5Sc^{1/2}Bo^{3/8}Ga^{1/4}$	Homogeneous flow
Schüergel et al[65]	$Sh = 0.15Re^{1/2}Sc^{1/2}$	Homogeneous flow
Ruthyia et al. [46]	$Sh = 0.083Re^{1/2}Sc^{1/2}Bo^{0.768}$	The heterogeneous regime and large bubbles $d_b > 20mm$

Most correlations used to calculate mass transfer were developed for gas-liquid systems and didn't consider solid properties.

In another study, Chilekar et al[43] found that the gas-liquid mass transfer coefficient was independent of particle lyophobicity in both regimes, which is in contradiction with the finding of Ruthyia et al.[46]

More recently, Mena et al.[66] were among the few authors who considered the effect of solid properties on $k_l a_l$ in SBCR. They developed an empirical correlation where the particles' diameter and concentration are present: $k_l a = a_1 u_g{}^{a_2}\left(1 + d_p\right)^{a_3}(1 - C_s)^{a_4}$. They took this exponential form from studies on a three-phase fluidized bed where liquid and gas are circulating. It should be mentioned that they used three polystyrene beads mean diameters (d_p=1100µm; d_p=770µm; d_p=591µm) and 0-30 % vol concentrations to study the simultaneous effect of diameter and loading on $k_l a_l$.

They observed that $k_l a_l$ increased with superficial gas velocity, and this increase was subdued by increasing solid concentration. On the other hand, they observed that $k_l a_l$ decreased with decreasing particles' diameter. The attractive point of their study is that they compared the effect of two types of polystyrene beads for each mean diameter. The first type is "new" polystyrene beads that contain fine particles, and the second is "washed" polystyrene beads where fines were removed. Interestingly, they developed two $k_l a_l$ correlations for each type and found that the form of the model they proposed didn't predict well the case for "new" beads were fine particles are present.

Consequently, they reported that the fine hydrophobic particles (d<20µm) they used affect negatively mass transfer as they adhere to bubble surface and hinder mass transfer. Moreover, when using hydrophilic glass beads fine particles, they observed a dual effect of solid on k_la_l (Figure 2.18[66]).

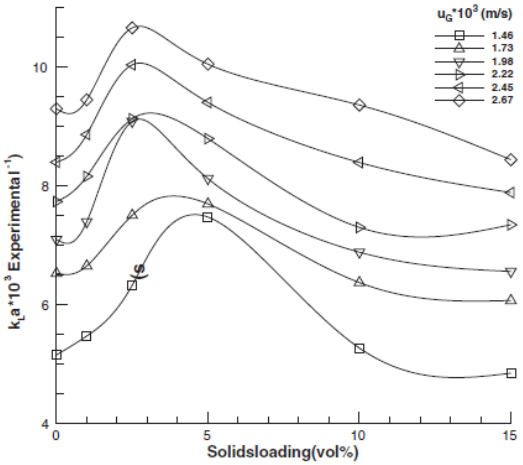

Figure 2.18 Volumetric mass transfer coefficient versus hydrophilic glass beads concentration[66]

From these findings, it is clear that the mechanisms that govern the effect of solid particles on k_la_l cannot be restricted to the physicochemical properties of gas and liquid but also the size and surface properties. These properties should be considered in k_la_l correlations development.

Hashemi et al. [67] conducted an experimental study to investigate the effect of pressure (varying between 0.1 to 4MPa), temperature (ranging between 277K and ambient temperature), superficial gas velocity (up to 0.2 m/s) and solid loading (up to 10%) on gas-liquid mass transfer in slurry bubble columns. The authors were interested in mimicking CO_2 hydrate forming operating conditions. They used ion-exchange resin wettable particles, tap water and oxygen/nitrogen mixture as solid, liquid and gas phases, respectively. However, they didn't find any solid effect on k_la_l in all the range of conditions used. Once again, this finding gives rise to discrepancies in this field in terms of solid effect and which of its properties is affecting hydrodynamics and mass transfer.

Another interesting finding is that the carbon dioxide hydrates slurry they used showed non-Newtonian shear thinning behaviour from a 6% concentration. Hence, it is necessary to know the

solid properties that directly influence the critical concentration at which the liquid phase properties (viscosity, density, and rheology) are altered. Thus, this limit concentration defines how we can model hydrodynamic and mass transfer parameters.

2.3.6 Effect of elevated pressure and temperature on the hydrodynamics and mass transfer of SBCR

Most of the chemical reactions that are conducted in industrial processes within SBCR require high pressure, high temperature and high gas velocity operating conditions to increase reactor performance and reach the needed conversion.

For instance, the most famous process carried out in SBCR is the Low-Temperature Fischer-Tropsch (LTFT) process that enables to convert syngas ($CO+H_2$) obtained from carbon-containing sources (coal-biomass…) to heavy hydrocarbons that can be transformed by upgrading to lubricating oil or diesel fuel. Generally, the reaction is catalyzed using carbon or iron catalysts [17, 68]. Typical conditions for LTFT process include temperatures ranging from 180º to 260º, pressures higher than 25 bar, superficial gas velocities higher than 0.15m/s, and micron-sized cobalt or iron catalyst[69].

Consequently, it is highly essential to understand the effect of such extreme conditions on hydrodynamics and mass transfer to reach the proper design and scale-up of SBCR.

However, although interest was given recently to SBCR, the effect of high pressure and high temperature on hydrodynamics and mass transfer is not yet understood and is limited if compared to the studies carried out in ambient conditions. Only a few studies were interested in the simultaneous effect of high pressure and high temperature, and most of the researchers studied the impact of high pressure at ambient temperature or the impact of high temperature at high pressure[55, 70].

Overall, global hydrodynamic parameters such as gas holdup, bubble size and bubble size distributions are mostly investigated in the literature. Moreover, the volumetric liquid-side mass transfer coefficient is the mass transfer parameter studied.

The most important studies on hydrodynamics and mass transfer in SBCR at relatively extreme conditions are summarized in Table 2.3:

Table 2.3 Previous studies on hydrodynamics and mass transfer of SBCR

Author	Three-phase system	Reactor dimensions	Operating variables	Parameters investigated
Sehabiague et al.[68]	N_2/He mixture Molten reactor wax Iron-based catalyst	ID=5.8m	P (4-31bar) T (380-500K) U_g (0.1-0.3 m/s) C_S (0-45 wt %)	ε_g , d_{32}, k_la
Sehabiague and Morsi [69]	N_2/He mixture Paraffin mixture / light F-T cut / heavy F-T cut Alumina / Puralox alumina / spent iron oxides	ID=0.29m H=3m	P (8-30 bar) T (300 – 530 K) U_g (0.14-0.26 m/s) C_v (0-20 vol %)	ε_g, d_{32}, bubble size distribution, k_la
Behkish et al.[71]	N_2 & He Isopar-M Alumina powder	ID=0.29m H=3m	P (0.67-3 MPa) T (300 – 473 K) U_g (0.07-0.39 m/s) C_v (0-20 vol %)	ε_g, d_{32}, bubble size distribution.
Chilekar et al.[43]	Air & N_2 Demineralized water& Isopar-M organic oil Activated carbon & Silica	ID=0.15m H=1.4m	P (0.1 – 1.3 MPa) T_{amb} U_g (0-0.4m/s) C_v (0-3 vol %)	ε_g , k_la, $d_{b,avg}$, U_{gtrans}
Vandu et al.[72]	Air C_9-C_{11} paraffin oil Puralox (Al_2O_3)	ID=0.1	P_{atm} T_{amb} U_g (0-0.4m/s) C_v (0-25 vol %)	ε_g , k_la
Krishna et al. [73]	Air	ID=0.38	P_{atm}	ε_g

	Paraffin oil Silica		T_{amb} U_g (0-0.5m/s) C_v (0-36 vol %)	
Bukur et al.[55]	N_2 FT-300 paraffin wax / Arge wax / Mobil reactor wax Iron oxide / Silica	ID=0.05m &0.21m H=3m	Patm T up to 538 K U_g (0-0.15m/s) C_s (10-30 wt %)	ε_g
Deckwer et al.[74]	N_2 paraffin wax Al_2O_3	ID=0.04m &0. 1m	P up to 11 bar T=416 & 543 K U_g (0-0.04m/s) C_s (0-16 wt %)	ε_g , k_la

- **Effect of pressure:**

The effect of pressure has been investigated in the previous studies (Table 2.3), and accordingly, it was observed that gas holdup increases with pressure at all solid concentrations. This behaviour is related to the effect of pressure on gas density. More specifically, increasing pressure increases gas density and then gas-phase momentum, which increases the bubble breakup rate of large bubbles to small bubbles[68, 69].

It should be mentioned that the effect of gas density on decreasing bubble size by increasing bubble breakup rate can be explained by the Kelvin-Helmotz theory that describes the stability of the gas-liquid interface in response to wave-like disturbances. The theory states that a liquid-gas surface is unstable to a disturbance of k wave number and c velocity if $k^2c^2<0$ with $k^2c^2 = gk + \frac{k^3\sigma}{\rho_L} - k^2\frac{\rho_G}{\rho_L} \times \left(v_g - v_l\right)^2$ (2.32) [75]. The disturbance increases with $\exp\left(\sqrt{-k^2c^2}t\right)$ growth factor which explains the effect of increasing gas density that results in increasing instability in the gas-liquid interface of large bubbles and then causing high bubble breakup rates and then a higher number of small bubbles.

The increasing of small bubbles gas holdup due to high breakup rates was observed by Behkish et al.[71], who found that with increasing pressure, large bubbles gas holdup $\varepsilon_{g,large}$ was constant

whereas the total gas holdup increased. This means that increasing pressure increases small bubbles gas holdup $\varepsilon_{g,small}$ (Figure 2.19[71]).

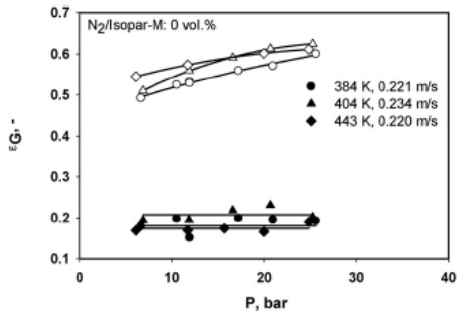

Figure 2.19 Effect of pressure on total and large gas holdups (plain: ε_g; solid: $\varepsilon_{g,\,large}$)[71]

For bubble Sauter mean diameter d_{32} and bubble size distribution, most of the findings are supporting the pressure effect. Thus, d_{32} decreases and the population of small gas bubbles increases with pressure [69, 71].

Moreover, the volumetric liquid-side mass transfer coefficient $k_l a_l$ was found to increase with pressure. This effect can be related principally to the increase of gas-liquid interfacial area with pressure. Thus, increased gas holdup and decreased d_{32} with pressure results in increasing gas-liquid interfacial area as $a = \frac{6\varepsilon_g}{d_{32}(1-\varepsilon_g)}$ (2.33)if a spherical shape for the bubbles is assumed [69].

For solid particles, it was found that the pressure effect on hydrodynamics and mass transfer was overshadowed by the high concentrations of solid particles (> 10 % vol).[71]

- **Effect of temperature:**

Most of the previous studies concluded that gas holdup increases with temperature. Hence this effect is related to temperature impact on liquid properties, especially viscosity and surface tension [68, 69, 71]. Thus, increasing temperature decreases liquid surface tension and then the cohesive forces between liquid molecules that maintain bubbles surface as a rigid spherical shape are reduced and then the bubble breakup rate is increased. Also, when viscosity decreases, bubble coalescence decreases and the number of small bubbles increases.

According to these findings, increasing temperature decreases $d_{32,}$ and the bubble size distribution is shifted to smaller diameters due to large bubble breakup.

However, the presence of particles seems to affect the conventional influence of elevated temperature on bubble size. Indeed, Sehabiague et al.[69] found that at c_v= 2% vol d_{32} increased with temperature. This effect was also observed by Behkish et al.[71] but at solid concentrations between 5 and 10% vol. They explained this effect by the fact that increasing temperature increases the number of small bubbles that will form clusters or froth. However, adding solid will increase the instability of the froth at the top of the liquid mixture. This will cause its destruction and will lead to more small bubble coalescence and then the increase of d_{32}. Sehabiague et al.[69] reported that unstable foam was observed in their system when using a small amount of solid up to 3%.

In another study, Chilekar et al.[43] stated that foaming is a characteristic of SBCR operating with lyophobic particles at elevated pressure. Sehabiague and Behkish didn't report the nature of their particles. All these findings lead us to ask about the effect of particles' properties on altering the effect of high temperature on hydrodynamics and mass transfer of SBCR, especially al low concentrations for which the slurry properties are not affected.

Another interesting finding can prove the importance of particles properties especially wettability on hydrodynamics and mass transfer: Sehabiague et al.[69] found that the gas holdup when using alumina (Al_2O_3) in heavy F-T cut is higher than the gas holdup when using iron oxide in heavy F-T cut with the same operating variables (23 bar pressure). However, the authors didn't explain this difference and concluded that alumina is different from iron oxide in terms of their effect on hydrodynamics without focusing on their intrinsic properties.

Regarding mass transfer, it was found that increasing temperature increases the gas-liquid interfacial area (a) due to gas holdup increase and d_{32} decrease and also increases k_l due to the increase of gas diffusivity D_{AB} with temperature[69].

CHAPTER 3 RESEARCH STRATEGY

3.1 Problem identification

Solid particles are generally used in slurry bubble column reactors as catalysts in many chemical and biological processes. Consequently, their presence greatly affects hydrodynamic and mass transfer parameters that determine the performance of such reactors. However, the presence of solid particles and their effect on hydrodynamics and mass transfer is a subject of debate in the literature.

The general trend adopted by most of the researchers is to treat the issue of solids' impact from a macroscopic scale. Hence, they consider that the liquid phase properties such as viscosity or density are affected by solids, then develop corrected quantities such as apparent viscosity or apparent density by considering the system as a gas-slurry two-phase system. The disadvantage of this approach is that the researchers who adopt it apply all the findings of gas-liquid bubbles columns in terms of hydrodynamic and mass transfer correlations and models to design and scale-up slurry bubble column reactors. However, except considering concentration and density, all the intrinsic properties of solids are neglected, which can render this approach very risky.

Moreover, considering the slurry bubble columns as a two-phase system in literature is attributed to high solid concentrations. However, it is not specified precisely at which concentration we can consider a two-phase system instead of a three-phase system or what are the parameters that determine this threshold concentration. Below this concentration, liquid properties are not altered, and the system is considered as a three-phase system. In this case, solid particles have an independent effect on bubble-particle adhesion, which determines the further behaviour of bubbles within the column. In literature, the value of this quantity ranges from 3vol% to 10vol% based on experimental findings. So, no agreement about a unique value leads to asking whether the three phases' intrinsic properties or the operating conditions that affect this threshold concentration.

Coalescence and breakup are hydrodynamic phenomena that determine bubble parameters viz. bubble size, bubble rise velocity and bubble radial and axial distribution. It should be mentioned that solids present in bubble column can have two distinct behaviours: They can collide or adhere to bubbles or either be present in the bulk liquid and then affect bubbles coalescence or breakup. Solid intrinsic properties that are believed to affect bubble-particle interaction or particles' presence

in the bulk liquid are particle size distribution and solid lyophobicity or lyophilicity. In literature, studies that are interested in the direct effect of lyophobicity/lyophilicity or particle size on coalescence and breakup are very scarce. Even less are perceived the physical mechanisms that underlie the type of this effect in bubble columns. Findings regarding the effect of solid particles on hydrodynamics and mass transfer are often ambiguous or even contradictory.

In addition, most of the investigations that are generally interested to bubble-particle interaction were conducted in stationary systems (flotation process – single bubble behaviour – antifoaming studies) in which particles are necessarily placed in the gas-liquid interface and probability of bubbles detachment from gas-liquid interface due to gravity or high shear rates is much less than the probability of bubble-particle collision and bubble-particle adhesion. However, in bubble columns, bubbles and particles are moving freely, and then bubble-particle interaction is different. Consequently, the effect of solid properties on bubble-particles interaction needs to be extensively investigated in the real conditions of slurry bubble columns.

The effect of solid properties and particle size distribution can be elucidated if local hydrodynamic parameters are studied. Bubble size, bubble chord length, bubble rise velocity and their radial and axial positions will give valuable information about bubble-particle interaction. The effect of solid on bubble dynamics in literature was only studied in high concentration systems. So far, the investigation of the effect of solid intrinsic properties on local hydrodynamic parameters and bubble dynamics is in its elementary stage, and more studies are needed to explore this effect.

In addition, models being used to design and scale-up of slurry bubble column reactors are too much simplified. Hydrodynamic and mass transfer phenomenological models and correlations don’t include the effect of solids intrinsic properties. In the models available, the solid effect is present by adding a concentration correcting factor to the models developed for two-phase systems. So, it is necessary to develop a reliable phenomenological model for hydrodynamics (gas holdup) and mass transfer that can be applicable to a variety of solid particles and experimental conditions.

Another interesting point is that slurry bubble columns generally operate at high pressures and high temperatures. Even less, the effect of solid intrinsic properties on hydrodynamics and mass transfer at these extreme conditions is not yet studied seriously, and only very few works were conducted in this field. Whereas the effect of temperature and pressure on liquid and gas properties that

directly affects hydrodynamics and mass transfer is progressing, the effect of such extreme conditions on solid intrinsic properties goes unnoticed.

3.2 Objectives

As already mentioned, there is a great need to have a complete understanding of the effect of solid-phase properties and operating pressure on hydrodynamics and mass transfer bubble column reactors. Thus, the main objective of this research work is *to investigate the hydrodynamics and mass transfer of two-phase and three-phase bubble column reactors.*

The following specific objectives are defined to achieve this main objective:

- Understand the simultaneous effect of particle size and solid concentration on the global hydrodynamics holdup of slurry bubble column reactors and develop a new correlation to estimate the total gas holdup. The aim is to improve the scaling-up and design of SBCR by taking into account the intrinsic properties of the solid phase
- Elucidate the physical impact of solid particles on the volumetric gas-liquid mass transfer coefficient $k_l a_l$ in slurry bubble column reactors
- Investigate the effect of pressure on the hydrodynamics of a pilot-scale bubble column operating with low and moderate-viscosity Newtonian liquids

3.3 Methodology

The experimental work of this research work was performed in two-different pilot-scale bubble columns. The series of experiments related to the first and second objectives were carried out at ambient pressure and ambient temperature in a 0.292 m diameter and 2.7 m height Plexiglas bubble column. The setup was adapted to handle the use of heavy solid particles. The series of experiments corresponding to the third objective were performed at elevated pressure and temperature in a stainless steel 0.152 m inside diameter and 4.8 m height bubble column. The strategy of the three-phase experimental work was to choose inert non-porous heavy solid particles in the micron size. Besides, the experimental plan was based on increasing the solid concentration step by step in order to explore all the potential phenomena that could occur by adding particles to a gas-liquid system. The most important achievement was to provide extensive and reliable experimental data on the effect of solid particles on global hydrodynamics and mass transfer. For the third objective, two

hydrocarbons with different range of viscosities were strategically chosen to give an insight into the effect of pressure on the global hydrodynamics. Several available measurement techniques such as differential and absolute pressure transducers, dissolved oxygen probe as well as several data processing methods were used to determine and interpret global gas holdup, regime transition points, bubbles classes, bubble size and gas holdup axial distribution. Moreover, one important part of this work was to introduce a novel phenomenological correcting factor for predicting the total gas holdup in three-phase systems.

3.4 Measurement techniques

3.4.1 Pressure transducers

Several phenomena can generate pressure fluctuations within SBCR. Thus, small bubbles generated by the gas distributor rise in the column and their size changes continuously as a result of coalescence and breakup phenomena. Also, bubbles drag liquid when rising, which results in macro-scale liquid circulations, which affects the trajectories of rising bubbles and also their breakup [76]. Besides, rising bubbles are erupting when they arrive at the liquid surface. Generally, pressure fluctuations are divided into global and local pressure fluctuations. Phenomena causing each type of those fluctuations are illustrated in Figure 3.1.

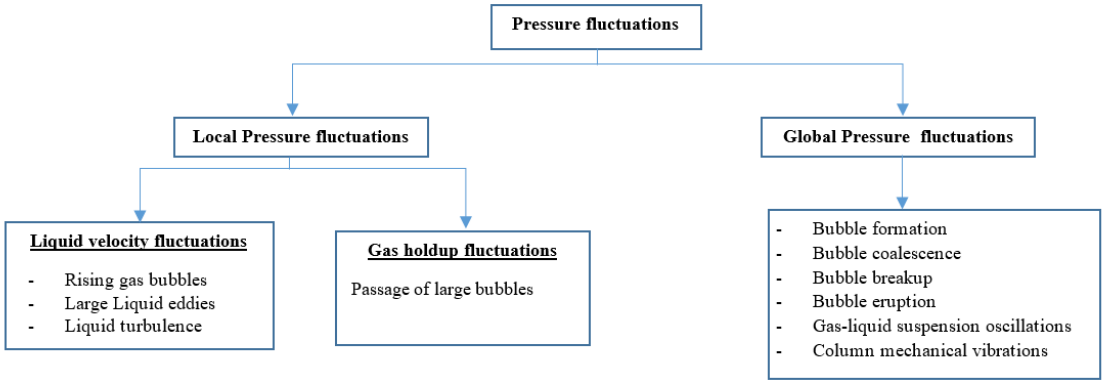

Figure 3.1 Pressure fluctuation sources in slurry bubble columns

Pressure measurement in slurry bubble column reactors is a non-invasive, simple, and inexpensive measurement technique that is used generally in lab-scale, pilot-scale and industrial-scale installations. The challenge with this measurement technique is the processing of pressure fluctuations signals and the differentiation between each fluctuation source within those signals.

3.4.1.1 Differential pressure transducers:

Differential pressure transducers (DPT) enable to determine gas holdup fluctuations in a three-phase flow by the following equation:

$$\frac{\mathrm{dP}}{\mathrm{dz}} = \left(\rho_g \varepsilon_g + \rho_l \varepsilon_l + \rho_s \varepsilon_s\right) g \tag{3.1}$$

Total gas holdup and its axial distribution in the bubble column are evaluated using the following equation:

$$\varepsilon_g = 1 - \frac{1}{\rho_l + C_v \times (\rho_S - \rho_l)} \times \frac{\Delta P}{g \Delta H} \tag{3.2}$$

With C_v is the volumetric concentration of solid particles

3.4.1.2 Absolute pressure transducers:

- **Statistical analysis of pressure time series:**

Analyzing pressure fluctuations in the time domain is generally based on the evaluation of signals amplitude[77]. The Standard deviation of the signal quantifies this evaluation.

The Standard deviation (SD) for N pressure sampling points is defined as:

$$\sigma = \sqrt{\frac{1}{N-1} \sum_{n=1}^{N} (P_n - \bar{P})^2} \tag{3.3}$$

With

$$\bar{P} = \frac{1}{N} \sum_{n=1}^{N} P_n \tag{3.4}$$

The passage of large bubbles is believed to be the phenomenon that causes pressure to diverge from its steady value. As generally known, the standard deviation is a measure of data set dispersion from its mean value (which corresponds to the steady-state of the column). Therefore, the standard deviation has a strong relation with bubble size in a specific region of the column.

- **Spectral analysis of the pressure time series:**
  - **Power spectral density:**

Power spectral density (PSD) is an analysis in the frequency domain. It characterizes the frequency content of the signal and displays the contribution of each frequency to the overall signal power [77]. One aim of spectral density analysis is to detect periodicities in the signal, which are represented by frequency peaks. Thus, each frequency peak corresponds to the phenomenon that dominates in the bubble column with a significant periodicity.

The pressure time series are converted from the time domain to the frequency domain by the discrete Fourier Transform [76]:

$$\mathcal{F}_x(f) = \frac{1}{T}\int_0^T P_x(t)e^{-2\pi ift}dt \quad (3.5)$$

The PSD of a pressure signal measured at position x in the column, $P_{xx}(f)$ is:

$$P_{xx}(f) = \frac{1}{f_s}\mathcal{F}_x(f)\mathcal{F}_x^*(f) \quad (3.6)$$

With f_s the sampling frequency of the signal and $\mathcal{F}_x^*$ the complex conjugate of $\mathcal{F}_x$.

PSD is an efficient tool to give an idea about the size of bubbles that are in the column. Esmaeili et al.[40] reported that small rising bubbles (4 mm) generate pressure fluctuations at high frequencies up to 50 Hz, whereas large rising bubbles (4-5 cm) generate pressure fluctuations at low frequencies (2-5 Hz). Hence, bubble properties and their behaviour can be characterized by the amplitude, dominant frequency and frequency distribution of the PSD curve[40]

To clearly show the utility of this analysis, we discuss the amplitude of a PSD curve obtained in a 2Dimension SBCR at different gas velocities and at a 83.5 cm height from the distributor, as reported by Chilekar et al.[76] and illustrated in Figure 3.2.

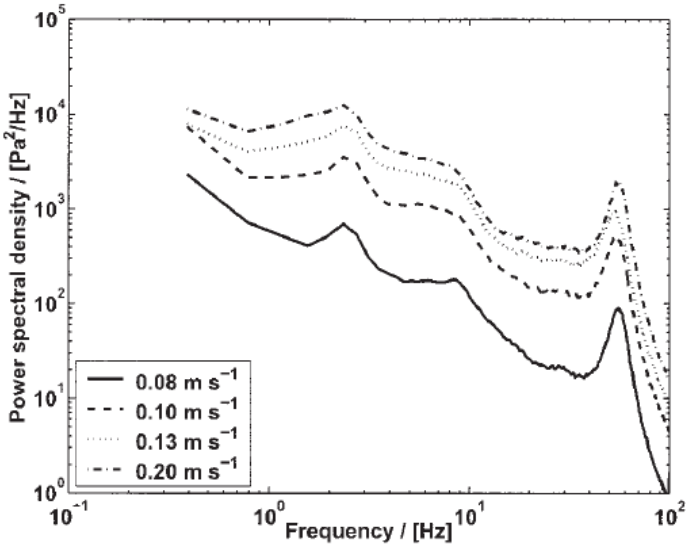

Figure 3.2 PSD curve of pressure time series at different gas velocities[76]

As can be seen from the curve, the overall power is low at low gas velocities due to the existence of smaller gas bubbles. At the homogeneous regime, small bubbles rise at low velocities and don't generate high power. When increasing gas velocity, the system goes toward the heterogeneous regime where larger bubbles are formed and generate higher power fluctuations. Also, in the same curve for one gas velocity, power is higher in the low frequencies region and is related to the existence of mainly large bubbles. Then, the power drops in the high frequencies region and is related to the existence of mainly small bubbles.

- **Bubble size estimation by signal decomposition method:**

This method is explained in detail in the experimental procedure of chapter 5.

3.4.2 Dynamic gas disengagement technique

Dynamic gas disengagement technique (DGD) is a measurement technique used to study bubble classes, bubble holdup structures and bubble rise velocities[12]. The principle of the technique is based on plotting the dispersion height drop when the gas flowing at a certain velocity is suddenly shut off. The main assumption characterizing this technique is that large bubbles have high rise velocities and then disengage first after shutting-off the gas. Small bubbles have lower rise velocities and disengage afterwards [71]. More precisely, when faster large bubbles are disengaging, the drop of the gas holdup is very fast. After the large bubbles have disengaged, small

slow bubbles will disengage, and the rate of drop of gas holdup will be lower, as illustrated in Figure 3.3.

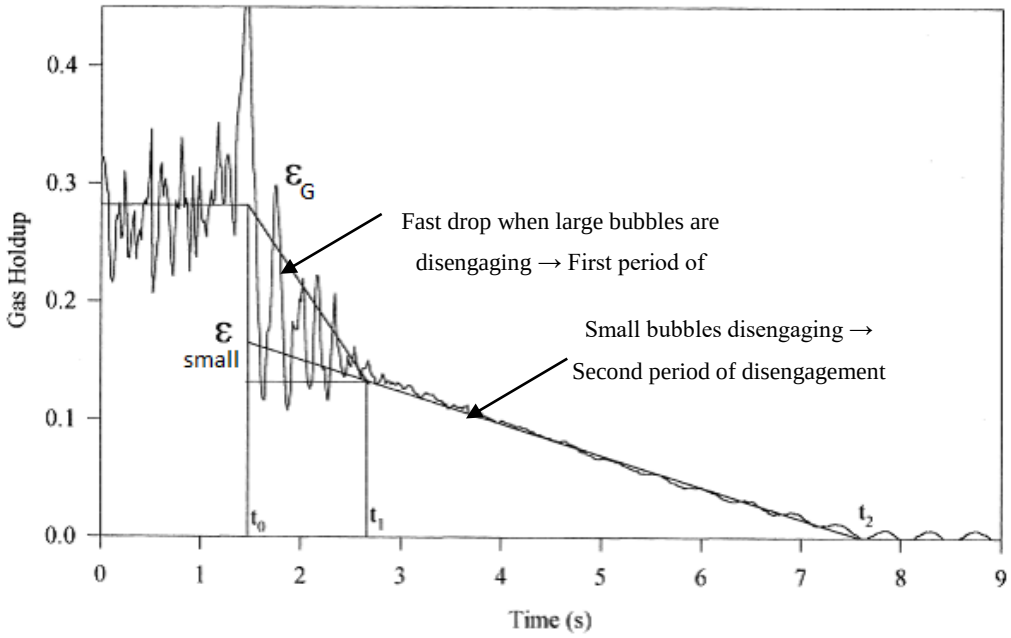

Figure 3.3 Typical gas holdup drop for a specific velocity in the DGD technique. Modified from reference[78]

This technique enables to determine the contribution of each of the two classes of bubbles (small and large) on the total gas holdup. Hence, it permits to provide a large amount of information about the effect of operating variables on each bubble class.

It should be mentioned that the DGD technique applied in SBCR is based on several assumptions:

- During disengagement, bubble interactions don't affect the gas holdup structure.
- The gas holdup has a uniform axial profile.
- Solid concentration within slurry remains constant during gas disengagement.

The large bubbles gas holdup is then calculated from the small bubbles gas holdup as follows:

$$\boldsymbol{\varepsilon_{large} = \varepsilon - \varepsilon_{small}} \quad (3.7)$$

Where ε_{small} is the small bubbles'gas holdup determined from the disengagement curve as depicted in Figure 3.3

and ε is the total gas holdup under the chosen steady-state gas velocity at the start of the disengagement experiment.

3.4.3 Dissolved oxygen optical probe (Visiferm DO325)

The dissolved oxygen probe is used to measure the volumetric gas-liquid mass transfer coefficient $k_l a_l$. The principle of measurement is called oxygen-dependent luminescence quenching.

3.4.3.1 Oxygen-dependent luminescence quenching principle

The principle is explained in more detail in Chapter 5

3.4.3.2 Experimental procedure

The measurement of the volumetric liquid-gas mass transfer ($k_l a_l$) is performed by the dynamic oxygen absorption technique by considering the use of the saturation method. This method is discussed in more significant detail in Chapter 5.

3.5 Thesis organization

The present chapter contains the problem under investigation, the objectives of the research work, the methodology as well as the used measurement techniques. Chapter 2 presents an extensive literature review on bubble column applications, the fundamentals of bubble-particle interaction in slurry bubble column reactors, a description of hydrodynamic and mass transfer aspects in bubble columns, and critical review on the recent advances in investigating the effect of solid particles' presence and the high pressure and high temperature on bubble properties. Chapter 4 provides an insight into the simultaneous effect of particle size and solid concentration on the global hydrodynamics of slurry bubble column reactors. Chapter 5 is dedicated to elucidating the impact of solid particles' presence on the volumetric gas-liquid mass transfer coefficient $k_l a_l$. Chapter 6 explains the effect of increasing pressure on the total and axial gas holdup distribution for two hydrocarbons with low and moderate viscosity liquids. Besides, each chapter contains a specific literature review on the related subjects. Chapter 7 includes a general discussion on the different

results obtained during this research work. Finally, a brief conclusion and recommendations for future researches on the topic are given in chapter 8.

CHAPTER 4 ARTICLE 1: SIMULTANEOUS EFFECT OF PARTICLE SIZE AND SOLID CONCENTRATION ON THE HYDRODYNAMICS OF SLURRY BUBBLE COLUMN REACTORS

El Mahdi Lakhdissi [1], Iman Soleimani [1], Christophe Guy[2], Jamal Chaouki[1,*]

[1]Dpt. of Chemical Engineering, École Polytechnique de Montréal, P.O. Box 6079, St. C.V., Montréal, Qc., Canada H3C 3A7

[2] Dpt. of Chemical & Materials Engineering, Gina Cody School of Engineering & Computer Science, Concordia University, 1455 Boulevard de Maisonneuve W., Montréal, Qc., Canada H3G 1M8

*Corresponding author: jamal.chaouki@polymtl.ca;

(Published in American Institute of Chemical Engineers (AIChE) journal, DOI: 10.1002/aic.16813)

Abstract:

The simultaneous effect of particle size and concentration on the total gas holdup of slurry bubble column reactors was investigated in this work. The total gas holdup was measured for air-water-glass beads systems. Three solid concentrations (up to 5%) and three particle diameters (up to 256 µm) were used. It was found that increasing particle size at high constant concentration decreases gas holdup. Moreover, increasing solid concentration decreases gas holdup and this decreasing effect is higher for larger particles. Also, solid particles have two effects on hydrodynamics, namely changing the viscosity and density of the liquid phase as well as hindering the bubbles from rising within the column by the collision phenomenon. Therefore, a new correcting factor was introduced to correct the gas holdup. The hindering factor considers both the collision efficiency affected by the particle size as well as the solid concentration. A novel correlation was developed to predict the experimental data of the three-phase gas holdup.

Keywords: slurry bubble column, hydrodynamics, particle size, solid concentration, collision efficiency, dimensional analysis

4.1 Introduction

Slurry bubble column reactors (SBCR) have widespread applications in chemical, petrochemical, biochemical and environmental processes[79-81]. Indeed, SBCR are one of the most preferred reactors to conduct a multitude of well-known industrial applications, namely Fischer-Tropsch synthesis (FT)[82], catalytic chlorination of alkenes[80] and the hydroconversion of petroleum residues and heavy oils[83]. They are characterized by their low maintenance and operating costs and the absence of mechanically moving parts. Almost all the applications of SBCR are based on catalytic reactions where solid particles – catalyst – are suspended in a gas-liquid system. Several works were interested to determine the successful method for the design and scaleup of SBCR. The critical points in the scaleup are hydrodynamics and mixing[84]. Hence, it is important to maintain the same hydrodynamic parameters and mixing patterns when we extrapolate the lab scale unit to the industrial scale unit. This will make it possible to obtain the same performance as the small unit in terms of conversion and selectivity[84]. Therefore, hydrodynamics, in addition to kinetics, are the key parameters to successfully design and scaleup SBCR. However, if the effect of the solid catalyst nature and its amount on the intrinsic kinetics and the conversion respectively has been tackled by many researchers[85], the understanding of its influence on gas and liquid flow behaviours is still an object of debate.

There are two general approaches to view the problem of adding solid particles to a gas-liquid system. The first one is called the two-phase approach and considers that solid particles are homogeneously mixed with the liquid phase and then form a slurry or pseudo-homogeneous phase. Therefore, all theories and models developed for hydrodynamics and applicable for the gas-liquid system can be used for three-phase systems. This approach was adopted by several authors[1, 2]. Rabha et al.[86] considered that this approach could only be applicable for particles having a Reynolds number Re_p lower than 0.3 and, then Stokes law is still relevant. However, they stated that by using large particles with a Reynolds number Re_p higher than 0.3, we could not neglect the effect of solid particles on the gas-liquid flow. The second approach is called the three-phase approach. It considers that the three phases (gas-liquid-solid) should be studied separately and then we should include the properties of each phase in the developed models and correlations. Rabha et al.[86] were one of the few authors who brought up the importance of the three-phase approach. They found that the structure of the gas flow in a three-phase system is profoundly different from

a solid-free two-phase system even if the apparent viscosity of the former and the liquid viscosity of the latter were the same. They reported that bubble coalescence is more pronounced in the presence of solid particles and concluded that the use of the two-phase approach is not reliable for relatively large particles (50 µm, 100 µm, and 150µm). However, Krishna et al.[2] reported that for highly concentrated slurries (40% v/v) and small particles (38 µm), using highly viscous liquid could predict the gas holdup of the three-phase system.

Consequently, it is of prime importance to determine when we can apply each of the two approaches. Also, if we target the use of the three-phase approach, we should pinpoint which solid properties more significantly affect the hydrodynamics of bubble columns. Hence, we should thoroughly investigate the effect of particle size, shape, degree of wettability and density as well as concentration to clearly understand the interaction between gas, liquid and solid. For instance, we can combine the effect of particle size with the effect of one of the other parameters, such as solid concentration, superficial gas velocity or liquid properties[87].

4.1.1 Effect of increasing solid concentration on the global gas holdup

Investigating the effect of solid concentration on gas holdup was done by many authors[73, 78, 88-91]. The common finding is that increasing solid concentration decreases gas holdup and then increases bubble size. Sasaki et al.[89] found that, for 100µm of porous hydrophilic silica particles, gas holdup decreases with increasing concentration up to 40% v/v and it is independent for larger concentrations. They justified this effect by the findings of Ojima et al.[58] who found that increasing solid concentrations enhances bubble coalescence. In another work, Li et al.[78] investigated the influence of solid concentration on the gas holdup due to small and large bubble populations by using the dynamic gas disengagement technique (DGD). For an air-water-glass beads system of 35µm and a concentration up to 40%v/v, they reported that increasing the solid concentration has more effect on decreasing small bubble gas holdup compared to large bubble gas holdup. They attributed this effect to enhancing small bubbles coalescence. Indeed, small bubbles are more willing to coalesce with each other compared with large bubbles that are close to the maximum stable bubble size before breakage. In agreement with Li et al.[78], Krishna et al.[73] reported that increasing solid concentration affects the gas holdup related to the dense phase more (liquid – particles – small bubbles) by enhancing small bubbles coalescence. In contrast, particles

don’t affect the gas holdup of the dilute phase (big bubbles). Wu et al.[90] showed, by using local measurements based on a four-tip optical fiber probe, that increasing 75μm alumina particles loading from 9% to 25% v/v decreases local gas holdup, bubble frequency, and bubble surface area and increases bubble chord length significantly. They explained this effect by the two-phase approach in which the increased apparent viscosity of the slurry enhances bubble coalescence. However, they found that bubble rise velocity changes slightly with the concentration, although increasing solid loading increases the bubble size (average bubble chord length) significantly. As generally believed, a larger bubble must have a larger rise velocity. This finding brings about the question of the additional impact of particles on bubble flow independently of their effect on the apparent viscosity of the slurry. In their work, Gandhi et al.[91] attributed the decrease of the gas holdup of the 35μm glass beads-air-water system at high concentrations (up to 40% v/v) to the decrease of the bubble breakup rate. Rabha et al.[88] reported that by increasing the solid concentration from 5% to 36% for 100μm glass particles, solid particles have a dual effect on gas holdup. They showed that at low concentration, bubble coalescence is enhanced while at large concentrations, bubble breakup is enhanced. They explained the apparition of the bubble breakup regime by the increase of bubble-particle interaction at large concentrations. However, despite the advanced, ultrafast electron beam X-ray tomography used, their work was performed in a small diameter column and they concluded that more experimental work should be done at larger diameter columns with small increments of concentrations. This will enable taking into consideration the same hydrodynamics as a real system, avoiding wall effects and investigating at which concentration we have the increase of gas holdup by solid particles or whether this effect is only a feature of small columns. The common observation about all the above reported works is that they didn’t provide enough scientific explanation about why increasing solid concentration enhances bubble coalescence except the increase of the apparent viscosity of the slurry phase considered as a pseudo viscous phase. However, solid particles have their intrinsic effect on bubble behaviour and this was shown by the findings of Wu et al.[90] and Rabha et al.[86].

4.1.2 Effect of particle diameter and solid concentration on the global gas holdup

In literature, the effect of particle size and concentration on the hydrodynamics of slurry bubble columns is scarce and several conflicting results have been found. Hence, the effect of particle diameter on global hydrodynamics and especially total gas holdup was reported by only a few

authors[1, 58, 87, 92-94]. Rabha et al. [87] investigated the effect of particle size and solid concentration on the hydrodynamics of a 0.07m diameter bubble column at a very low superficial gas velocity (up to 5cm/s). They found that the average gas holdup is independent of particle size and solid concentration when the diameter is below 100 µm and mass concentration is below 3%. In contrast, at larger diameters and solid concentrations, they observed that the average gas holdup decreases significantly with increasing particle size and solid concentrations. They stated that, by increasing particle size and concentrations more bubbles are covered by the solid and the remaining solid increases the apparent viscosity of the liquid phase. The increased viscosity subsequently enhances bubble coalescence. However, they didn't report the effect of the solid present on the bubble surface on the gas flow behaviour and which of the parameters (particle size or concentration) affects the gas holdup more. In addition, they only observed the homogeneous and slug flow regimes in their work, while the heterogeneous flow couldn't be reached [86]. A similar trend has been reported by Kim et al.[93] and JamialAhmadi and Muller-Steinhagen [54] who reported that gas holdup decreases when particle size increases. On the contrary, Ojima et al.[58] found that decreasing particle size and increasing solid concentration enhance bubble coalescence and then decrease gas holdup. They related this effect to the fact that decreasing particle diameter increases particle number density in the liquid film surrounding the bubble. Consequently, the liquid film will have a finer and more fragile porous-like structure at which point the critical film thickness before rupture increases, which enhances bubble coalescence. The authors were among the few researchers who studied the microscopic effect of the particles on bubble behaviour by measuring the time elapsed between the first contact between two bubbles and film rupture. They also stated that the contact between bubble interface and particles is a local phenomenon and doesn't depend on the macroscopic behaviour of the bubble-particle interface. However, the use of hydrophilic particles in their work couldn't result in a high presence of particles in the liquid surrounding the bubble but, on the contrary, particles were preferably present in the continuous liquid phase. Also, their experiment was based on a single-hole gas injector and rectangular 2D and 3D bubble columns, which is not relevant to the real columns. In another work, Li et al.[94] reported that changing glass beads particle size from 11µm to 93µm has no effect on the total gas holdup. Kara et al.[1] found that increasing particle from 10µm to 70 µm decreases gas holdup, but they stated that the reason of this effect is still unknown. From the literature, we can observe that

there is no strong scientific understanding of the effect of particle size and concentration on the total gas holdup in SBCR.

Therefore, in the present study, the main objective was to experimentally investigate the simultaneous effect of particle size and concentration on the global hydrodynamics of a pilot-scale SBCR. We then developed using a new approach a model that can predict global gas holdup by including the appropriate parameters directly affected by particle size and concentration.

4.2 Experimental procedure

4.2.1 Experimental setup and materials

The experimental work was conducted in a Plexiglas bubble column of 2.61m height and 0.292m inside diameter. The gas phase is oil-free compressed air, the liquid phase is tap water and the solid phase is glass beads. Air was injected into the system through a perforated plate distributor. The latter consists of 94 holes with 1mm orifice diameter and 1400 holes/m^2 density. The column has two rotameters (King Instrument), with which the air flow rate can be adjusted, and the entire superficial gas velocity range can be covered (0 – 0.25 m/s). This range was chosen to perform experiments in both homogeneous and heterogeneous regimes. The slurry phase (water – glass beads) operated in batch mode and the initial slurry level without aerating was set to 1.1m before each experiment. Regarding the solid phase, non-porous hydrophilic glass beads particles with three mean diameters (35µm - 71µm - 156µm) were used. Experiments were conducted, in addition to a solid-free system, for three initial solid volume fractions C_v (1% v/v – 3% v/v – 5% v/v). These low values were chosen to work with small increments of concentrations. The properties of the glass beads solid phase are summarized in Table 4.1.

Table 4.1 Glass beads properties

Solid nature	10% Finer than	Mean diameter (µm)	90% Finer than	Density
Hydrophilic glass beads	18 µm	**35 µm**	60 µm	2500 kg/m^3
	59 µm	**71 µm**	85 µm	
	125 µm	**156 µm**	192 µm	

A schematic of the bubble column setup is shown in Figure 4.1

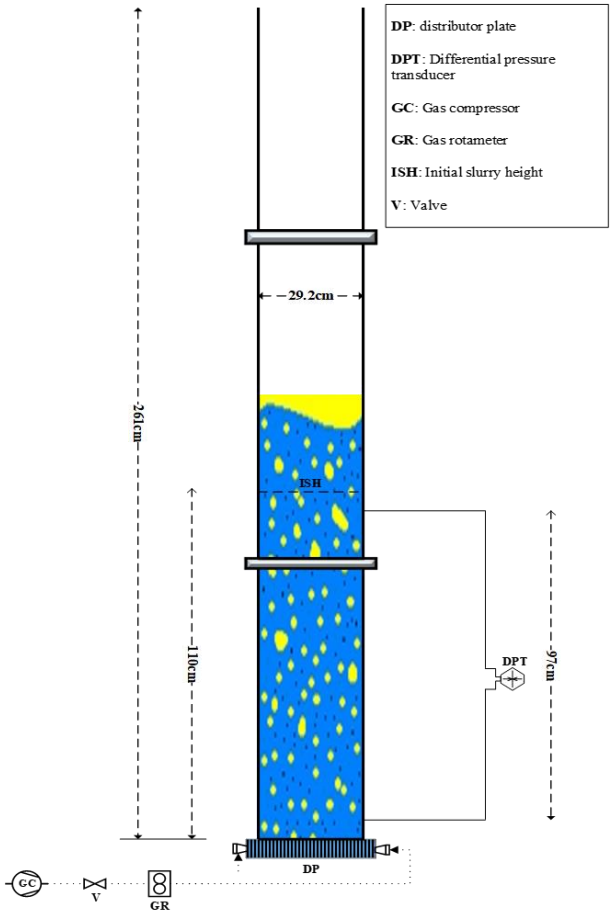

Figure 4.1 schematic of slurry bubble column setup

4.2.2 Measurement techniques

The measurement technique used is a JUMO dTRANS p20 DELTA differential pressure transducer DPT. The specifications of the DPT are summarized in Table 4.2.

Table 4.2 Specifications of JUMO differential pressure transducer

Measuring input range	0 to 240 mbar
Accuracy as % of the Full scale	0.1%
Output range	4 to 20 mA
response time T_{60} without damping	≤ 190ms

This technique is based on measuring the differential pressure between two levels that delimit a certain zone in the column. As it is used to measure the gas holdup within the measuring zone, the DPT was set-up in a way to cover the entire bubble column system. The difference between the levels was set to 97cm. The bottom leg of the transducer was installed 4cm above the distributor plate.

Gas holdup in the bubble column can be related to the pressure gradient in the measuring zone by the following equation[78]:

$$\varepsilon_g = 1 - \frac{1}{\rho_l + C_v \times (\rho_S - \rho_l)} \times \frac{\Delta P}{g \Delta H} \tag{4.1}$$

We used the same data acquisition card (National Instrument, PCI6023E) and LabVIEW software used in the work of Esmaeili et al.[40] to record the data. We recorded pressure times series for 180s at the 512 Hz frequency. We repeated experiments three times and each experiment was performed with a new slurry batch. The average of the three readings is used to present our hydrodynamic results.

A quick-closing valve was installed to perform the dynamic gas disengagement technique (DGD). It's a measurement technique used to study bubble classes, bubble holdup structures and bubble rise velocities[12]. Its principle is based on plotting the dispersion gas holdup drop when the gas flow at a certain velocity is suddenly shut off. The main assumption characterizing this technique is that large bubbles have high rise velocities and then disengage first after shutting-off the gas.

Small bubbles have lower rise velocities and disengage afterwards [71]. More precisely, when faster large bubbles are disengaging, the drop of the gas holdup will be very fast. In our experimental procedure, we ran the system for 30 seconds and at t=30s we shut-off suddenly the gas and recorded the time dependent differential pressure by the same transducer we used to measure the total gas holdup.

4.3 Results and Discussion:

4.3.1 Effect of increasing particle diameter at constant concentration

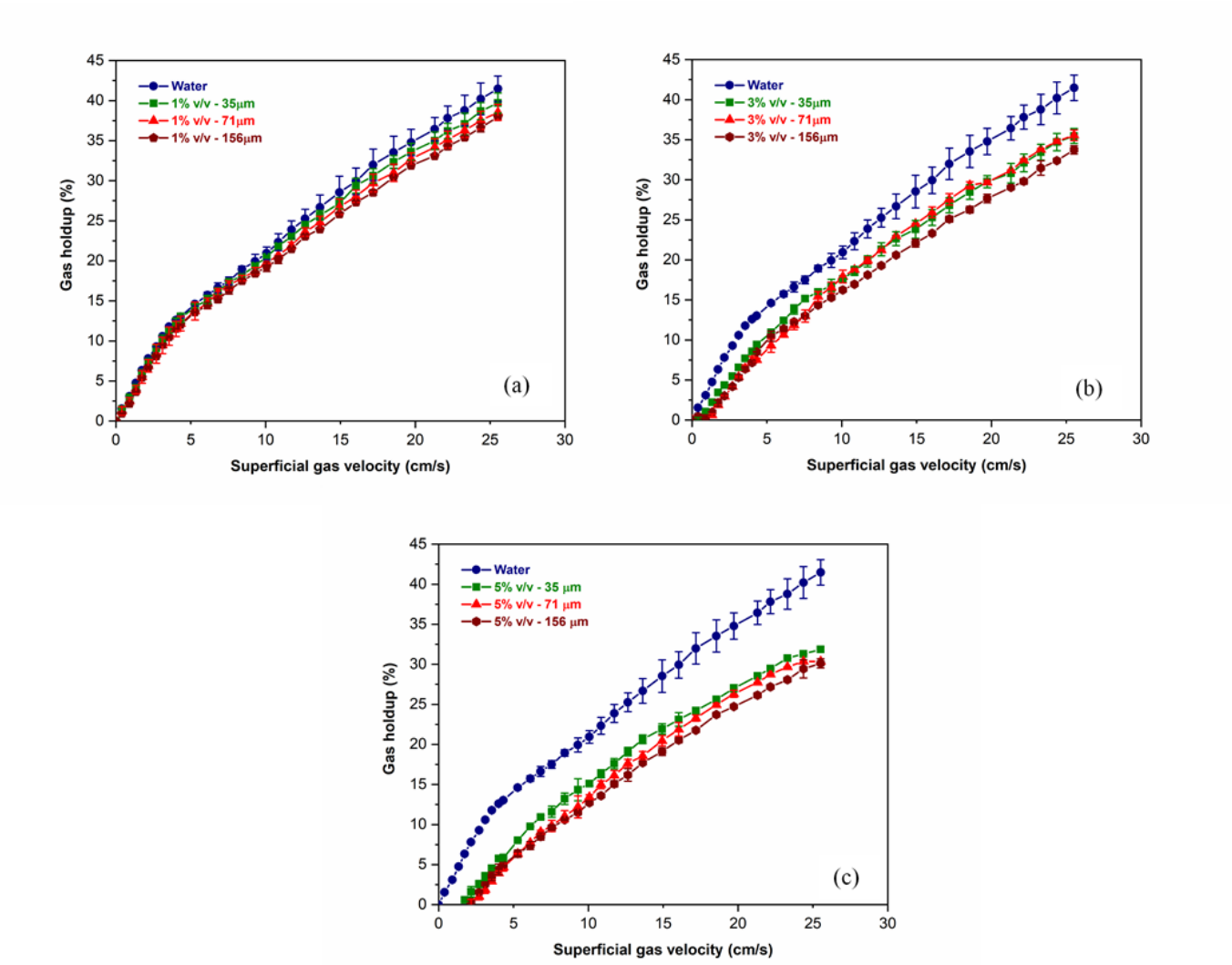

Figure 4.2 Effect of increasing particle size on total gas holdup at constant concentration: a) 1%v/v b) 3%v/v c) 5%v/v (Error bars represent the standard deviation of three gas holdup experimental values)

Gas holdup or gas voidage is one of the key hydrodynamic parameters in SBCR; it was experimentally obtained by the pressure transducer. Figure 4.2 shows the influence on total gas holdup of increasing particle size and superficial gas velocity at constant concentration. As a first observation, adding solid particles decreased gas holdup for all concentrations and particle sizes if

compared with an air-water system, which agrees with the findings of the other works[73, 90, 94]. The second observation is about the flow regime prevailing in the SBCR as a function of superficial gas velocity, particle size and concentration. It is worth mentioning that we can generally observe two flow regimes in a bubble column. The first one is called the homogeneous or bubbly flow regime. This regime generally prevails at low superficial gas velocities and bubbles are small and have narrow size distribution. The second regime is called the heterogeneous or churn turbulent regime. This regime prevails at high superficial gas velocities. Also, the onset of bubble coalescence and breakup phenomena is due to increasing turbulence within the system as well as high liquid circulation. Hence, small and big bubbles appear and result in a wide bubble size distribution[18]. Many parameters can affect the occurrence of one of those regimes[40]. We can determine at which regime we are operating by analyzing the global gas holdup vs superficial gas velocity curve. Indeed, for a simple air-water system, the increase of gas holdup as a function of superficial gas velocity is almost linear at low velocities and non-linear at high velocities[18]. Therefore, the change of slope in the global gas holdup curve determines the transition point from the homogeneous to the heterogeneous regime. From Figure 4.2a we can notice the presence of both homogeneous and heterogeneous regimes by a clear change in the slope (The transition velocity is about 5cm/s). However, when we increased concentration to 3% and 5%, no change of slope could be clearly defined, and we can conclude that only the heterogeneous regime was prevailing even at low superficial gas velocities (lower than 5cm/s). The early onset of the heterogeneous regime is attributed to the enhanced bubble coalescence due to high solid concentration. The third observation is about the effect of particle size. At very low concentrations (1%v/v and 3%v/v), the effect of particle size on gas holdup was not significant (Figure 4.2a, Figure 4.2b). However, at 5%v/v, we observed that increasing particle size decreased gas holdup (Figure 4.2c). Also, the effect of particle size on decreasing gas holdup prevailed at higher velocities. For instance, Figure 4.2c shows that changing particle size had no effect on gas holdup at very low velocities. This means that changing particle size influenced bubble coalescence and breakup phenomena occurring at high velocities. The decreasing effect of particle size agrees with the findings of Rabha et al.[87] who found that at low concentration (1% and 3%), the effect of particle size (50 µm, 100 µm and 150 µm) on radial gas holdup is not significant. At 5%, they found that increasing particle size decreases gas holdup due to large bubbles formation. The difference is that

our work was performed with a relatively large diameter bubble column and wide range of superficial gas velocities.

4.3.2 Effect on increasing solid concentration at constant diameter

Figure 4.3 shows the effect on gas holdup of increasing solid concentration at constant particle diameter. The decreasing effect of solid concentration agreed with most of the findings of other authors. In addition, increasing solid concentration for one particle size (Figure 4.3c for 156μm for instance) shows the early onset of the heterogeneous regime. Also, the interesting finding is that the decreasing effect of solid concentration on gas holdup was more pronounced at a larger particle size. For instance, at 15cm/s superficial gas velocity, increasing solid concentration from 3%v/v to 5%v/v decreased gas holdup by 15% for 156μm but only by 9% for 71μm. Consequently, the effect of solid concentration could not be separated from the effect of particle size.

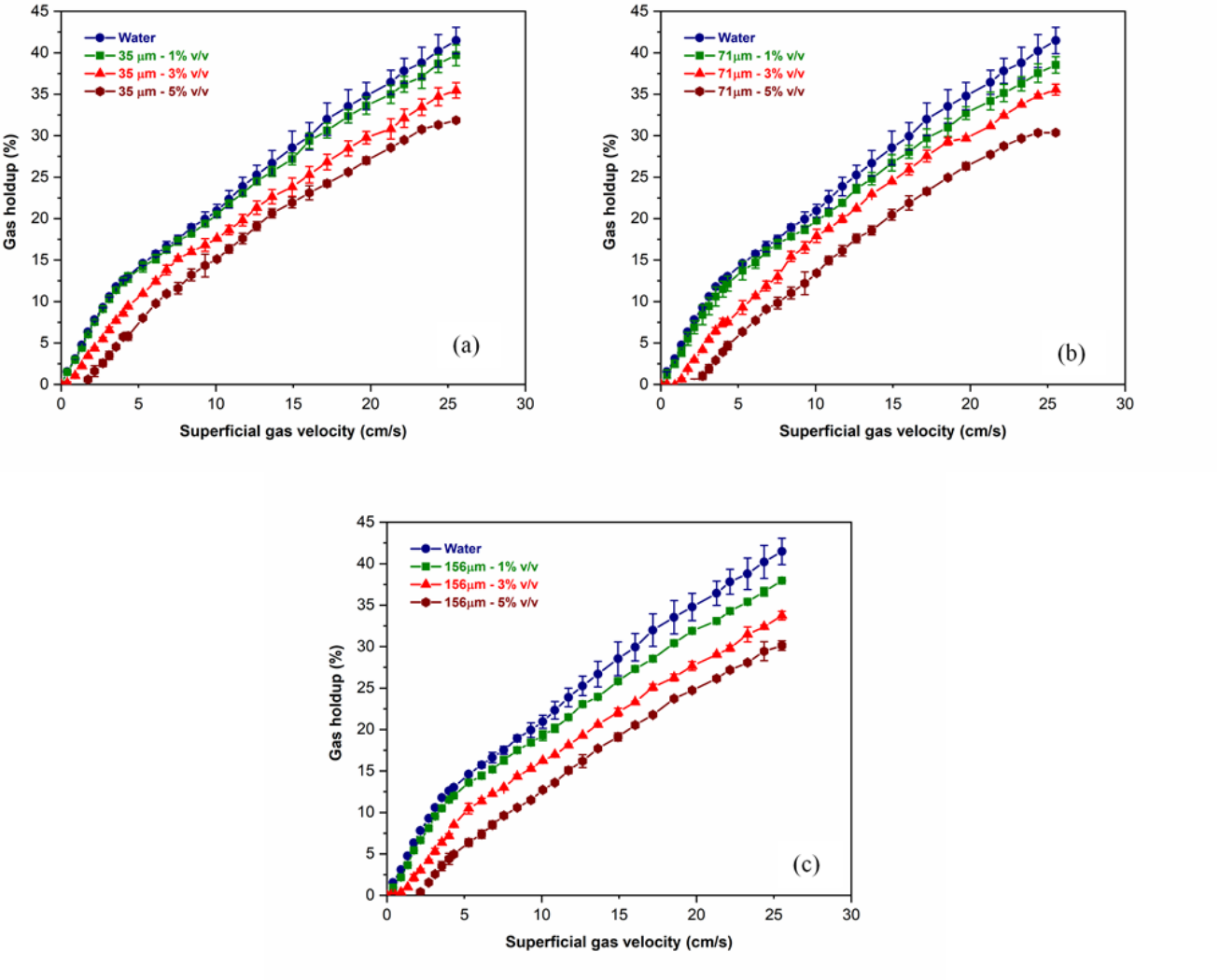

Figure 4.3 Effect of increasing solid concentration on total gas holdup at constant particle size: a) 35µm b) 71µm c) 156µm (Error bars represent the standard deviation of three gas holdup experimental values)

4.3.3 Verification of the applicability of the two-phase approach on the experimental gas holdup data

To prove that solid particles have an additional effect on bubble flow besides their effect on changing liquid viscosity, we compared the experimental gas holdup data with the gas holdup predicted by the two-phase approach.

The first step was to develop a correlation that could predict the total gas holdup in an air-liquid system (two phases) for the same operating conditions as our work. To do so, we used the gas holdup points that we obtained experimentally for the air-water system in our bubble column as well as the gas holdup data obtained in the same setup by Esmaeili et al.[40]. They performed their experiments with eight different liquids (Carboxymethyl Cellulose (CMC): 0.3; 0.5 and 0.7 wt.% in water, Xanthan Gum 0.3; 0.5 and 0.7 wt.% in water, Boger fluid and Glucose). The physical properties of these liquids can be found in their work. Then we performed a dimensional analysis to include all the properties and operating conditions in the developed model.

The observations made during the experimental work led to consider seven physical variables (k=7) to predict gas holdup. These variables include the operating conditions and properties of gas and liquid phases i.e.,

$$\varepsilon_g = f\left(U_g, g, D_c, \rho_g, \rho_l, \sigma_l, \mu_l\right) \tag{4.2}$$

Where $U_g, g, D_c, \rho_g, \rho_l, \sigma_l,$ and μ_l are superficial gas velocity, gravitational acceleration, bubble column diameter, gas density, liquid density, liquid surface tension and liquid viscosity respectively.

The physical variables are a function of three physical dimensions (r=3), namely mass (kg), length,(m), and time (t), and then, according to Buckingham's π theorem, we needed to determine $\pi' = k - r = 7 - 3 = 4$ dimensionless numbers to calculate gas holdup[95].

The four independent dimensionless numbers found were:

$$\pi_1 = \frac{U_g}{\sqrt{gD_c}} \quad \pi_2 = \frac{gD_c{}^2\rho_l}{\sigma_l} \quad \pi_3 = \frac{gD_c{}^3\rho_l{}^2}{\mu_l{}^2} \quad \pi_4 = \frac{\rho_g}{\rho_l} \tag{4.3}$$

The first dimensionless number is Froude number (Fr), the second is Bond number (Bo), the third is Galilei number (Ga) and the last is the ratio of gas density to liquid density.

Therefore, the gas holdup for an air-liquid two-phase system was expressed as follows:

$$\varepsilon_g = a_1 \times \left(\frac{U_g}{\sqrt{gD_c}}\right)^{a_2} \times \left(\frac{gD_c{}^2\rho_l}{\sigma_l}\right)^{a_3} \times \left(\frac{gD_c{}^3\rho_l{}^2}{\mu_l{}^2}\right)^{a_4} \times \left(\frac{\rho_g}{\rho_l}\right)^{a_4} \tag{4.4}$$

We used the Genetic Algorithm function (GA) in MATLAB to determine the constants of equation (4.4) by fitting 167 gas holdup points.

The final form of gas holdup correlation in a two-phase air liquid-system was:

$$\varepsilon_g = 0.45 \times Fr^{0.69} \times Bo^{0.19} \times Ga^{0.03} \times \left(\frac{\rho_g}{\rho_l}\right)^{0.23} \quad (4.5)$$

$$0.0023 \leq Fr \leq 0.15$$

$$10801 \leq Bo \leq 14620$$

$$1.015 \times 10^{7} \leq Ga \leq 2.42 \times 10^{11}$$

$$9.43 \times 10^{-4} \leq \frac{\rho_g}{\rho_l} \leq 1.227 \times 10^{-3}$$

The mean absolute percentage error (MAPE), standard error (SE), and 95% confidence interval of the fitting were 7.65%, ±1.6% and ±3.17%, respectively.

After the development of the two-phase system gas holdup correlation, we compared the experimental gas holdup $\varepsilon_{g,exp}$ for a three-phase system with the prediction of the two-phase approach $\varepsilon_{g,2\varphi}$. It should be mentioned that $\varepsilon_{g,2\varphi}$ was calculated by equation (4.5) by changing ρ and μ to slurry density ρ_{slurry} and slurry viscosity μ_{slurry} respectively. Also, the addition of solid particles doesn't affect, in general, the liquid surface tension according to Brian and Chen[96].

μ_{slurry} was calculated by the correlation of Saxena and Chen[97]:

$$\mu_{slurry} = \mu_{liquid} \times (1 + 4.5 \times C_v) \quad (4.6)$$

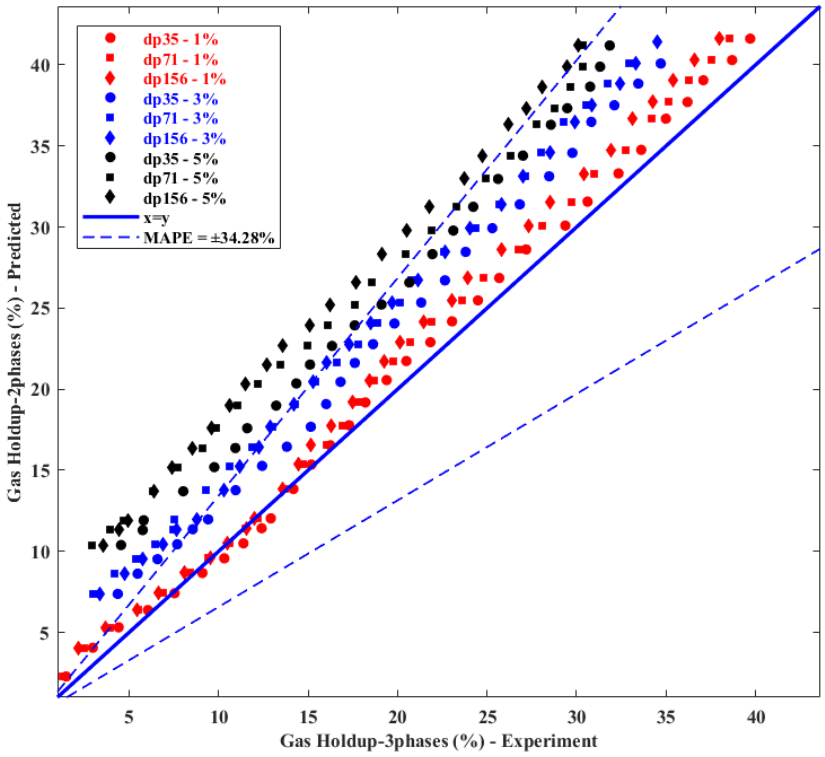

Figure 4.4 Comparison between the experimental and the predicted value of gas holdup by the two-phase approach

Figure 4.4 shows the comparison between the gas holdup predicted by the two-phase approach and the gas holdup obtained experimentally for the three solid concentrations and the three particle sizes used. We can clearly observe that the two-phase approach overestimated gas holdup with an average MAPE of 34.28%. Also, the error increased when we increased the solid concentration and particle size. Therefore, gas holdup in a slurry bubble column could not be predicted by simply correcting liquid viscosity and density. This finding is in agreement with the work of Rabha et al.[86]. Based on this result, solid particles have two different types of effect on the gas-liquid system. The first effect is changing the properties of the liquid phase. Indeed, by adding particles, a new slurry phase with corrected viscosity and density is formed. An additional effect decreases gas holdup to a larger extent than predicted by the two-phase approach. Also, this additional effect is more significant when increasing concentration and particle size. Hence, the lowest error is obtained in the case of 1% and 35µm particles.

4.3.4 The additional effect of solid particles on bubble behaviour

4.3.4.1 Collision Efficiency E_c

In addition to the bubble column field, froth flotation is an industrial process in which bubble-particle interaction takes place. In the aim to selectively separate valuable hydrophobic particles from hydrophilic gangues, air bubbles are fed to the flotation cell to capture particles and drive them to the froth zone. Hence, three main subprocesses control the performance of the flotation process. The first one is called the collision subprocess in which a particle approaches and collides with an air bubble. After the collision, the contact between bubble and particle will result either in attachment or driftage of the particle. This step is called the attachment subprocess. The third subprocess is called the stability of the bubble-particle aggregate against the detachment forces in the flow field. Attachment forces between the particle and bubble should be higher than the external detachment stresses[34]. Regarding experiments performed in the bubble column, we had the idea to use the same subprocesses of the flotation field to explore the effect of solid particles on hydrodynamics. However, not all the three subprocesses could be used. Hence, if we compare the turbulence between a flotation cell and a bubble column, we can easily conclude that higher turbulence occurs in the bubble column, especially in the case of the heterogeneous regime. Also, the particles attached to air bubbles in flotation should be hydrophobic to reach the goal of separation while we have used hydrophilic glass beads in our work. Therefore, and based on those differences, we can state that only the collision subprocess should be considered for bubble-particle interaction in bubble columns for hydrophilic particles. In addition, no attachment or detachment is present under our work conditions. It should be mentioned that it's the collision efficiency E_c parameter that is used to quantify the collision subprocess in flotation rate calculation[98].

Schulze[99] defined collision efficiency as " the ratio of the number of particles encountering a bubble per unit time to the number of particles approaching the bubble at a great distance in a flow tube with a cross-sectional area equal to the projected area of the bubble". In other words, the collision efficiency E_c quantifies the percentage of particles that will collide with the bubble on the basis of a certain number of particles present in the system.

4.3.4.2 Parameters affecting collision efficiency E_c

Collision efficiency is affected by three main parameters. The first parameter is bubble surface mobility. Consequently, the bubble surface could completely or partially adsorb impurities or surfactants added on purpose[100]. The surface mobility significantly affects the collision process. Dai et al.[98] reported that collision efficiency for bubbles with a fully mobile surface is ten times higher than the case of a completely immobile surface. Therefore, as we were working with tap water and no surfactants, we assumed that the bubble surface in the bubble column is completely mobile.

The second parameter that affects collision efficiency is the flow regime around the bubble surface. The regime is determined based on the bubble Reynolds number $\mathrm{Re_b} = \frac{\mathrm{v_b d_b \rho_f}}{\eta}$. Hence, we can distinguish between three regimes, namely Stokes flow regime ($\mathrm{Re_b} << 1$), intermediate flow and potential flow ($\mathrm{Re_b} >> 1$). According to Dai et al.[98], bubbles with a mobile surface demonstrate high rising velocities. Consequently, the flow regime around the bubble for our case was potential.

The third parameter to determine the collision efficiency is the quantification of inertial forces. Particle inertia is the main factor that determines whether a particle will cross liquid streamlines and collide with a bubble or not. The trajectory of particles within the flow field and also the amount of particles that can reach the bubble surface depend on the inertia of particles and also on the characteristics of the flow field[34] . It is quantified by the Stokes number, which is the ratio between the inertial force and the viscous drag force acting on the particle. It is also the ratio of the characteristic time of the particle to a characteristic time for the flow around the bubble: $St = \frac{v_{B\times\rho_p\times d_p^2}}{9\times\mu_{fluid}\times d_b}$ (4.7)

Following the value of the Stokes number, we can distinguish between three scenarios when a particle encounters a bubble. St_{cr} is defined as the minimal Stokes number for which a particle can reach a bubble surface due to inertial forces. St_{cr} is assumed to be equal to $\frac{1}{12}$ in literature[98, 101] . Therefore, if $St < St_{cr}$ particles follow the liquid streamlines and the effect is called interceptional effect. In this case, and due to its finite size, the particle may touch bubble surface only for a critical liquid streamline in which the particle is in a radial distance smaller than the sum of bubble and particle radii [102]. If $St_{cr} < St < 1$, particles have an individual settling velocity

and deviate from liquid streamlines. Bubble-particle collision can result from this deviation. This effect is called the gravitational effect. If $St > 1$ particles are large and heavy enough that they cannot follow liquid streamlines and then have a straight trajectory. This effect is called the inertial effect and bubble-particle collision is promoted due to inertia. Based on these three parameters, we can state that particle size and density directly affect the Stokes number and consequently the collision efficiency E_c (equation (4.7)). Therefore, introducing E_c in the gas holdup model could be a good way to quantify the effect of particle size on hydrodynamics.

4.3.4.3 Model to calculate collision efficiency E_c:

Several models were used to calculate the collision efficiency E_c. A review of these models and the range of their applicability can be found in the work of Dai et al.[98]. The most relevant model for our conditions is the Dukhin or generalized Sutherland Equation GSE model. It is an analytical expression of collision efficiency based on the basic Basset-Boussineq-Oseen (BBO) particle trajectory equation. It was developed for a completely mobile bubble surface with potential flow and by considering the negative effect of particle inertial forces. Indeed, GSE model is a correction of another model called the Sutherland model in which the negative effect of inertial forces are neglected[98].

The Sutherland model collision efficiency E_{c-SU} was calculated by: $E_{c-SU} = \frac{3 \times d_p}{d_b}$ (4.8)

Where d_p is particle diameter and d_b is bubble diameter.

We used the GSE model to calculate the collision efficiency E_{c-GSE} [98]:

$$E_{C-GSE} = E_{c-SU}.\ sin^2\theta_t.exp\left\{3K_3\left[cos\theta_t\left(ln\frac{3}{E_{c-SU}} - 1.8\right) - \frac{2+cos^3\theta_t - 3cos\theta_t}{2E_{c-SU}sin^2\theta_t}\right]\right\} \quad (4.9)$$

Where θ_t is the angle of tangency calculated by:

$$\theta_t = arcsin\left\{2\beta\left[(1+\beta^2)^{\frac{1}{2}} - \beta\right]\right\}^{\frac{1}{2}} \quad (4.10)$$

And β is a dimensionless number defined by: $\beta = \frac{4 \times E_{c-SU}}{9 \times K_3}$ (4.11)

And K_3 is defined by: $K_3 = St \times \frac{\rho_p - \rho_{fluid}}{\rho_p}$ (4.12)

4.3.4.4 Steps to calculate E_{C-GSE} :

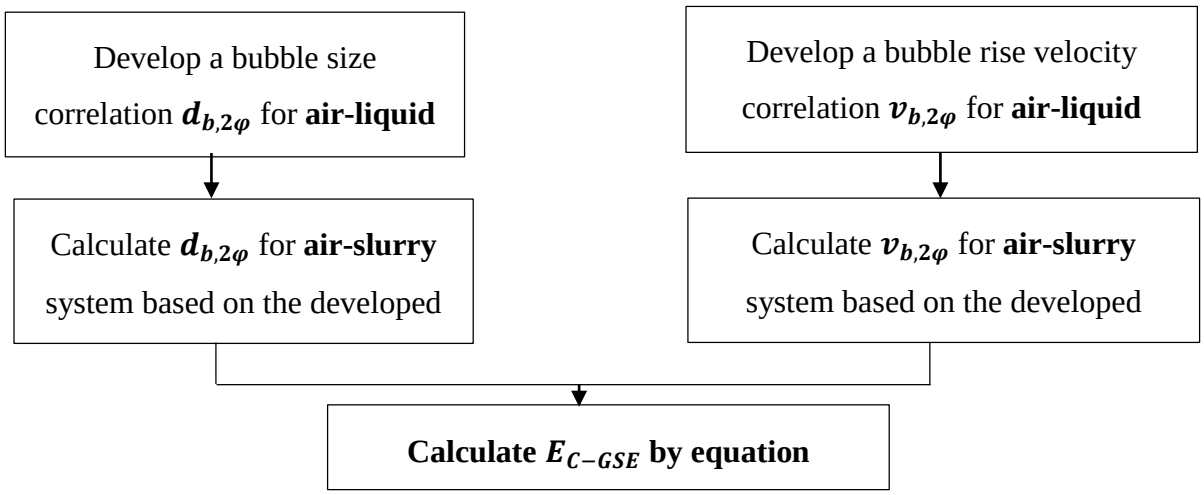

The same dimensional analysis used to develop the two-phase gas holdup correlation (equation (4.5)**)** was used to develop bubble size and bubble rise velocity correlations for the air-liquid system. The experimental measurements for bubble size and bubble rise velocity obtained by Esmaeili et al.[95] for the same liquids as above were used. The authors used a fiber optic probe to perform the measurements. The number of experimental points fitted for bubble size and bubble rise velocity correlations were 153 and 70 respectively.

The final form of bubble size correlation in the two-phase air-liquid system was:

$$d_b = D_c \times 0.6 \times Fr^{0.53} \times Bo^{0.35} \times Ga^{-0.14} \times \left(\frac{\rho_g}{\rho_l}\right)^{0.17} \quad (4.13)$$

$$0.016 \leq Fr \leq 0.138$$

$$10801 \leq Bo \leq 14620$$

$$1.015 \times 10^{7} \leq Ga \leq 2.42 \times 10^{11}$$

$$9.43 \times 10^{-4} \leq \frac{\rho_g}{\rho_l} \leq 1.227 \times 10^{-3}$$

The MAPE, standard error (SE), and 95% confidence interval were 9.55%, ±3.22mm and ± 6.35mm, respectively.

The final form of bubble rise velocity correlation in the two-phase air-liquid system was:

$$v_b = \sqrt{gD_c} \times 0.21 \times Fr^{0.51} \times Bo^{-0.96} \times Ga^{-0.01} \times \left(\frac{\rho_g}{\rho_l}\right)^{-1.6} \quad (4.14)$$

$$0.016 \leq Fr \leq 0.128$$

$$10944 \leq Bo \leq 14620$$

$$1.015 \times 10^{7} \leq Ga \leq 2.42 \times 10^{11}$$

$$9.43 \times 10^{-4} \leq \frac{\rho_g}{\rho_l} \leq 1.226 \times 10^{-3}$$

The MAPE, standard error (SE), and 95% confidence interval were 7%, ±4.09 cm/s and ± 8.83 cm/s, respectively.

4.3.4.5 Effect of operating conditions on the collision efficiency E_{c-GSE} and introduction of the hindering factor HF:

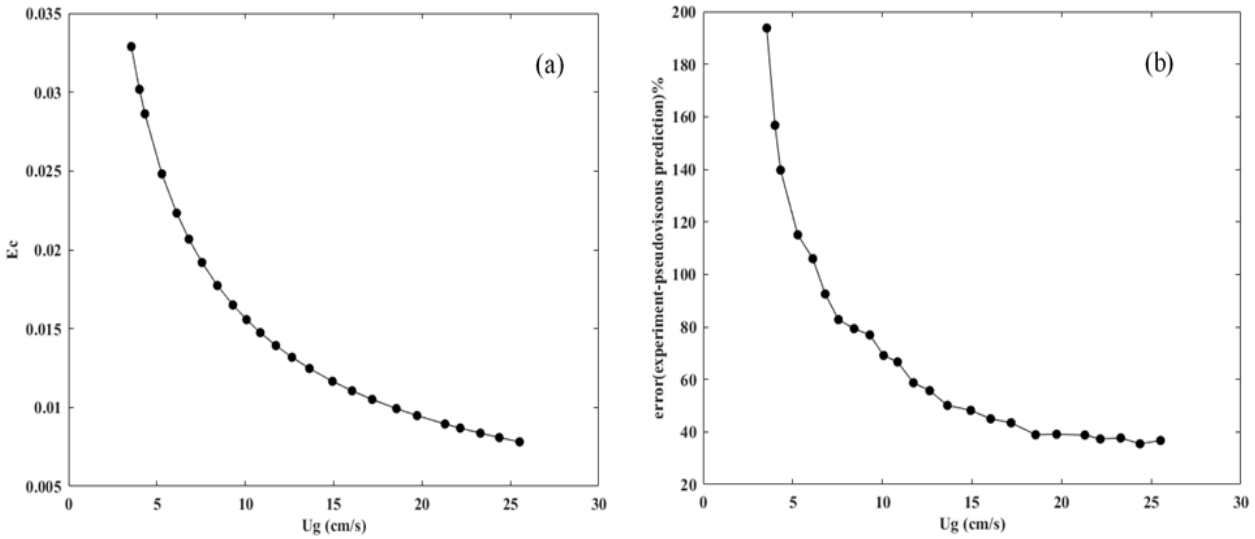

Figure 4.5 Effect of the superficial gas velocity on: a) collision efficiency b) error of the two-phase prediction (156µm-5%v/v)

Figure 4.5a shows the effect of superficial gas velocity on the calculated collision efficiency in the bubble column. It is clear that E_{c-GSE} decreased with increasing superficial gas velocity. Interestingly, Figure 4.5b shows that the error between the experimental gas holdup for the three-phase system and the prediction of the two-phase approach changed in the same way with superficial gas velocity. This finding gave us a hint that the source of error could be related to the collision phenomenon.

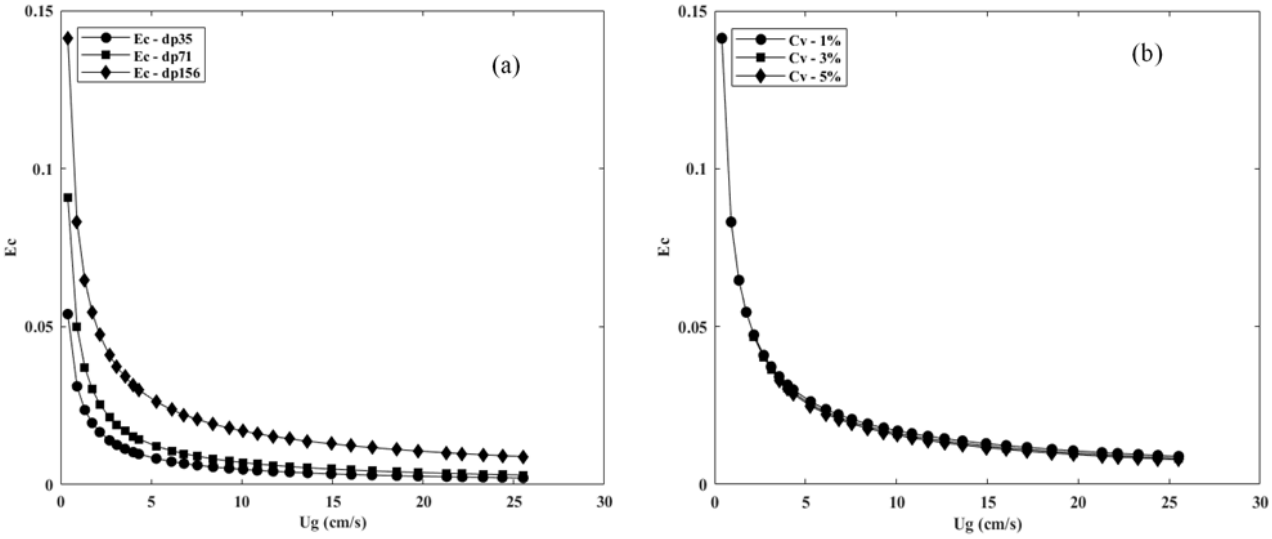

Figure 4.6 a) Effect of particle size on E_c b) Effect of solid concentration on E_c

However, we found that E_{c-GSE} was only affected by particle size (Figure 4.6). Indeed, bigger particles have high inertia and tend to deviate from liquid streamlines, which increases their collision efficiency compared with small particles. In addition, we found that solid concentration didn't affect collision efficiency for one particle size. For instance, for 156µm particles, collision efficiency was the same for all the three concentrations (Figure 4.6b). Based on these findings, we introduced a new factor called the Hindering Factor (HF). We assumed that this factor was responsible for the deviation between the two-phase approach and the three-phase experimental results and that it should be used to correct the prediction of the two-phase approach. Therefore, the three-phase gas holdup should be equal to the two-phase gas holdup multiplied by the Hindering Factor as follows:

$$\boldsymbol{\varepsilon_{g,3\varphi} = \varepsilon_{g,2\varphi}} \times [(\mathbf{1} - \boldsymbol{E_c}) \times (\mathbf{1} - \boldsymbol{C_v})]^{\boldsymbol{a}} \quad (4.15)$$

The authors wanted to develop a correlation that can be applied to both three-phase and two-phase systems. C_v value quantifies the number of particles present within the system. Hence, we multiplied a term involving C_v (Which is $(1 - C_v)$) by a term involving E_c (Which is $(1 - E_c)$). The choice of $(1 - E_c)$ and $(1 - C_v)$ instead of E_c and C_v respectively was because $\varepsilon_{g,3\varphi}$ should be equal to $\varepsilon_{g,2\varphi}$ if no solid particles are present within the system $((1 - E_c) \rightarrow 1;\ (1 - C_v) \rightarrow 1)$

and then no correction is needed. Therefore, the term $(1 - E_c) \times (1 - C_v)$ is interrelated to the number of particles that will really collide with one bubble.

The $[(\mathbf{1} - \boldsymbol{E_c}) \times (\mathbf{1} - \boldsymbol{C_v})]^{\boldsymbol{a}}$ term is called the hindering factor that makes it possible to adjust the error between the three-phase gas holdup and the two-phase gas holdup prediction data to the lowest possible value. It should be mentioned that, before correction, each particle size and each concentration showed a different error value (Figure 4.4). We then aimed to make each single error tend to zero by applying the same correcting factor.

Therefore, the hindering factor consists mainly of two parts. The first one is the collision efficiency, which depends only on particle size and not on particle concentration. The second part is the number of particles present in the system and on the basis of which we know the actual number of particles that will collide with bubbles by multiplying it by the collision efficiency. Consequently, we assume that the simultaneous effect of particle size and concentration on the total gas holdup can be formulated as the following: increasing particle size and concentration increases the hindering factor, HF. As a result, particles hinder bubbles from rising, which increases the probability of contact between bubbles and then enhances bubble coalescence.

To prove the hindering effect of solid particles, we present in Figure 4.7 the disengagement curves for 71µm and 156µm at 5%v/v for three different superficial gas velocities (11.73, 17.18 and 23.3 cm/s). The aim was to highlight the effect of particles on the time needed for the bubbles to disengage from the column and, more specifically, on their bubble rise velocity. As we have proven for the total gas holdup, increasing particle size decreased gas holdup. This is clearly shown in the disengagement curves before t=30s. The 71µm gas holdup was on average larger than the 156 µm gas holdup. This means that the bubbles in the 156 µm particle system had larger holdup equivalent bubble diameter than the bubbles in the 71 µm system. However, when the gas flow was stopped, the bubbles in the 71µm system disengaged faster than the bubbles in the 156µm one, even if they were smaller. The disengagement curve for the 71µm system shows a steeper slope and the rate of decrease of the gas holdup was steeper. This result brings about the hindering effect of solid particles. Indeed, 156µm particles hindered bubbles from rising and the rate of the gas holdup decrease was lower. We can conclude that increasing particle size increases the hindering effect.

Therefore, we can explain the findings of Figure 4.2. At very low concentrations (1%v/v and 3%v/v), the number of particles present in the system was low and then the number particles that would collide with bubbles was even less. This explains why we didn't see a significant effect of particle size on gas holdup. However, at 5%v/v, we started to see the effect of particle size as the number of particles within the system was higher. Also, for Figure 4.3, we can explain the fact that the decreasing effect of solid concentration on total gas holdup was more pronounced at a higher particle size because of the increase in the hindering factor, HF.

The final form of the gas holdup correlation of the three-phase system was obtained by a simple linear fitting in MATLAB of the logarithm of equation (4.15) as follows:

$$\boldsymbol{log\, \varepsilon_{g,3\varphi} = log\, \varepsilon_{g,2\varphi} \; + a \times log[(1 - E_c) \times (1 - C_v)]} \tag{4.16}$$

The correlation has the following final form:

$$\boldsymbol{\varepsilon_{g,3\varphi} = \varepsilon_{g,2\varphi} \; \times [(1 - E_c) \times (1 - C_v)]^{5.43}} \tag{4.17}$$

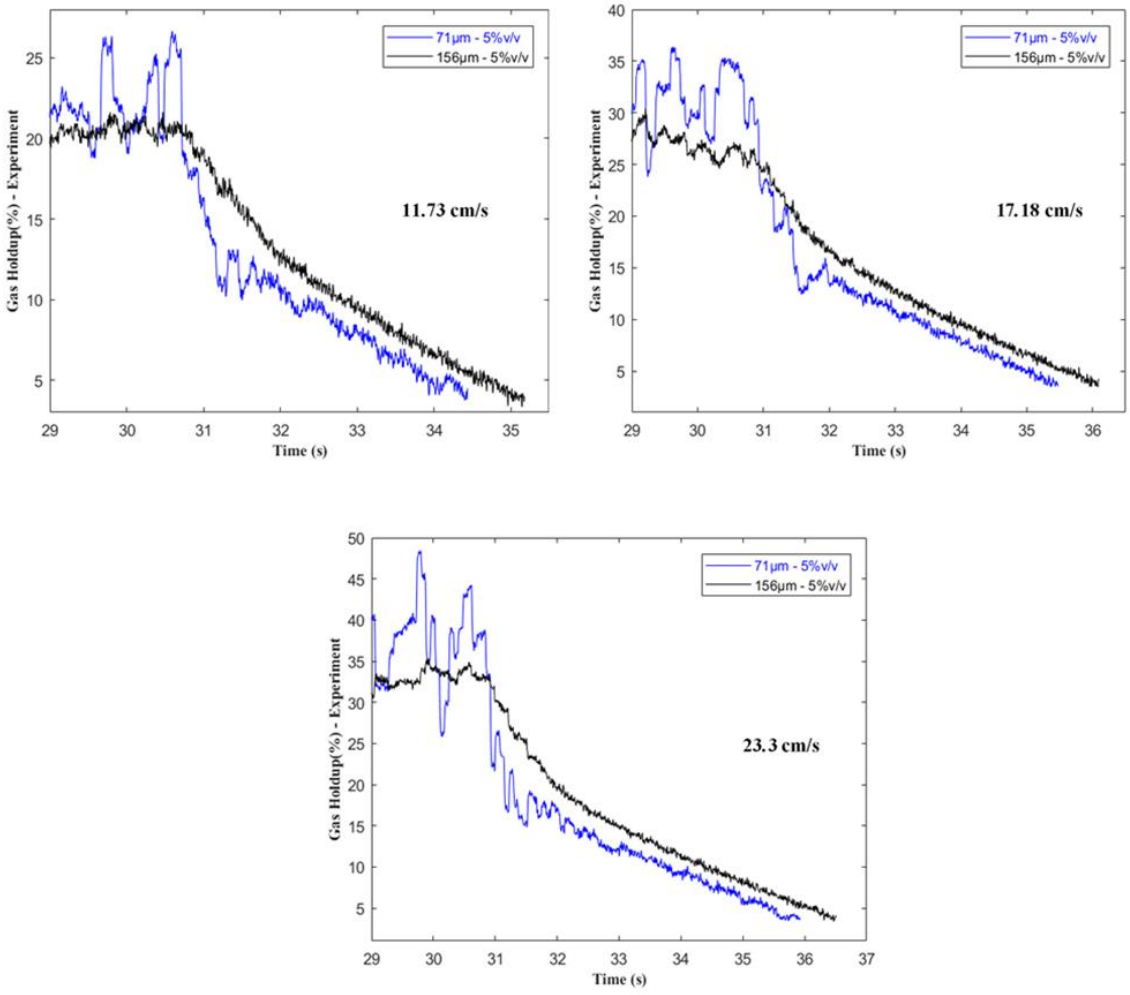

Figure 4.7 Disengagement curve for 71µm and 156µm at 5%v/v for three different superficial gas velocities

Figure 4.8 shows a comparison between the three-phase gas holdup measured experimentally and the gas holdup predicted by equation (4.17). The MAPE, standard error (SE), and 95% confidence interval of the fitting were 10.4%, ±1.29% and ±2.55%, respectively. The source of error of the fitting was the value of $\boldsymbol{C_v}$ at low superficial gas velocities. Indeed, at low Ug, the solid concentration in the region surrounding a bubble was not $\boldsymbol{C_v}$ but $\boldsymbol{C_{v,local}}$ which is the local concentration near the bubble. Mokhtari et al.[103] found that the local solid concentration increases with superficial gas velocity until it reaches a plateau in the heterogeneous regime. It's this constant value that could be equal to the initial solid volume fraction $\boldsymbol{C_v}$. This finding explains the large error of the fitting at low superficial gas velocities if

compared with high superficial gas velocities. Therefore, knowing the local solid concentration at each velocity could improve the proposed correcting factor.

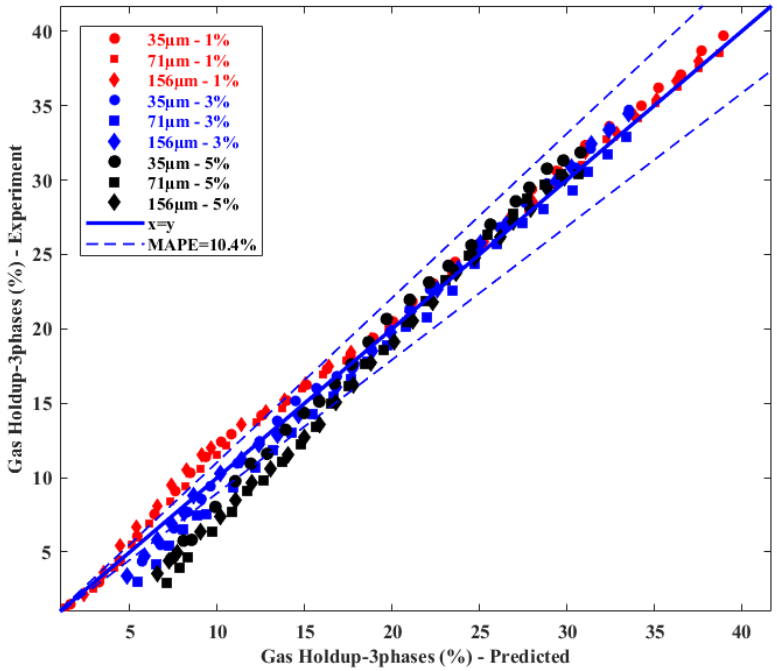

Figure 4.8: Comparison between the experimental gas holdup and the corrected gas holdup

4.3.5 Comparison between gas holdup correlations developed for three-phase system and the experimental gas holdup obtained in this work

We conducted a comprehensive literature review to find the most relevant correlations developed for gas-liquid-solid systems. The six correlations found are summarized in Table 4.3. Kito el al.[104] have developed a gas holdup correlation in a mobile bed where air and liquid are in countercurrent flow. They used different liquids namely water, aqueous glycerin solution and ethanol. The solid phase was light plastic material in the centimeter size range. They found good agreement between the experimental gas holdup and the one predicted by their correlation. Also, they reported that gas holdup is independent of liquid velocity and solid properties. Koide et al.[105] proposed a gas holdup correlation for the transition and heterogeneous regimes. They performed their experiments with water and different aqueous solutions and with heavy glass and bronze particles in the micron size. They developed their empirical equation based on the finding

that solid particles have a low effect on gas holdup in the heterogeneous regime. In another work, Reilly et al.[106] proposed an empirical correlation for gas holdup based on the experimental work conducted in bubble columns in the heterogeneous coalescing regime. The work was performed for different sizes of heavy micro glass beads in three different liquids and three different gases (air, helium and argon). Chen et al.[107] have developed a gas holdup correlation based on the work performed in a three-phase magnetic fluidized bed. Sehabiague et al.[108] proposed a gas holdup empirical correlation based on experimental work performed at high pressure and temperature for different gas mixtures and Fischer-Tropsch liquid cuts. More details about the range of application of these five correlations can be found in the work of Basha et al.[85]. The last correlation found was the one proposed by Götz et al.[109]. The authors were among the few authors who corrected the two-phase gas holdup to obtain a three-phase gas holdup as was proposed by our work. However, their correlation was developed only for a homogeneous regime. It was developed based on experimental data from various works and then from different systems and gas distributor design.

Figure 4.9 compares the prediction of the aforementioned models with the proposed correlation in this work. We report the prediction parameters in Table 4.4. According to this figure, we can state that most correlations reported in the literature could not accurately predict our experimental gas holdup especially at high superficial gas velocities.

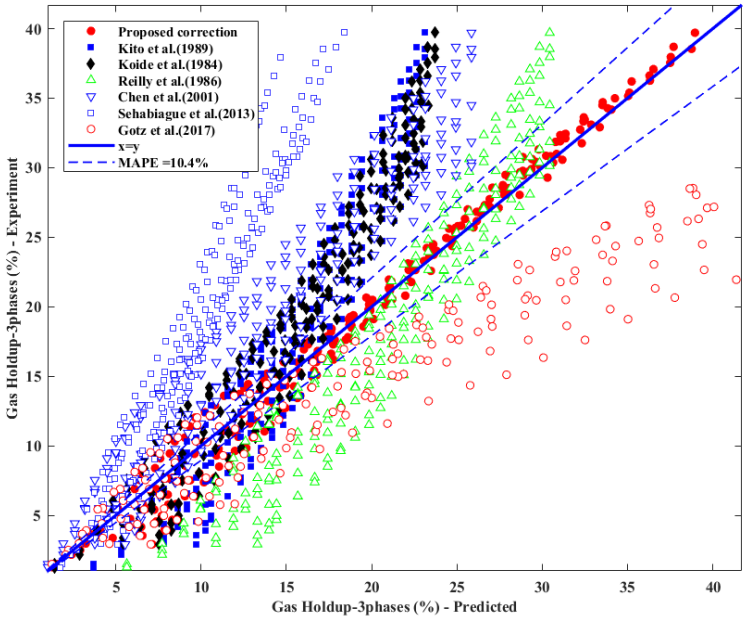

Figure 4.9 Comparison between predictions of different gas holdup correlations

Table 4.3 Summary of the gas holdup correlations developed for gas-liquid-solid systems

Authors	**Correlation**
Kito el al.[104]	$\varepsilon_g = 0.19\left(\frac{{U_g}^2 d_p \rho_l}{\sigma_l}\right)^{0.11}\left(\frac{U_g}{\sqrt{g d_p}}\right)^{0.22}$
Koide et al.[105]	$\frac{\varepsilon_g}{\left(1-\varepsilon_g\right)^4} = \frac{0.277\left(\frac{U_g \mu_l}{\sigma_l}\right)^{0.918}\left(\frac{g {\mu_l}^4}{\rho_l {\sigma_l}^3}\right)^{-0.252}}{1+4.35\left(\frac{C_s}{\rho_p}\right)^{0.748}\left(\frac{\rho_p-\rho_l}{\rho_l}\right)^{0.881}\left(\frac{D_c U_g \rho_l}{\mu_l}\right)^{-0.168}}$
Reilly et al.[106]	$\varepsilon_g = 296{U_g}^{0.44}{\rho_l}^{-0.98}{\sigma_l}^{-0.16}{\rho_g}^{0.19} + 0.009$
Chen et al.[107]	$\varepsilon_g = 0.75{U_g}^{0.78} exp(8.12 \times 10^{-6} H_c)$
Sehabiague et al.[108]	$\varepsilon_g = 11241.6\left(\frac{{\rho_g}^{0.174}{U_g}^{0.553}\Gamma^{0.053}}{{\mu_l}^{0.025}{\sigma_l}^{0.105}{\rho_l}^{1.59}}\right)\left(\frac{P}{P-P_s}\right)^{0.203}\left(\frac{D_c}{D_c+1}\right)^{-0.117}\exp(-1.2\times10^{-3}C_s - 0.4\times10^{-6}{C_s}^2 - 4339 d_p + 0.434 X_W$

Götz et.[109]	$\varepsilon_g = \frac{7.8391^{K_2 . GS^{K_3} . K_4{}^{Surf}} \left(\frac{U_g}{\sqrt{gL_c}}\right)\left(\frac{(\rho_L - \rho_G) g d_{b,ref}{}^2}{\sigma_L}\right)^{0.2204} \left(\frac{(\rho_L - \rho_G) g \rho_L d_{b,ref}{}^3}{\mu_L{}^2}\right)^{0.0476} \left(\frac{\rho_G}{\rho_L}\right)^{K_7}}{1 + \left(K_{S1}\left(\frac{\rho_p - \rho_L}{\rho_L}\right)^{0.755}\left(\frac{C_v}{(1-C_v)^2}\right)^{0.263}\left(exp\left(\frac{d_p}{d_{b,ref}}\right)\right)^{K_{S4}}\right)}$

Table 4.4 Prediction parameters for different gas holdup correlations

Author	**MAPE**	**Standard error (%)**	**95% confidence interval (%)**
Kito el al.[104]	33%	± 6.22	±12.26
Koide et al.[105]	24.34%	± 5.9	± 11.7
Reilly et al.[106]	45%	± 4.8	± 9.45
Chen et al.[107]	27.55%	± 6.23	± 12.27
Sehabiague et al.[108]	43%	± 10.9	± 21.46
Götz et.[109]	45.44%	± 13.23	± 26.09
Proposed correlation	10.4%	± 1.29	± 2.55

4.3.6 Validation and range of applicability of the proposed correction

To verify the applicability of equation (4.17) we performed the same correction procedure as described above on the experimental gas holdup data obtained in the work of Li et al.[110], Li et al.[94] and Ghandi et al.[91]. It should be mentioned that the proposed correction was valid for systems with relatively low solid concentrations (lower than 10% v/v), superficial gas velocities higher than 5 cm/s and relatively large diameter bubble columns. From these three works, we extracted the data that fit in our range of application. Figure *4.10* shows a comparison between the three-phase gas holdup measured experimentally in these

three works and the gas holdup predicted by our correlation. The prediction parameters are summarized in Table *4.5*. The correlation could predict the data with MAPE and a standard error of 21.5% and ±5.57, respectively. Moreover, experimental data obtained in systems with the same conditions as our work are scarce in literature.

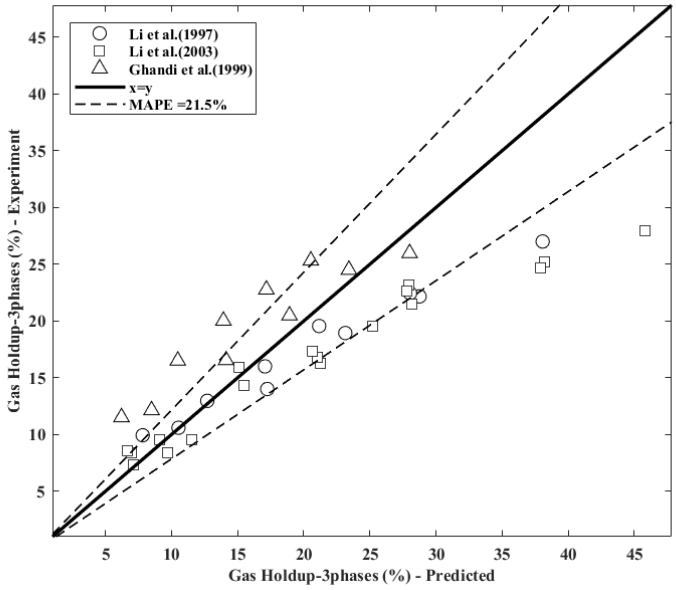

Figure 4.10 Comparison between the experimental and predicted gas holdup by the proposed correlation for other experimental data

Table 4.5 Prediction parameters for different gas holdup data series

Data series	**System**	**Number of points**	**MAPE before correction**	**MAPE After correction**	**Standard error (%)**
Li et al.[110]	Air-water-glass beads (35µm)	10	76%	18%	± 5.4
Li et al.[94]	Air-water-glass beads (11-35-93 µm)	18	78 %	24.5%	± 7.31
Ghandi et al.[91]	Air-water-glass beads (35µm)	10	25%	22%	± 4
	Total	**38**	**60 %**	**21.5%**	**± 5.57**

4.4 Conclusion

In this study, we clarified the simultaneous effect of particle size and concentration on the total gas holdup of a relatively large slurry bubble column. The experimental results showed that, at a constant concentration, increasing particle size had no effect on gas holdup at low concentrations (1%v/v and 3%v/v) and decreased gas holdup at high concentration (5%v/v). Also, at a constant diameter, increasing solid concentration decreased gas holdup and the decreasing effect was more pronounced with a larger particle size. Moreover, the decreasing effect of solid particles on the total gas holdup was present in the heterogeneous regime where the bubble coalescence phenomenon occurs. Considering the three-phase system as a two-phase system with a corrected slurry viscosity and density was not applicable to our system. The two-phase approach overestimated our experimental data with an MAPE of 34.28%. Consequently, we introduced a novel hindering factor that considers the additional effect of solid particles on bubble flow in terms of collision phenomenon. The hindering factor consists of the collision efficiency parameter that is affected only by particle diameter and the solid concentration parameter. By applying this correcting factor, we could correct the two-phase prediction by a MAPE of 10.4%. However, more work should be done to widen the range of applicability of the proposed correction. First, the fitting shows a large error at low superficial gas velocities because the solid is not well dispersed at these velocities and the solid concentration is not equal to the initial solid volume fraction. Therefore, we can improve the correction factor if we can measure the local solid concentration at low velocities. Second, at a high solid concentration, we cannot correct the two-phase prediction by the same correcting factor because we assume that from 10% v/v, the particles will not have more space to collide with the bubble and the slurry phase might have a non-Newtonian behaviour. Third, the power a used in the hindering factor HF should be the subject of further studies. The parameter from the phase properties, operating conditions or reactor design that affects the error with respect to the two approaches more should be pinpointed. This parameter will then be directly linked to a . Fourth, it should be mentioned that the correlations used to calculate the parameters of the two-phase approach (gas holdup-bubble size-bubble velocity) should be chosen as a function of the appropriate range of application. Last, more experimental work with different solid properties (density – wettability – porosity) and relatively high concentrations is required to better understand

how the solid affects bubble column hydrodynamics. This novel correcting approach introduces a new method for investigating the intrinsic effect of solid particles.

4.5 Acknowledgments

The authors would like to acknowledge TOTAL American Services, Inc. and the Natural Science and Engineering Research Council, Canada (NSERC) for the financial support of this work. We also would like to appreciate Dr Esmaeili Amin for his assistance in the modeling part of this work.

CHAPTER 5 ARTICLE 2: EFFECT OF SOLID PARTICLES ON THE VOLUMETRIC GAS LIQUID MASS TRANSFER COEFFICIENT IN SLURRY BUBBLE COLUMN REACTORS

El Mahdi Lakhdissi [1], Afshin Fallahi[1], Christophe Guy[2], Jamal Chaouki[1,*]

[1]Department of Chemical Engineering, Polytechnique Montréal, P.O. Box 6079, St. C.V., Montreal, QC, Canada H3C 3A7

[2] Department of Chemical & Materials Engineering, Gina Cody School of Engineering & Computer Science, Concordia University, 1455 Boulevard de Maisonneuve West, Montreal, QC, Canada H3G 1M8

*****Corresponding author: jamal.chaouki@polymtl.ca;

(Published in Chemical Engineering Science, DOI: 10.1016/j.ces.2020.115912)

Abstract

The effect of solid particles on the volumetric gas liquid mass transfer coefficient $k_l a_l$ in slurry bubble column reactors was investigated in the present work. $k_l a_l$ was measured for an air-water-glass bead system using the dynamic oxygen absorption technique. Three solid concentrations (1-3-5% v/v) and two particle diameters (71 µm-156µm) were used. Solid particles had a negligible effect on $k_l a_l$ due to two opposite effects. First, a fraction of the particles tends to be located in the bulk liquid, altering its viscosity. In the heterogeneous regime, increasing the solid concentration enhances bubble coalescence, which led to an increase in size and, as a result, a decrease in the gas-liquid interfacial area a_l. Second, another fraction of particles moves to the bubble surface due to the collision phenomenon and tends to accumulate in the liquid film, resulting in local turbulence and an increase in the liquid-side mass transfer coefficient k_l. The *hydrodynamic effect* mechanism was the governing mechanism of the effect of solid particles on gas-liquid mass transfer within the range of the investigated operating conditions.

Keywords: slurry bubble column, volumetric gas-liquid mass transfer coefficient, particle size, solid concentration, hydrodynamic effect, dynamic oxygen absorption technique, signal decomposition method

5.1 Introduction

Slurry bubble column reactors (SBCR) are one of the simplest three-phase systems to operate. The absence of agitators and the low operating costs make them ideal for a number of industrial applications, including Fischer-Tropsch synthesis, waste water treatment, and hydroconversion of heavy oils. In addition to hydrodynamics, gas-liquid mass transfer is one of the key parameters for designing and scaling up this type of reactor[111]. This parameter is even more critical when the chemical reaction between the gas and liquid reactants is mass transfer limited. Several theories were developed to describe mass transfer phenomena for a gas-liquid system. Lewis and Whitman[60] introduced the two-film model to describe steady-state mass transfer. The interface between the two phases is delimited by a gas film and a liquid film, each with a specific thickness. Mass transfer occurs within these films. Other models, such as the penetration and surface renewal theories, were subsequently developed to describe unsteady state mass transfer for gas-liquid contactors[112, 113]. Alper and Öztürk[114] and Alper et al.[115] reported that these models cannot describe mass transfer phenomena in the presence of solid particles suspended in the liquid phase very well. They thus introduced the concept of gas-liquid mass transfer enhancement by solid particles. Four mechanisms have been proposed to describe enhancement phenomena. The first mechanism called the *hydrodynamic effect* is in the boundary layer between the gas and liquid. In this case, solid particles present in the gas-liquid interface tend to decrease the effective thickness of the boundary layer, which is mainly related to the local turbulence induced by solid particles or to their collision with the gas-liquid interface. Also, the mass transfer coefficient k_l increases due to the larger refreshment rate of the liquid in the gas-liquid interface. More details about this mechanism can be found in the work of Ruthyia et al.[116] and Kluytmans et al.[117] The second mechanism, which was introduced by Alper et al.[115], is called the *shuttle effect*. It considers that particles with a certain porosity and, as such, a high specific area adsorb more gas in the diffusion layer and desorb it into the bulk liquid. The presence of particles thus enables more gas transport, which increases k_l. The third mechanism is called the *coalescence inhibition effect*, by which some

particles attach to gas bubbles to some extent, depending on their properties and the surrounding operating conditions. Particle-to-bubble adhesion (PBA) hinders bubble coalescence by stabilizing the bubble surface, which increases the specific gas-liquid interfacial area and thus the volumetric gas-liquid mass transfer coefficient $k_l a_{l[118]}$. The fourth mechanism is called the *reaction enhancement effect*. Solid particles used as catalysts in three-phase systems catalyze the chemical reaction at the gas-liquid interface, increasing conversion in the film layer as well as the rate of mass transfer[118].

Several researchers have focused on determining the mechanisms that govern mass transfer at the gas-liquid interface in the presence of solid particles. However, it is difficult to determine exactly which conditions result in a given mechanism. Kluytmans et al.[117] studied the effect of carbon particles and electrolytes on mass transfer in a 2D slurry bubble column and a stirred tank reactor. In the slurry bubble column, they found that $k_l a_l$ and a_l are independent of the carbon particle concentration for a nitrogen-water-carbon system. Behkish et al.[119] reported that increasing the concentration of two different solids (iron oxide catalyst and glass beads) from 0 to 36% (v/v) in a large-scale slurry bubble column markedly decreases $k_l a_l$, mainly due to the decrease in the gas-liquid interfacial area caused by the increase in bubble coalescence. Vandu and Krishna[120] studied the effect of varying porous alumina catalyst volume fractions on $k_l a_l$ in a slurry bubble column operating with paraffin oil in the heterogeneous regime. They reported that the solid concentration has no effect on the mass transfer coefficient but did not provide a physical reason to explain this phenomenon, only saying that their finding was not in agreement with previously published results and concluding that more work will be required to determine which solid or liquid property controls the effect of catalyst concentration. Other authors reported that, under Fischer-Tropsch conditions (particles smaller than 50 µm and weight concentrations lower than 16%), solid concentration has a negligible effect on the mass transfer coefficient[74, 121]. Mena et al.[66] found that the effect on $k_l a_l$ differs depending on some solid properties. For 9.6-µm hollow glass spheres they observed a dual effect of the solid concentration on $k_l a_l$. However, for an air-water-polystyrene system with three different particle sizes and different volume fractions (up to 30% (v/v)), they observed that an increase in the solid concentration causes a decrease in $k_l a_l$. As can be seen in the literature, there are many discrepancies with respect to the effect of the presence of solid particles on the volumetric mass transfer coefficient. It is clear, nonetheless, that these

disagreements arise from differences in parameters related to (1) liquid physicochemical properties, (2) solid properties such as wettability, size, and density, (3), reactor size, geometry, and design, and (4) operating conditions, such as gas and liquid velocities, solid concentration, pressure, and temperature.

The objective of the present work was to narrow the range of parameters studied and provide reliable experimental data on the physical effect of the presence of solid particles on gas-liquid mass transfer in a slurry bubble column reactor. We performed the experiments in a pilot-scale bubble column slurry reactor with fixed gas, liquid, and solid phases, and only changed the particle size, particle concentration, and superficial gas velocity. The ultimate goal was to determine the physical mechanism that describes the effect of solid particles on mass transfer within the range of applications relevant to our research.

5.2 Experimental procedure

5.2.1 Experimental setup and materials

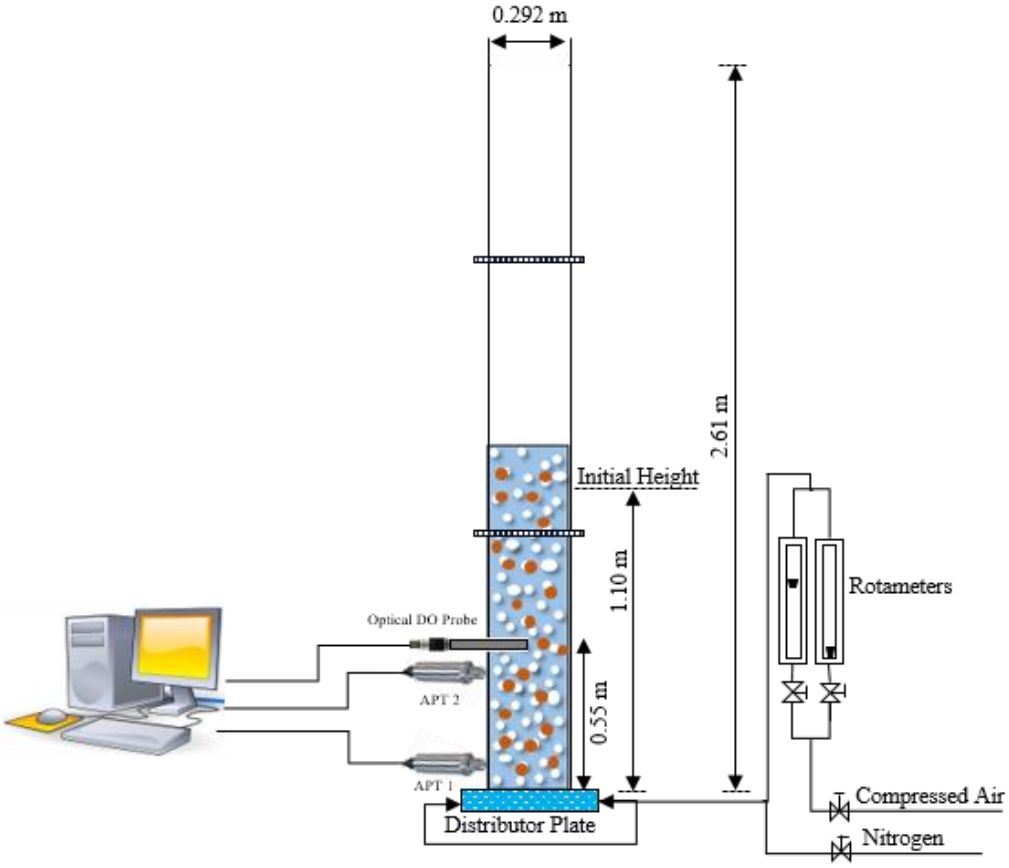

Figure 5.1 Schematic of the slurry bubble column setup and measurement techniques

The experiments were conducted in a 2.61-m high Plexiglas slurry bubble column with a 0.292-m inside diameter (Figure 5.1). The solid phase was composed of nonporous hydrophilic glass beads, the gas phase was oil-free compressed air, and the liquid phase was tap water. The experiments were conducted using two particles sizes (71 µm and 156 µm) and three initial solid fractions C_v (1% (v/v), 3% (v/v), 5% (v/v)). More details on the characteristics and operating mode of the setup, can be found in a previous publication[122]. The properties of the glass bead solid phase are summarized in Table 4.1.

Table 5.1 Glass beads properties

Solid nature	10% Finer than	Mean diameter (µm)	90% Finer than	Density
Hydrophlic glass beads	59 µm	**71 µm**	85 µm	
	125 µm	**156 µm**	192 µm	

5.2.2 Measurement techniques and methods

5.2.2.1 Gas-liquid mass transfer coefficient k_la_l measurement

The volumetric gas-liquid mass transfer (k_la_l) was measured with the dynamic oxygen absorption technique using the saturation method. Nitrogen was injected into the column until the dissolved oxygen concentration in the liquid phase was equal to zero. Afterwards, air was injected into the column, and the concentration of dissolved oxygen was monitored using an optical probe. By assuming that the liquid phase is characterized by perfect mixing and the depletion of oxygen from the gas bubble is negligible, the mass balance of dissolved oxygen gave the oxygen concentration C at each instant[123]:

$$\frac{dC}{dt} = k_l a(C^* - C) \tag{5.1}$$

where C^* is oxygen solubility (the oxygen saturation concentration), $k_l a$ is the volumetric mass transfer coefficient, and C is the oxygen concentration in the liquid.

This equation was integrated by considering that, at time t_0, the concentration of oxygen in the liquid phase was equal to 0. The following equation was obtained:

$$C(t) = C^*\left[1 - exp\left(-k_l a(t - t_0)\right)\right] \tag{5.2}$$

A Visiferm DO325 optical probe (Hamilton) was used to measure the dissolved oxygen (DO) concentration in the liquid phase. The measurement of the dissolved oxygen by the Visiferm mass transfer probe is based on the oxygen-dependent luminescence quenching method. Thus, in the absence of oxygen, a luminophore present in the sensing element of the probe absorbs an excitation

(light) and releases by luminescence fluorescence a part of the absorbed energy. If oxygen is introduced in the sensing element of the optical probe, the luminophore transfers a part of the energy absorbed from excitation to the oxygen and then the intensity of luminescence decreases. The oxygen concentration and the intensity of luminescence are related by the Stern-Volmer equation:

$$\frac{I_0}{I} = 1 + k_q t_0 \times O_2 \quad (5.3)$$

Where I_0 is the intensity of luminescence when the quenching molecule (O_2) is absent, I is the intensity of luminescence when the quenching molecule (O_2) is present, k_q is the quencher rate coefficient and t_0 is the luminescence of the luminophore to be quenched

The DO probe was installed axially 0.55 m above the distributor in the center of the radial position in order to record the oxygen concentration in a representative zone of the column (Figure 5.1). Performing the $k_l a_l$ measurements in the center radial position stemmed from the air-water system experimental results where a flat $k_l a_l$ radial profile for low and large superficial gas velocities was obtained. Furthermore, the $k_l a_l$ measurements were performed in the center axial zone because it is representative of the column far from the distributor zone where the bubbles are formed and the surface free zone where they erupt. Also, it is assumed that all liquid flow patterns are fully developed within this zone.

The probe measured dissolved oxygen over a range of 4 ppb to 25 ppm by oxygen-dependent luminescence quenching. A data acquisition card (National Instrument, PCI6023E) and LabVIEW software were used to record dynamic DO concentrations. All measurements were recorded for 180 s at a frequency of 512 Hz and were made in triplicate. The 180s recording time was chosen to ensure reaching the oxygen saturation condition for all the operating conditions. According to the Shannon-Nyquist criterion[124], the 512Hz sampling rate corresponds to a spectrum of 200 Hz frequency, and in which the best dissolved oxygen signal resolution has been obtained. The average of the three readings was used to determine our mass transfer results.

5.2.2.2 Average bubble size estimation using the signal decomposition method

Global pressure fluctuations could result from several phenomena, such as column mechanical vibration, bubble formation, bubble eruption, bubble coalescence, bubble breakup and the natural

oscillations of the slurry suspension. Global pressure waves generated by global pressure fluctuations travel rapidly from their origin to different points in the column. As these global fluctuations have a high propagation velocity, which is generally greater than 50 m/s, they can be measured almost instantaneously throughout the whole height of the column[125]. In other words, the global pressure time series $P^{glob}(t)$ measured at an axial position x are almost the same as the ones measured simultaneously at another axial position y: $a_y P^{glob}(t+\Delta t)$. a_y is the attenuation of the global pressure fluctuations at the position y compared to the position x, and Δt is the time lag. The two measured global pressure time series are coherent and have a constant time lag. Ruthiya et al.[125] stated that this time shift is nearly equal to zero for the global pressure waves measured simultaneously at two different axial positions in the slurry bubble column.

On the other hand, local pressure waves generated by local pressure fluctuations are caused mainly by the passage of large gas bubbles and travel at a low velocity from the source (< 2 m/s)[125]. However, local pressure fluctuations can only be measured near the source of fluctuation. When a gas bubble is generated at the gas distributor, it changes in size, shape, and velocity as it rises in the column, and the pressure fluctuation created by its passage, at a certain point, is different from the fluctuation measured at the gas distributor. Consequently, local pressure fluctuations measured at a higher axial position from the distributor, and caused by the passage of a bubble are not coherent with the pressure fluctuations measured just above the gas distributor where large bubbles do not exist.

The signal decomposition approach in SBCR was introduced by Ruthiya et al.[125] It is based on the separation of phenomena attributed to high velocity pressure waves that are highly coherent from phenomena attributed to low velocity pressure waves with low coherence. The rise of large gas bubbles is the dominant phenomenon that causes low velocity pressure waves. This method thus makes it possible to determine the size of large gas bubbles from pressure fluctuations.

The coherence of two pressure signals P_x and P_y measured at a height x just above the gas distributor and at a height y in the column respectively was assessed using the following coherence function:

$$\boldsymbol{\gamma_{xy}}^{\mathbf{2}}(\mathbf{f}) = \frac{\mathbf{P_{xy}(f)P^{*}_{xy}(f)}}{\mathbf{P_{xx}(f)P_{yy}(f)}} \tag{5.4}$$

where $P_{xx}(f)$ and $P_{yy}(f)$ are the power spectral densities of the pressure time series at positions x and y, respectively:

$$\mathbf{P_{xx}(f)} = \frac{\mathbf{1}}{\mathbf{f_s}} \boldsymbol{\mathcal{F}}_{\mathbf{x}}\mathbf{(f)}\boldsymbol{\mathcal{F}}_{\mathbf{x}}{}^{*}\mathbf{(f)} \tag{5.5}$$

where $\mathcal{F}_x(f)$ is the discrete Fourier Transform that converts the pressure time series from the time domain to the frequency domain defined by:

$$\boldsymbol{\mathcal{F}}_{\mathbf{x}}\mathbf{(f)} = \frac{\mathbf{1}}{\mathbf{T}} \int_{\mathbf{0}}^{\mathbf{T}} \mathbf{P_x(t)e^{-2\pi ift}dt} \tag{5.6}$$

where $P_{xy}(f)$ is the cross-power spectral density (CSD) of the two signals defined by:

$$\mathbf{P_{xy}(f)} = \frac{\mathbf{1}}{\mathbf{f_s}} \boldsymbol{\mathcal{F}}_{\mathbf{x}}\mathbf{(f)}\boldsymbol{\mathcal{F}}_{\mathbf{y}}{}^{*}\mathbf{(f)} \tag{5.7}$$

and $\mathbf{P^{*}_{xy}(f)}$ is its conjugate.

The coherence function values are between 0 and 1. Coherence equal to 0 means that the two signals are completely incoherent and coherence equal to 1 means that the two signals are completely coherent.

After calculating the coherence function, the next step involved calculating the coherent-output power spectral density (COP) and the incoherent-output power spectral density (IOP), which represent global coherent pressure fluctuations and local incoherent pressure fluctuations, respectively:

$$\mathbf{COP_y(f)} = \boldsymbol{\gamma}_{\mathbf{xy}}{}^{\mathbf{2}}\mathbf{(f)P_{yy}(f)} \tag{5.8}$$

$$\mathbf{IOP_y(f)} = (\mathbf{1} - \boldsymbol{\gamma}_{\mathbf{xy}}{}^{\mathbf{2}}\mathbf{(f)})\mathbf{P_{yy}(f)} \tag{5.9}$$

According to Chilekar et al.[76], the amplitude of pressure fluctuations caused by the passage of a bubble is proportional to the size of the gas bubble to a certain power. Hence, they proposed the following relation between bubble size and σ_i, the standard deviation of IOP representing the power of pressure fluctuations attributed to rising bubbles:

$$\boldsymbol{d_b} \approx \mathbf{0.153}\left(\frac{\boldsymbol{\sigma_i}}{\boldsymbol{\rho_s g}}\right)^{\mathbf{0.434}} \tag{5.10}$$

The standard deviation σ_i can be obtained by applying the Parseval theorem[76]:

$$\boldsymbol{\sigma_i}^{\mathbf{2}} = \int_{\mathbf{0}}^{\infty} \boldsymbol{IOP}(\mathbf{f})\boldsymbol{df} \tag{5.11}$$

which is the area under the incoherent output power curve.

We used this method to estimate the average large bubble size by spectral analysis of the pressure time series. In order to do so, two absolute pressure transducers (Omega) were positioned 0.02 m and 0.45 m, respectively, above the distributor to record the pressure time series at these two locations (Figure 5.1). To generate the pressure time series, we used the same data acquisition and LabVIEW software as for the dissolved oxygen concentration measurements. In addition, we recorded the pressure time series for 180 s at 512 Hz and repeated the experiments in triplicate for each experimental condition.

If the contribution of small bubbles to the average bubble size is negligible compared to that of the large bubble, the opposite is the case for the gas-liquid interfacial area. However, we are assuming that at large gas velocities, the number of small bubbles is negligible, and large bubbles have a more pronounced presence in the system due to the dominance of the coalescence phenomenon occurring in the heterogeneous regime. The dominance of the large bubble presence could be approximately verified by analysing the dynamic gas disengagement (DGD) data reported in a previous work of the authors[122]. It was observed that by increasing the superficial gas velocity, the change of slope in the disengagement curve was hardly detectable, and then the assumption of the presence of approximately one bubble population (large bubbles) was adopted. For some operating conditions, this finding was also observed visually when performing the experimental work. It should be mentioned that all the results reported in this work are based on this assumption. Therefore, in the heterogeneous regime, the average large bubble size estimated by the signal decomposition method is assumed to be equal to the average bubble size. All conclusions reported in this work corresponded to the heterogeneous regime conditions. Furthermore, the heterogeneous regime was found to occur at lower superficial gas velocities when increasing solid concentration[122]

Figure 5.2 shows the average bubble size calculated using the signal decomposition method for two concentrations of 156-μm particles at (1% (v/v), 5% (v/v)). Increasing the solid volume fraction increased the bubble size, which was in agreement with reports in the literature[88, 90], indicating that the coalescence phenomenon was enhanced by increasing particle loading due to

the effect on liquid viscosity. We compared the bubble size values calculated in the present work with those measured by Rabha et al.[87] by ultrafast electron beam X-ray tomography in a lab-scale slurry bubble column 70-mm in diameter. Interestingly, for almost the same conditions (150-µm glass beads, 5% (v/v), and 5-cm/s superficial gas velocity), Rabha et al.[87] reported an average bubble size of 22 mm, which is very close to our value. It should be mentioned that we could not compare bubble sizes at higher gas velocities as 5 cm/s was the maximum velocity that could be attained in the 70-mm diameter column. Although this comparison was between two works performed in different scale setups, we could make a preliminary assumption that the signal decomposition method provides a good indication of the average bubble size in slurry bubble columns. Experimental bubble size data obtained for large setups and low solid concentrations are thus needed to validate the results obtained by the signal decomposition method

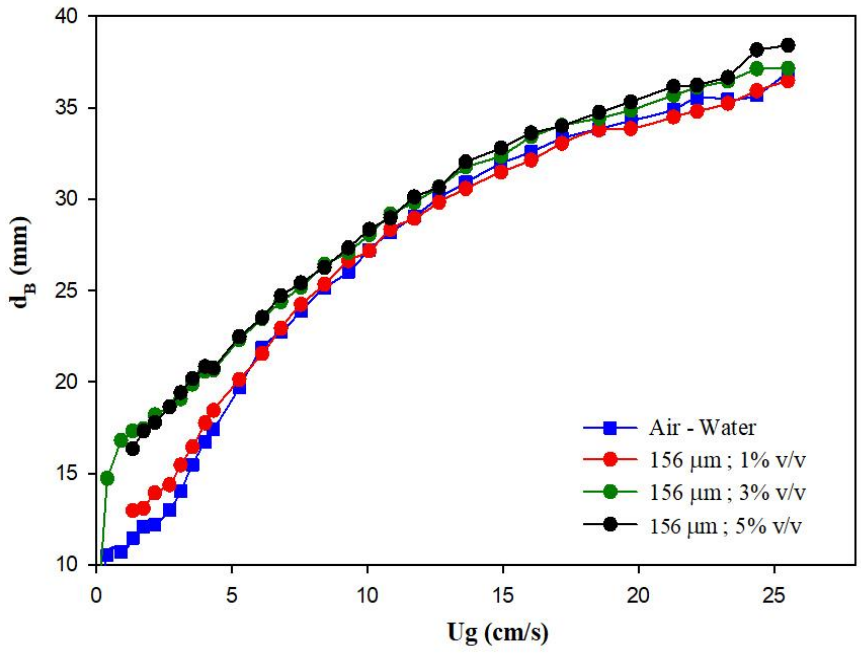

Figure 5.2 Effect of particle size on the bubble size calculated using the signal decomposition method

5.3 Results and discussion

5.3.1 Effect of solid particles on the volumetric mass transfer coefficient k_la_l

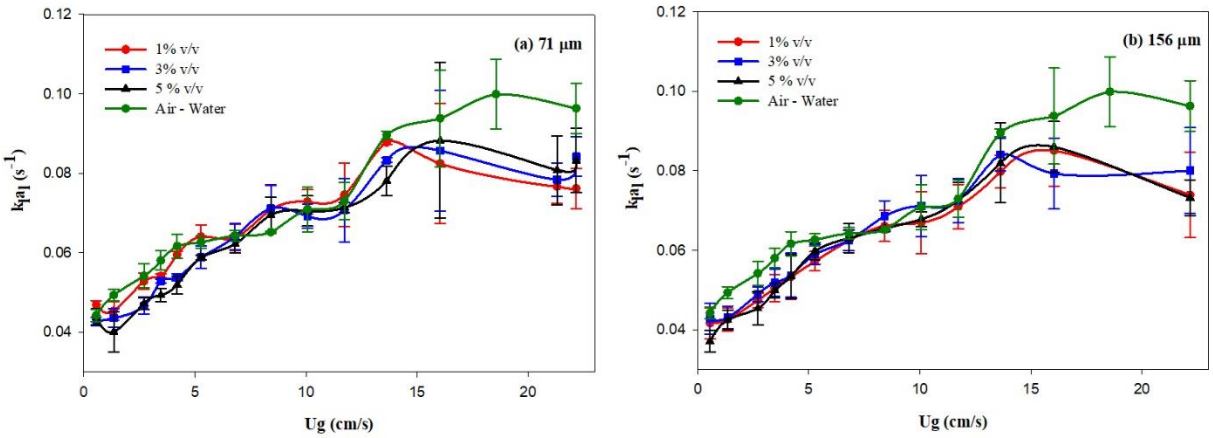

Figure 5.3 Effect of increasing the solid concentration on the volumetric gas liquid mass transfer coefficient k_la_l at a constant particle size: (a) at 71 µm ; (b) at 156 µm

Figure 5.3 shows the effect of increasing the solid particle concentration on the volumetric gas-liquid mass transfer coefficient k_la_l at two different particle sizes (71 µm and 156 µm) and different superficial gas velocities. As can be seen, k_la_l increased in tandem with the superficial gas velocity, which was expected given that increasing the amount of gas in the column enhances gas-liquid mass transfer. However, there was no dependency between the glass bead volume fraction and k_la_l for the two particle sizes. Before explaining this effect, it should be mentioned that we used inert, nonporous glass beads to avoid the *shuttle effect* and *reaction enhancement* mechanisms. Our aim was to study the *hydrodynamic effect* and the *coalescence inhibition effect* and determine which of the two was the governing mechanism within the range of our operating conditions. Our result was in agreement with that of Kluytmans et al.[117] However, these authors reported that the measured a_l does not depend on the solid concentration in their system. They concluded that particle loading has no effect on k_l, which could explain the observed effect on k_la_l. It is well known that increasing the solid concentration enhances bubble coalescence and generates large bubbles that rise faster within the column, which reduces the interfacial area[73, 78, 91]. Indeed, the common statement in literature is that increasing solid increases the apparent viscosity of the slurry phase considered

as a pseudo homogeneous phase. Therefore, the turbulent eddies that tend to break the bubbles are dampened by the high viscosity of the medium, and then the bubble coalescence phenomenon is more pronounced than the bubble breakup[49]. Other authors have reported that the interfacial area a_l decreases when the solid concentration is increased[90, 126]. Our finding was in disagreement with that of Mena et al[66], who used an air-water-polystyrene system with three particle sizes (1100 µm, 770 µm, 591 µm) and all volume fractions. They reported that solid concentration has a decreasing effect on $k_l a_l$ and attributed this to enhanced bubble coalescence by solid particles due to the effect on suspension viscosity. The gas-liquid interfacial area a_l thus decreases because the bubbles increase in size. It should be mentioned that the density of the polystyrene beads they used is similar to that of water (1050 kg/m^3). As a result, the particles tend to follow the liquid streamlines as their Stokes number ($St = \frac{v_{B\times\rho_p\times d_p^2}}{9\times\mu_{fluid}\times d_b}$) is lower than that of heavy particles. In a previous report[122], we showed that heavy glass beads (2500 kg/m^3) tend to deviate from the liquid streamlines and collide with the bubble surface. Hence, in addition to the effect on liquid viscosity, particle movement toward the bubble surface induces local turbulence in the gas-liquid film, leading to an increasing effect on k_l. Indeed, Ruthyia et al.[118] reported that collisions of particles with the gas-liquid boundary layer decrease the thickness of the layer and increase k_l. Given this, the discrepancy between our findings and those of Mena et al.[66] can be explained by the difference between the densities of the particles used. It is worth mentioning that the discrepancies between the findings on the effect of solid particles on $k_l a_l$ reported in literature could be resolved by knowing which solid property causes these discrepancies and which physical phenomena are associated with one or a combination of solid properties. Behkish et al.[119] reported that solid concentration has a decreasing effect on $k_l a_l$ for glass beads (2500 kg/m^3, 11.4 µm), which are heavier than water, unlike the polystyrene beads used by Mena et al.[66] Behkish et al.[119] also attributed the decreasing effect of solid concentration to enhanced bubble coalescence and thus a larger bubble size. Compared to the work of Behkish et al.[119], the particles used in this study were smaller in size and their Stokes number was lower. Low Stokes numbers mean that particles exhibit a preference for following the liquid streamlines and then have more effect on the liquid medium properties. However, for the large particles used in the work of Behkish et al.[119], particles may have deviated from the liquid streamlines and tended to be placed at the bubble surface . Vandu et al.[72] also reported that solid concentration has no effect on $k_l a_l$

for porous alumina particles (3900 kg/m^3, 16 µm, and 70% porosity, with concentrations up to 25%). In this case, two opposite phenomena may be responsible for the effect. This is in agreement with the results of Mena et al.[66] and Behkish et al.[119], who both used particle sizes and densities of the same order of magnitude (low particle size, high density) and reported that solid loading decreases k_la_l. The second effect is related to the porosity of the particles as k_la_l also increases in the presence of solids due to the *shuttle effect*. As such, k_la_l is not changed by an increase in solid loading. Chen et al.[127] observed a dual effect of solid concentration on k_la_l for ultrafine hollow glass microspheres (1400 kg/m^3, 8.624-µm mean diameter, superficial gas velocity up to 8.5 cm/s). They reported that, for concentrations up to 5 wt.%, k_la_l increases with solid loading while k_la_l decreases for concentrations between 5 and 25 wt.%. They attributed the increase in k_la_l to the *hydrodynamic effect* and the decrease in k_la_l to enhanced bubble coalescence, which causes a decrease in the air-liquid interfacial area.

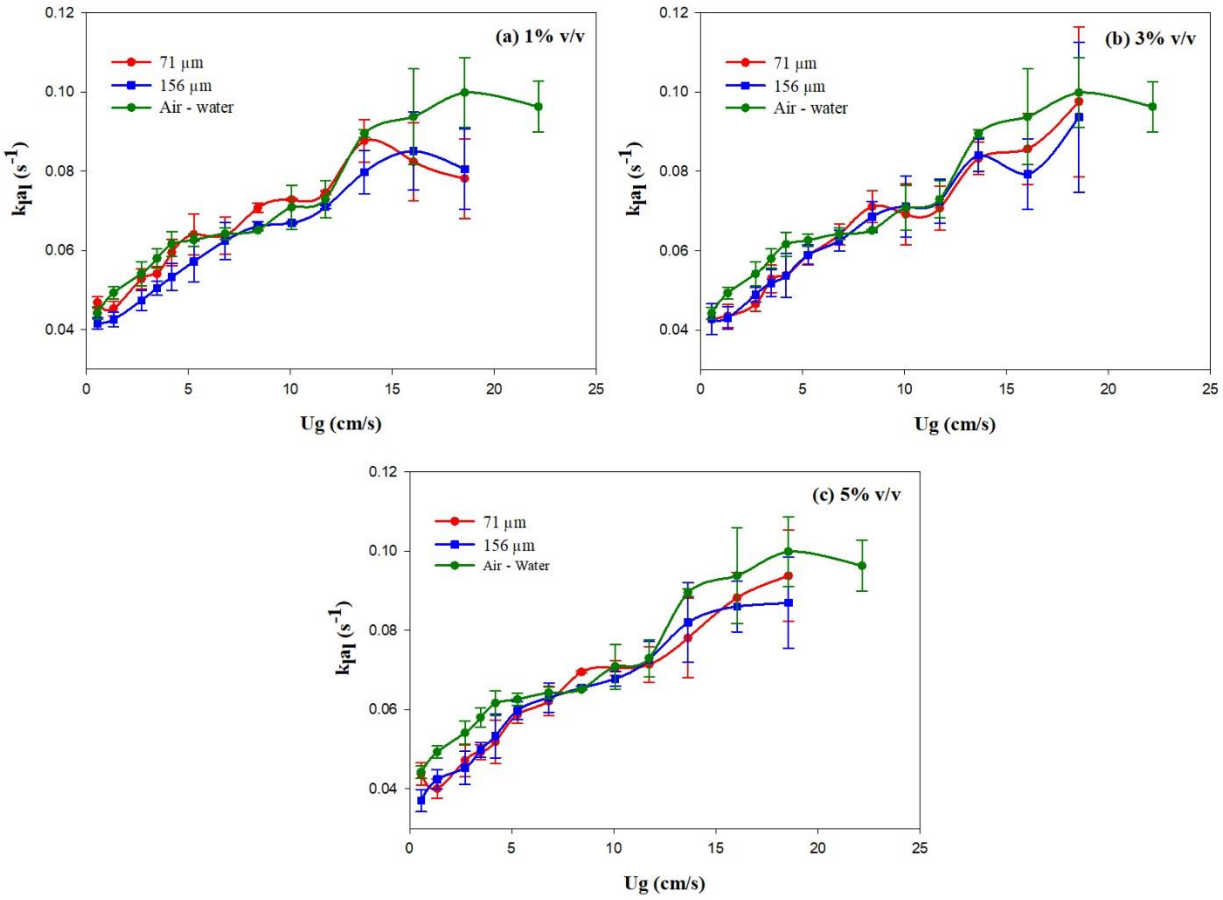

Figure 5.4 Effect of increasing particle size on the volumetric gas liquid mass transfer coefficient $k_l a_l$ at a constant solid concentration

Figure 5.4 shows the effect of doubling the particle size (71 µm and 156 µm) on the measured $k_l a_l$. Increasing particle size had no effect on $k_l a_l$ for the three solid volume fractions (1% (v/v), 3% (v/v), 5% (v/v)). Little is known about the effect of particle diameter on $k_l a_l$. Mena et al.[66] reported that, for solid concentrations up to 5% (v/v), changing the particle size (591 µm, 770 µm, 1100 µm) had a negligible effect on $k_l a_l$ while, at higher concentrations, increasing the particle size increases the mass transfer coefficient. However, they did not propose a physical explanation for their findings. Zheng et al.[128] reported that, for glass beads (0.53 mm and 0.755 mm) larger than those used in the present study but with almost the same density (2338.1 kg/m^3), increasing the particle size decreases $k_l a_l$ and that this effect is more pronounced at higher gas velocities. However, they did not provide an explanation for this effect. The discrepancy between our findings and those

of Zheng et al.[128] may be related to the difference between the range of particle sizes used in the two studies. When large particles are used (in the mm range), the *steric effect* induced by the presence of solid particles is more pronounced. The solid particles thus occupy their own space in the column independently of the gas and liquid phases. Mena et al.[38] reported that the gas holdup in their gas-liquid-solid system is $\left(1-\frac{C_V}{100}\right)$ times lower than in a gas-liquid system of the same volume. As such, using particles in the mm range decreases the volume of gas and thus gas-liquid mass transfer. Kim et al.[129] observed a similar trend to that reported by Zheng et al.[128] using glass beads lower than 1 mm in size with almost the same density (2500 kg/m^3). However, they observed the opposite effect for particles larger than 1 mm in size. Interestingly, Koide et al.[130] found that increasing the particle diameter of large Ca-alginate gel particles $\left(1.88\ \text{mm} \leq d_p \leq 3.19\ \text{mm}\right)$ with almost the same density as water (1070 kg/m^3) had no effect on $k_l a_l$ for solid concentrations up to 20%.The authors did not, however, provide an explanation for this effect. The low density of Ca-alginate gel particles compared to the glass beads used by Zheng et al.[128] may explain the difference between the two studies.

To gain more insight into these findings, the effect of the presence of solid particles on k_l and the air-liquid interfacial area a_l must be differentiated. The mass transfer coefficient was then deduced from the measured $k_l a_l$ and the calculated a_l.

5.3.2 Effect of solid particles on the air-water surface area a_l

The air-water surface area a_l was calculated using the following equation by assuming that bubbles have a spherical shape:

$$\boldsymbol{a_l = \frac{6\varepsilon_g}{d_{32}(1-\varepsilon_g)}} \tag{5.12}$$

where ε_g is the total gas holdup measured previously[122] and d_{32} is the Sauter mean diameter calculated using the signal decomposition method.

Figure 5.5 shows the effect of solid concentration on the calculated a_l at different superficial gas velocities. In the heterogeneous regime and in agreement with several authors[90, 126, 127], an increase in the solid concentration causes a decrease in a_l for both particle sizes due to enhanced bubble coalescence.

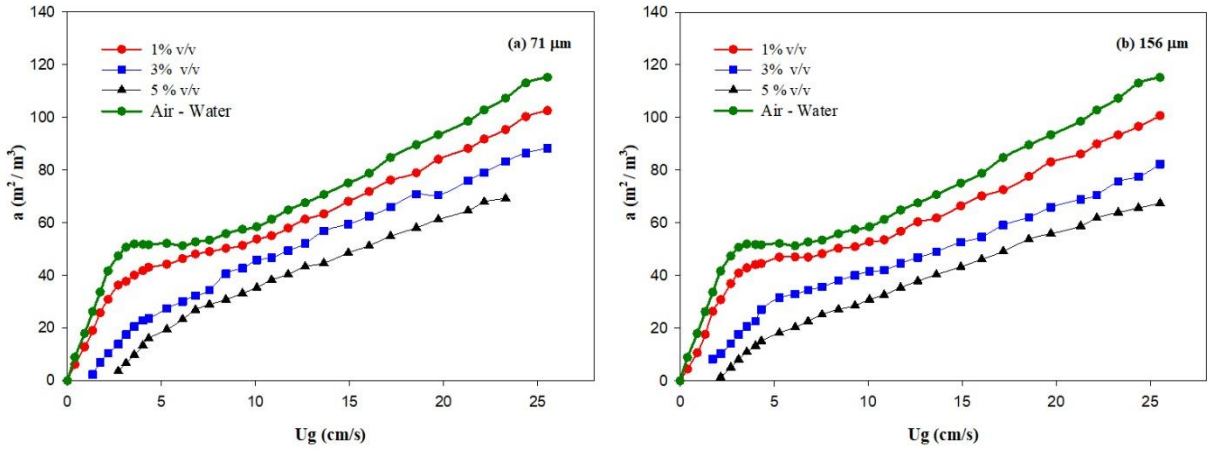

Figure 5.5 Effect of increasing the solid concentration on the air liquid interfacial area a_l at a constant particle size

Figure 5.6 shows that an increase in particle size resulted in a decrease in a_l starting from a 3% (v/v) concentration in the heterogeneous regime (high superficial gas velocities). In a previous work of the authors[122], a new correcting factor called the hindering factor (HF) $[(1-E_c)\times(1-C_v)]^{5.43}$ has been developed to quantify the simultaneous effect of particle size and solid concentration on the total gas holdup. This factor includes a particle size depending term $[(1-E_c)]^{5.43}$ and a concentration depending term $[(1-C_v)]^{5.43}$. The simultaneous effect of particle size and solid was clarified based on the following statement: Increasing particle size and concentration increases the hindering factor. As a result, particles tend to hinder bubbles from rising, which increases the probability of contact between bubbles and then enhances bubble coalescence and increases bubble size. At low solid concentration (1%), the hindering factor is lower than at high solid concentrations (3% and 5%). Therefore, the effect of increasing particle size in decreasing gas holdup and then decreasing the air-liquid interfacial area a is more pronounced at higher concentrations. At low superficial gas velocities (homogeneous regime), the coalescence phenomenon doesn't occur as the bubbles are small and rise in a vertical direction throughout the column. Consequently, solid particles do not affect the bubble size and the interfacial area a_l at these low velocities.

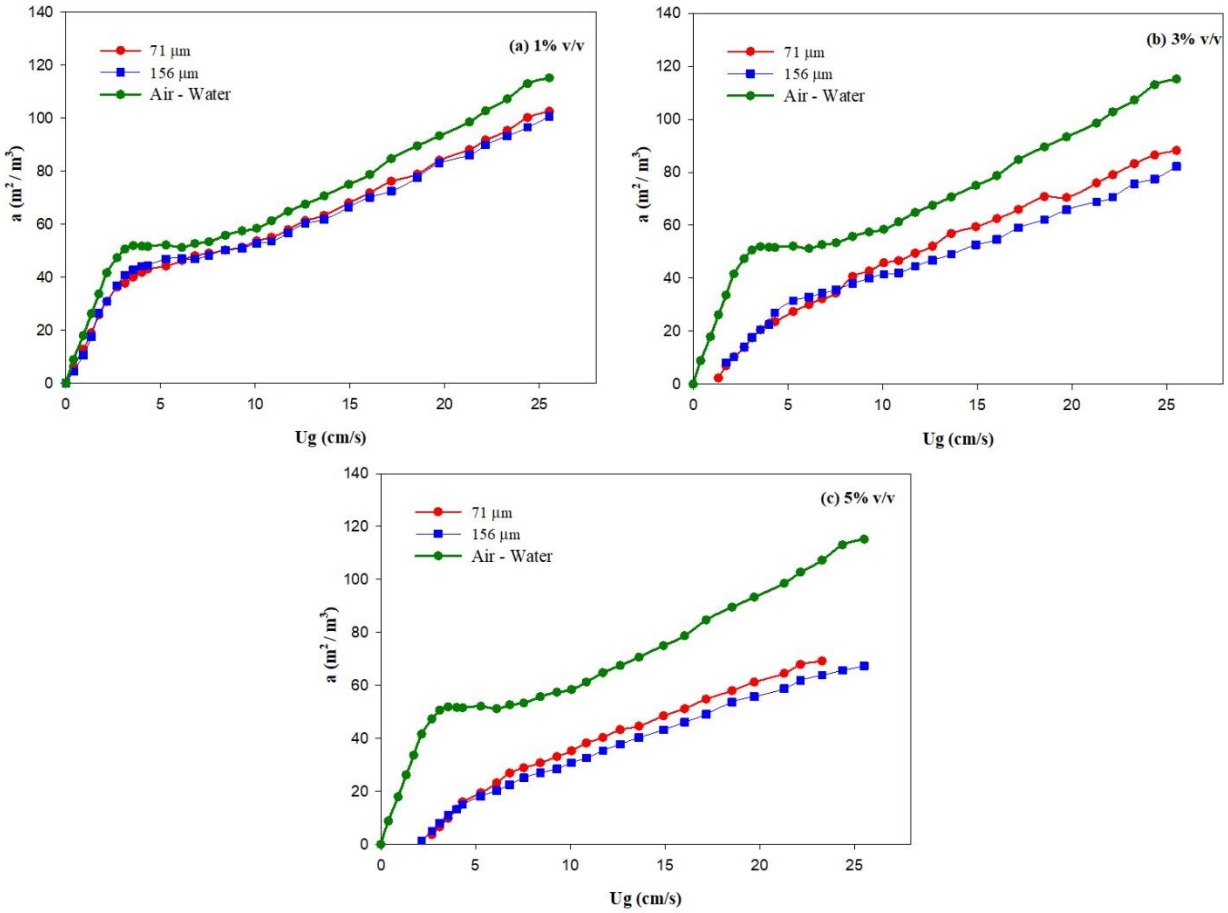

Figure 5.6 Effect of an increase in particle size on the air-liquid interfacial area a_l at a constant solid concentration

Based on the effect on a_l, the *coalescence inhibition effect* can be discarded for the range of operating conditions used in the present work as the hydrophilic glass beads promote bubble coalescence and increase bubble size. n the heterogeneous regime, increasing particle size and concentration increases the hindering effect of the hydrophilic particles that tend to hinder bubbles from rising, which increases the probability of contact between bubbles and then enhances bubble coalescence. The hindering effect has been discussed in more detail in a previous work of the authors[122].

5.3.3 Effect of solid particles on the liquid side mass transfer coefficient k_l

Figure 5.7 shows the liquid side mass transfer coefficient k_l obtained based on the measured $k_l a_l$ value and the calculated a_l value. Increasing the superficial gas velocity decreased k_l for all the

operating conditions studied. Glass beads in slurry bubble columns tend to reach the bubble surface by the collision phenomenon[122]. However, as they are hydrophilic, they do not adhere or attach to the surface due to the absence of an adhesion force. Following collision, they preferably enter the liquid film surrounding the bubble or the bulk liquid, depending on the shear stress. A high shear stress tends to displace particles from the liquid film and move them to the bulk liquid as the mixing intensity is higher. The shear stress in bubble columns is proportional to the superficial gas velocity[118]. When the particles enter the liquid film, *the hydrodynamic effect* mechanism is more pronounced, which increases k_l. At higher superficial gas velocities, the particles are displaced into the bulk liquid, lessening the *hydrodynamic effect* and decreasing k_l. The decrease in the effect of the superficial gas velocity on k_l is more pronounced at a high solid concentration (5% (v/v)) than at a low solid concentration (1% (v/v)) as there are more solid particles and the difference between the number of particles in the liquid film and bulk liquid is more pronounced.

Increasing solid loading from 1% to 5% (v/v) increased k_l for the same superficial gas velocity and for both particle sizes. This is in agreement with the findings of Chen et al. [127], who reported that, at low concentrations (up to 5wt. %), an increase in solid loading increases k_l. For the range of concentrations used in the present work (1 to 5% (v/v)), increasing the solid volume fraction at a specific superficial gas velocity increased the number of particles in the liquid film and led to a more pronounced *hydrodynamic effect*. These findings provide a clear explanation of the effect of the presence of solid particles on the volumetric gas-liquid mass transfer coefficient $k_l a_l$ for the operating conditions used. Solid particles have two effects when added to a gas-liquid system. The first effect consists of a change in the bulk liquid viscosity and density. Increasing the solid concentration increases the liquid viscosity, which enhances bubble coalescence and thus bubble size. Consequently, in the present study, the gas-liquid interfacial area a_l decreased as a result of the first effect. The second effect involves the movement by collision of a certain number of hydrophilic particles toward the liquid film surrounding the bubble and enhances mass transfer by the *hydrodynamic effect*. In the present study, the liquid side mass transfer coefficient k_l increased as a result of the second effect. The two opposite effects of decreasing a_l and increasing k_l by increasing solid concentration cancelled any potential effect of the solid on the volumetric gas-liquid mass transfer coefficient $k_l a_l$.

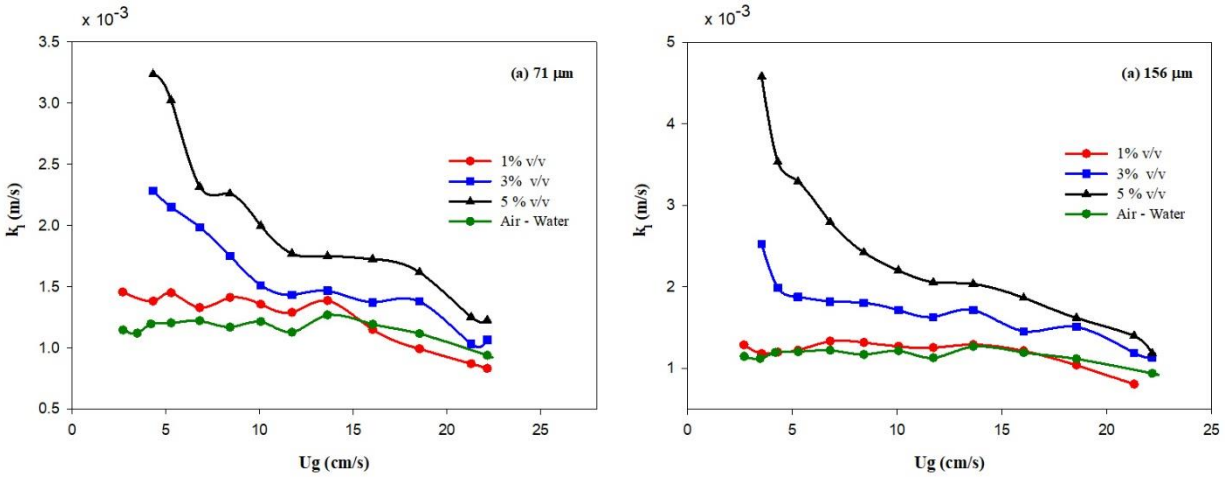

Figure 5.7 Effect of increasing the solid concentration on the liquid side mass transfer coefficient k_l at a constant particle size

The collision effect is a function of particle size. Hence, it was found in a previous work of the authors[122] that increasing particle size depends on the collision efficiency parameter E_c. The latter quantifies the number of particles that deviate from the liquid streamlines and move toward the bubble surface. Increasing particle size increases the collision efficiency parameter and then the bubble-particle collision[122].

If the collision is more pronounced, the *hydrodynamic effect* increases the liquid side mass transfer coefficient k_l in the heterogeneous regime, which can be clearly seen in Figure 5.8.

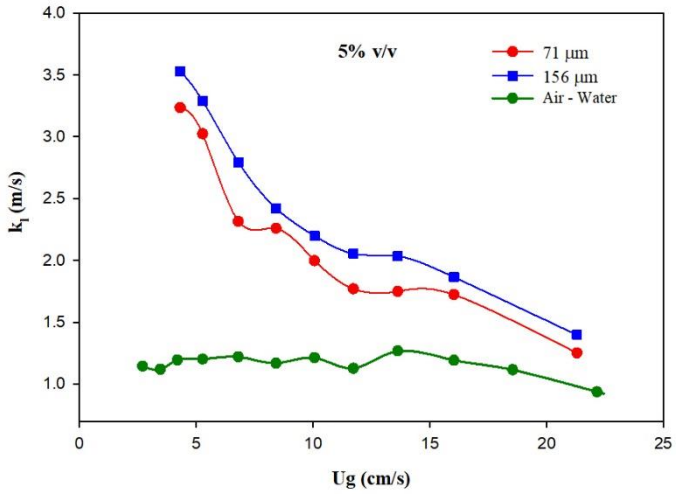

Figure 5.8 Effect of increasing the particle size on the liquid side mass transfer coefficient k_l at a particle concentration of 5% (v/v)

5.3.4 Verification of the applicability of the two-phase approach on predicting the experimental volumetric mass transfer coefficient k_la_l

The two-phase approach consists of considering a three-phase system (gas-liquid-solid) as a two-phase system (gas-slurry). By applying this approach, all correlations developed previously to predict hydrodynamic or mass transfer parameters in gas-liquid systems can be used for three-phase systems by only adjusting liquid properties to slurry properties. In our previous study[122], we demonstrated that the two-phase approach overestimated the experimental gas holdup and could not be applicable to the used air-water-glass beads system. In the same frame, we compared the experimental k_la_l data with the k_la_l predicted by the two-phase approach. To do so, we conducted a comprehensive literature review to find the most relevant correlations developed for gas-liquid systems. The five correlations found are summarized in Table 5.2. Akita and Yoshida[131] developed a k_la_l correlation from experimental data obtained with different gas-liquid systems and inside diameters of bubble columns. The gas-liquid systems investigated were: water-oxygen; 3 and 7 centipoise glycerol solution-oxygen; 30, 70 and 100 Vol% glycol solution-oxygen; Methanol-oxygen and 0.15M Na_2SO_3 solution-air. Hikita et al.[132] performed their experiments, prior to developing their correlation, in bubble columns with inside diameters of 10 cm and 19 cm using several gases and pure liquids and aqueous non-electrolyte solutions, such as air-water, air-30 wt.% sucrose, air- n-butanol, air-15 wt.% methanol, CH_4-water, CO_2-water. In other works,

Shah et al.[133] reported a correlation for an air-water system in a bubble column with an inside diameter of 20 cm and Letzel et al.[123] developed a correlation for the same system in a 15 cm inside diameter setup. The last correlation used was from Vandu and Krishna's[134] work where the experimental work was performed for air-water system in bubble columns with three different diameters (10, 15 and 38cm).

Table 5.2 Summary of $k_l a_l$ correlations developed for gas-liquid systems

Authors	**Correlation**
Akita and Yoshida[131]	$\frac{k_l a_l {D_c}^2}{D_l} = 0.6\left(\frac{\mu_l}{\rho_l D_l}\right)^{0.5}\left(\frac{g{D_c}^2\rho_l}{\sigma}\right)^{0.62}\left(\frac{g{D_c}^3{\rho_l}^2}{{\mu_l}^2}\right)^{0.31}{\varepsilon_g}^{1.1}$
Hikita et al.[132]	$\frac{k_l a_l U_g}{g} = 14.9\left(\frac{U_g\mu_l}{\sigma}\right)^{1.76}\left(\frac{{\mu_l}^4 g}{\rho_l\sigma^3}\right)^{-0.248}\left(\frac{\mu_g}{\mu_l}\right)^{0.243}\left(\frac{\mu_l}{\rho_l D_l}\right)^{-0.604}$
Shah et al.[133]	$k_l a_l = 0.467{U_g}^{0.82}$
Letzel et al.[135]	$k_l a_l = 0.5\varepsilon_g$
Vandu and Krishna[134]	$k_l a_l = 0.48\varepsilon_g$

It should be mentioned that $k_l a_{l,2phase-approach}$ was calculated for each of the aforementioned models by changing ρ , μ and D_l to slurry density ρ_{slurry} ,slurry viscosity μ_{slurry} and oxygen molecular diffusivity in the slurry phase D_{slurry} respectively. Also, the addition of solid particles doesn't affect, in general, the liquid surface tension[96]

μ_{slurry} and D_{slurry} were calculated by the correlation of Saxena and Chen[97] and Öztürk et al[136] respectively:

$$\boldsymbol{\mu_{slurry} = \mu_{liquid} \times (1 + 4.5 \times C_v)} \quad (5.13)$$

$$\boldsymbol{D_{slurry} = 5 \times 10^{-11} \times {\mu_{slurry}}^{-0.57}} \quad (5.14)$$

In addition, the experimental data chosen to verify the two-phase approach were in the range of the applicability of the five correlations.

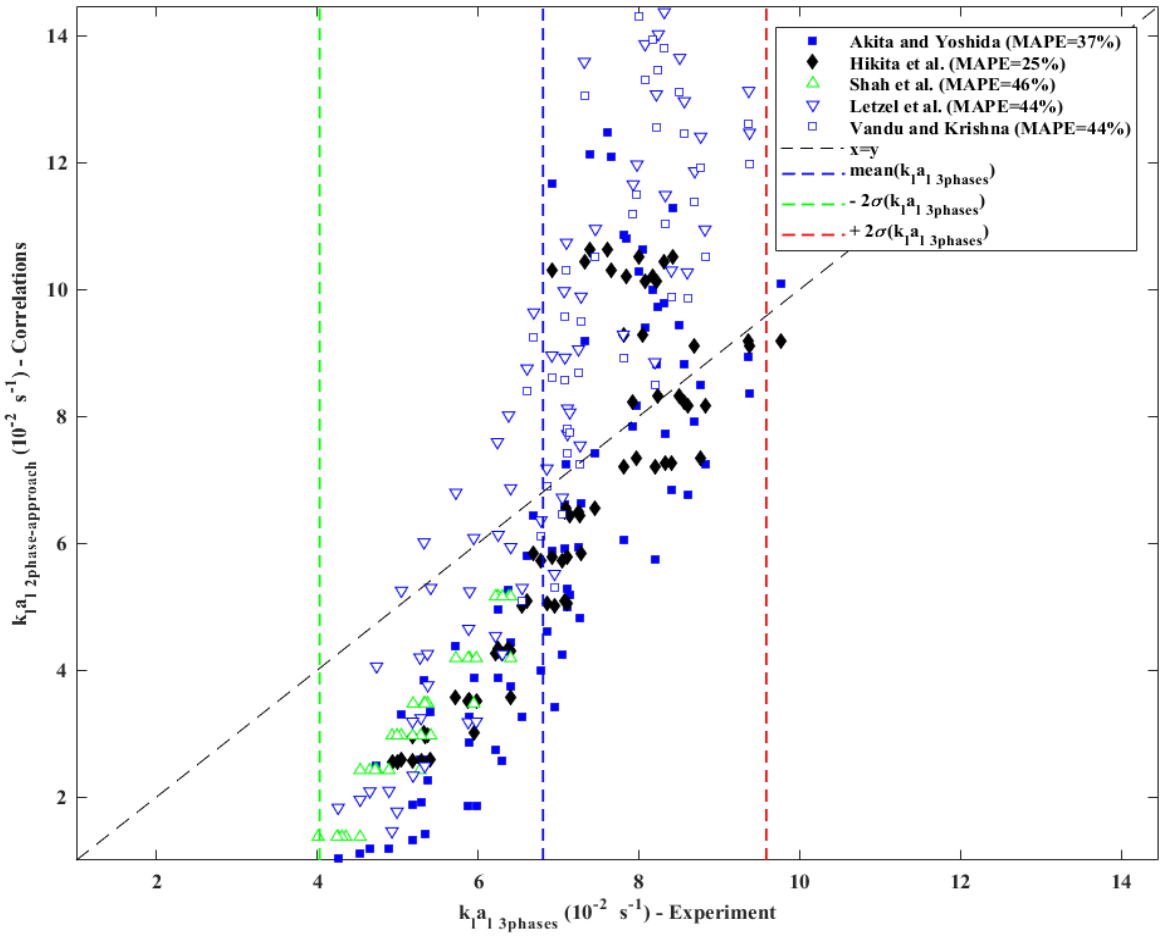

Figure 5.9 Comparison between the $k_l a_l$ estimated by the two-phase approach and the experimental $k_l a_l$

Figure 5.9 shows the comparison between the $k_l a_l$ estimated by the two-phase approach and the $k_l a_{l,3phases}$ obtained experimentally for the three solid concentrations and the two particle sizes used. The mean value of $k_l a_{l,3phases}$ and the two standard deviations (±2σ) from this mean are also shown in this figure. As a first observation, the two-phase approach didn't predict well the three-phase $k_l a_l$ and the mean absolute percentage error MAPE of prediction was 25%. Second, contrary to gas holdup results found in our previous study[122], the error of two-phase prediction did not depend

on solid concentration nor on particle size within the range of conditions used. This finding confirms that $k_l a_l$ did not depend on solid concentration and particle size. The third most interesting finding is that the range of variability of $k_l a_l$ narrowed drastically when moving from the two-phase approach to the three-phase approach. The $k_l a_l$ estimated by gas-liquid correlations had a mean value of $6.9 \times 10^{-2}\ s^{-1}$ and a standard deviation value of $4.17 \times 10^{-2}\ s^{-1}$ whereas the three-phase $k_l a_{l,3phases}$ had almost the same mean value of $6.8 \times 10^{-2}\ s^{-1}$ but a standard deviation of $1.38 \times 10^{-2}\ s^{-1}$. Hence, we can conclude that the two-phase approach couldn't predict the low variability of $k_l a_l$ when changing solid concentration and particle size. However, it is of prime importance to focus the efforts on the development of correcting factors that can describe and quantify accurately the physical phenomena resulting from particle presence in addition to altering the liquid viscosity, density or gas-liquid diffusivity. The above correcting factors would make it possible to estimate the experimental $k_l a_l$ by correcting the $k_l a_l$ predicted by the two-phase approach.

In addition, as the two-phase approach considers only the change in liquid properties and not the additional effect of solid particles on bubble behavior and liquid film turbulence, this finding could indicate that changing solid particle properties has less effect on $k_l a_l$ compared to a liquid system with the same properties. However, more experiments with different solids, concentrations, and particle sizes as well as with liquids having the same slurry properties should be performed to corroborate the aforementioned statements.

5.4 Conclusion

In the present work, we clarified the effect of the presence of solid particles on the volumetric gas liquid mass transfer coefficient $k_l a_l$ in a relatively large slurry bubble column in the heterogeneous regime. The experimental results showed that, at a constant particle size, increasing the solid concentration from 1% (v/v) to 5% (v/v) had no effect on $k_l a_l$ for all the superficial gas velocities studied. We could not increase the concentration more than 5% (v/v due to the hard fluidization of the heavy particles used (2500 kg/m^3). Also, at a constant concentration, increasing the particle size in the micron range had a negligible effect on $k_l a_l$. Our strategy aimed to narrow the range of different operating conditions and solid properties to pinpoint the mechanism that governs how particles affect mass transfer. We used inert nonporous hydrophilic glass beads to investigate the

occurrance of the *hydrodynamic effect* and *coalescence inhibition* mechanisms and determine whether one or both of them govern the solid effect on gas-liquid mass transfer. Based on the results of the present study, we were able to explain the effects of three solid properties, that is, density, particle size, and concentration on the gas-liquid mass transfer phenomenon. These three properties can be brought together in the Stokes dimensionless number that describes particle trajectories within a gas-liquid system. In the heterogeneous regime, the presence of particles in the bulk liquid affects its viscosity and decreases the gas-liquid interfacial area a_l. On the other hand, the presence of solids in the liquid film increases the liquid side mass transfer coefficient k_l. These two opposing effects of decreasing a_l and increasing k_l by solid concentration suppress any effect of the solid on $k_l a_l$. However, more work should be done to understand the effect of other solid properties on the mechanisms governing the enhancement of mass transfer. These properties must be investigated in order to accurately associate each property with the corresponding physical phenomena, which will make it possible to understand all the discrepancies reported in the literature. In addition, when reporting an effect, the range of operating conditions used must be provided. We also confirmed the collision phenomenon, which we introduced in a previous study, and showed that it was mainly affected by particle size. Finally, we demonstrated that the two-phase approach couldn't predict well the low variability of the experimental three-phase $k_l a_l$. However, this statement requires further investigation with more concentrations and particle sizes to be verified.

5.5 Acknowledgements

The authors thank TOTAL American Services, Inc. and the Natural Science and Engineering Research Council of Canada (NSERC) for their financial support.

CHAPTER 6 ARTICLE 3: EFFECT OF PRESSURE ON THE HYDRODYNAMICS OF A PILOT-SCALE BUBBLE COLUMN OPERATING WITH LOW AND MODERATE VISCOSITY NEWTONIAN LIQUIDS

El Mahdi Lakhdissi [1], Shuli Shu[1], Sherif Farag [1,2], Christophe Guy[3], Jamal Chaouki[1, *]

[1]Dpt. of Chemical Engineering, Polytechnique Montréal, P.O. Box 6079, St. C.V., Montréal, Qc., Canada H3C 3A7

[2]Mohammed VI Polytechnic University, Ben Guerir, Morocco

[3] Dpt. of Chemical & Materials Engineering, Gina Cody School of Engineering & Computer Science, Concordia University, 1455 Boulevard de Maisonneuve W., Montréal, Qc., Canada H3G 1M8

*****Corresponding author: jamal.chaouki@polymtl.ca;

(Submitted to Chemical Engineering Journal, May 30th ,2020)

Abstract

In a pilot-scale bubble column operating with low and moderate viscosity hydrocarbons, the effect of pressure on the total and axial gas holdup, as well as the regime transition velocity, was investigated. Experiments were performed for two air-Ketrul D100 and air-Hydroseal G250 HL gas-liquid hydrocarbon systems. It was found that increasing pressure increased gas holdup at the heterogeneous regime, and this effect was more pronounced for the low-viscosity liquid. Moreover, increasing pressure stabilized the homogeneous regime more, and again, this stabilizing effect was more significant for the low-viscosity liquid. Also, as a response to the pressure increasing, the axial gas holdup became more uniform in the case of the low-viscosity liquid and less uniform in the case of the moderate-viscosity liquid.

Keywords: Gas-liquid bubble column, elevated pressure, gas holdup axial distribution, regime transition, low-viscosity, moderate-viscosity

6.1 Introduction

Nowadays, growing global needs for chemical products result in more chemical processing and a growing shortage of non-renewable fossil resources. These resources dispense 86% of the world's energy and 96% of organic chemicals[3]. In addition, the new environmental considerations dictate a reduced energy consumption as well as a shift toward greener processes. Hence, it becomes of great interest to design and optimize processes that ensure maximum reactant conversion, minimum waste production, and renewable feedstock use[137]. Also, the production of green and sustainable chemicals requires the use of renewable resources to meet environmental constraints in the whole product life cycle. Bubble columns are known as one of the most utilized reactors in several industrial applications that treat these new feedstocks in addition to conventional fossil resources[138]. Chemical, petrochemical, biochemical, food, pharmaceutical and carbon dioxide capture processes take place in bubble columns. They are selected from among other gas-liquid reactors for their ease of operation as well as their low maintenance and operating costs.

The new approach of using biomass or other feedstocks to produce fuels, chemicals and materials gives rise to the question of the complexity of these new raw materials as well as the effect of their properties on the process performance in bubble columns. The use of highly viscous Newtonian and Non-Newtonian liquids as well as operation at elevated pressures and temperatures become a must to reach that goal. Therefore, it is of great interest to study, in addition to reaction kinetics, the bubble dynamics within those conditions. The knowledge of fluid dynamics at bubble scale (bubble size distribution, bubble velocity) and reactor scale (global, radial and axial gas holdups, mean residence time) can elucidate the impact of the above mentioned extreme conditions.

Liquid properties[139], such as density, viscosity, surface tension, specific heat capacity and electrical conductivity, are among the critical parameters that affect gas holdup and bubble size distribution in bubble columns. Several research studies investigated the effect of liquid viscosity on bubble behaviour. Generally, it has been observed that increasing liquid viscosity decreased gas holdup due to bubble coalescence enhancement. Schafer et al.[49] attributed this effect to low turbulence in the medium due to high viscosity, as the liquid eddies don't have sufficient energy to break the bubbles. Thus, bubble breakage decreases, which results in a bubble size increase and gas holdup decrease. Similarly, several previous studies reported a reduction of the gas holdup due

to a liquid viscosity increase (Akita and Yoshida[131], Wilkinson et al.[140], Kuncova and Zahradnik[141], Hwang and Cheng[142], Yang et al. 2010[143]). In contrast, other previous studies[144-146] reported that increasing liquid viscosity could increase gas holdup if the liquid viscosity is low. Consequently, they came up with the dual effect of viscosity on the gas holdup approach to explain the contradictory results in the literature. It should be mentioned that this dual effect was observed in previous works either for Newtonian liquids[145] or viscoelastic non-Newtonian liquids[147]. This dual effect was first investigated by the work of Eissa and Schurgel[148] who observed that the gas holdup increased for low viscosities (< 3mPa.s), decreased for moderate viscosities (3-11 mPa.s) and remained constant at higher viscosities. Similarly, Ruzicka et al.[145] reported that for low viscosity glycerol aqueous solutions (1-3 mPa.s), increasing liquid viscosity increased the gas holdup and stabilized the homogeneous regime. Conversely, they found that for moderate viscosity liquids (3-22 mPa.s), increasing liquid viscosity decreased the gas holdup and destabilized the homogeneous regime by reducing the transition velocity. Besagni et al.[149] also reported this dual effect, stating that the coalescence phenomenon is less pronounced at low viscosities, and the large drag force decreases bubble rise velocity. Therefore, gas holdup increases. At moderate/high viscosities, bubbles are more prone to coalesce into large bubbles that rise at a higher velocity within the column. Gas holdup decreases in consequence. Regarding the effect on the regime transition velocity, it was similarly observed that the homogeneous regime might either be stabilized or destabilized by increasing liquid viscosity[141, 143, 145, 146].

The effect of increasing pressure on global gas holdup and bubble size has been investigated in several previous studies[69, 71, 123]. Accordingly, it was observed that the gas holdup increases with pressure due to an increase in gas density, which results in increasing the gas-phase momentum and a more pronounced bubble breakup[68, 69]. Therefore, the effect of pressure on the global hydrodynamics (gas holdup) of gas-liquid bubble columns is investigated in the literature. Moreover, the effect of axial distance from the gas distributor on the gas holdup at different gas velocities and liquid properties has been well covered in the literature[40, 150-152]. Kumar et al.[150] reported that, for an air-water system, increasing the distance from the distributor increases the gas holdup. They stated that the bubbles formed at the distributor are larger and gradually break up as they rise through the reactor, which results in increasing gas holdup.

Similarly, Jin et al.[151] observed experimentally that for air-water and air-acetic acid systems, the local gas holdup increased with axial height in a bubble column having a 0.3m inside diameter and 6.6m in height.

The separate effect of the liquid viscosity, as well as the operating pressure on global and axial gas holdup, is well assessed in the literature for gas-liquid bubble columns. To our knowledge, however, there is a lack of research concerning the evolution of gas holdup axial distribution when increasing pressure for different ranges of liquid viscosities.

To reach this goal, we have conducted experiments with a hydrocarbon of low viscosity (2.9 mPa.s) and another with moderate viscosity (4.35 mPa.s). The two liquids have the same density and almost the same surface tension at the investigated operating conditions. By not omitting the importance of Non-Newtonian liquids as they are used in several chemical processes[40], the scope of this research work is to use Newtonian liquids of different viscosities.

In addition, studying the hydrodynamics by using those types of liquids is very important for several industrial processes. As an example, the hydroconversion of heavy oils is conducted at 100 atm pressure and 400˚C temperature by bubbling the hydrogen gas. Investigating the hydrodynamics in such extreme conditions is almost impossible. S*imilitude fluids* are fluids having nearly the same properties as the gas-liquid reactants used industrially but at relatively lower pressure and temperature (gas density, liquid viscosity). Therefore, it is of great interest to mimic the extreme industrial conditions by using those similitude fluids in a pilot-scale unit to study bubble behaviour.

6.2 Experimental

6.2.1 Bubble column setup

The experiments were conducted using a high-pressure and high-temperature gas-liquid bubble column unit. The schematics of the setup is shown in Figure 6.1. In addition to the bubble column reactor, a PLC control unit, two gas compressors, a liquid pump, electrical gas heating elements, two compressors, two gas-liquid separators, two air compressors, and a high-pressure air storage cylinder make up the multiphase unit. As the experiments were performed in a semi-batch mode, the initial static liquid height was adjusted to 1.1m before starting any set of experiments. The

bubble column unit was a stainless steel reactor with an inner diameter of 0.15m and 4.8m in height. It could operate at pressures up to 30 bars and temperatures up to 300˚C. The compressed air was conveyed from the cylinder storage and fed to the column through a stainless steel perforated plate distributor. The latter had 24 square-pitch spaced orifices of 1mm in diameter and 1316 orifices/m^2 to enable a uniform gas distribution through the column. More details about the design and the construction of this multiphase flow unit can be found in the work of Esmaeili et al.[19] . Two pneumatic ball valves were used to control and regulate simultaneously the system pressure as well as the superficial gas velocity. Experiments corresponding to this research work were conducted by varying the superficial gas velocity from 1 to 30 cm/s to cover both homogeneous and heterogeneous regime.

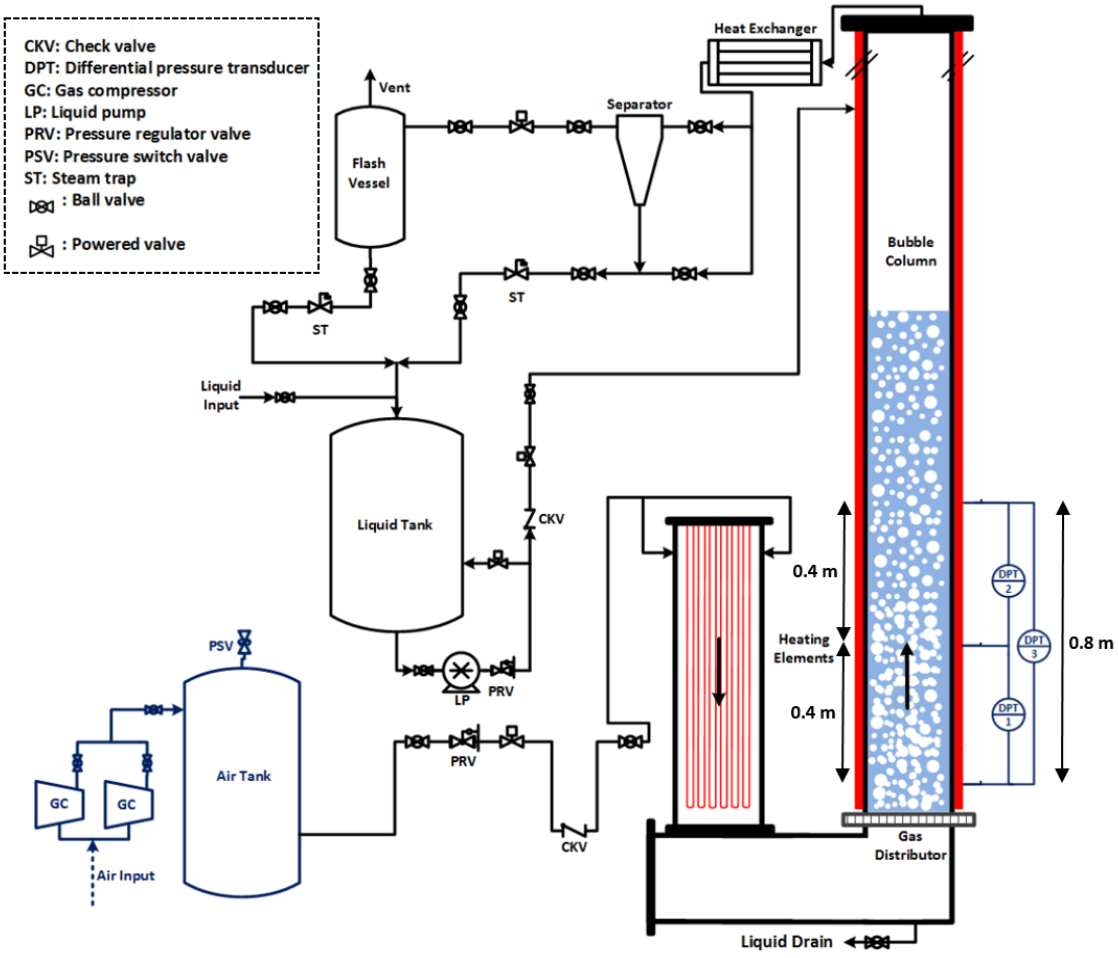

Figure 6.1 A schematic of the multiphase unit (Adapted from the work of Esmaeili et al.[153])

Three fast response differential pressure transducers (CE5NBA20, Viatran Inc.) flush-mounted on the reactor wall were used to measure the total gas holdup (DPT3) as well as the gas holdup in two different zones of the active height (DPT1 and DPT2). The gas holdup was calculated by the pressure drop method using the following equation:

$$\varepsilon_g = 1 - \frac{1}{\rho_l g}\left(\frac{\Delta P}{\Delta Z}\right) \tag{6.1}$$

where ρ_l is the liquid density, and ΔP is the differential pressure measured over a ΔZ height.

Two transducers were installed to record the differential pressure in two-equal volume zones (bottom zone and top zone). The third transducer was placed to measure the total gas holdup. It should be mentioned that the upper legs of the total gas holdup transducer, as well as the top zone transducer, were placed far from the free liquid surface. The reason is to avoid the effect of bubble eruption, occurring within the free liquid surface, on the bubble breakup and coalescence process. The pressure fluctuations were recorded for 120s at a 512 Hz frequency.

6.2.2 Materials and rheological and surface tension characterization

TOTAL Inc. provided two liquid hydrocarbons of low and moderate viscosities (Ketrul D100 and Hydroseal G250 HL) to our research group in order to perform hydrodynamic measurements. The rheological characterization of the two hydrocarbons was carried out at three different temperatures (25˚C, 50˚C and 75˚C) in a modular compact rheometer (MCR-501, Anton Paar) with a double-gap Couette geometry. The apparent viscosity (μ_{app}) was measured at different shear rates ranging from 10 to 1000 s^{-1} in order to mimic the effective shear rate inside the column. Nishikawa et al.[154] reported that the average shear rate is a linear function of the superficial gas velocity in a bubble column ($\dot{\gamma}_{av} = 5000U_g$). The range of the superficial gas velocity used in this study (0.01-0.3 m/s) results then in an effective shear rate range of 50-1500 s^{-1}. Figure 6.2 shows that, for both Ketrul D100 and Hydroseal G250 HL, the apparent viscosity was almost constant over the range of the applied shear rates as well as for the three temperatures. Therefore, both liquids were showing a Newtonian behaviour. In addition, both liquids' viscosities decrease with increasing temperature. The apparent liquid viscosities for both hydrocarbons are summarized in Table 6.1. At ambient temperature (25˚C), Hydroseal G250HL ($\mu_{app} = 4.35\ mPa.s$) is more viscous than

Ketrul D100 ($(\mu_{app} = 2.9\, mPa.s)$. Hydroseal G250HL is therefore a Newtonian liquid with a moderate viscosity at ambient conditions, whereas Ketrul D100 is a Newtonian liquid with a low viscosity. It should be mentioned that, in general, increasing pressure has an insignificant effect on the viscosity of the liquid for pressures less than 40 bars[155].

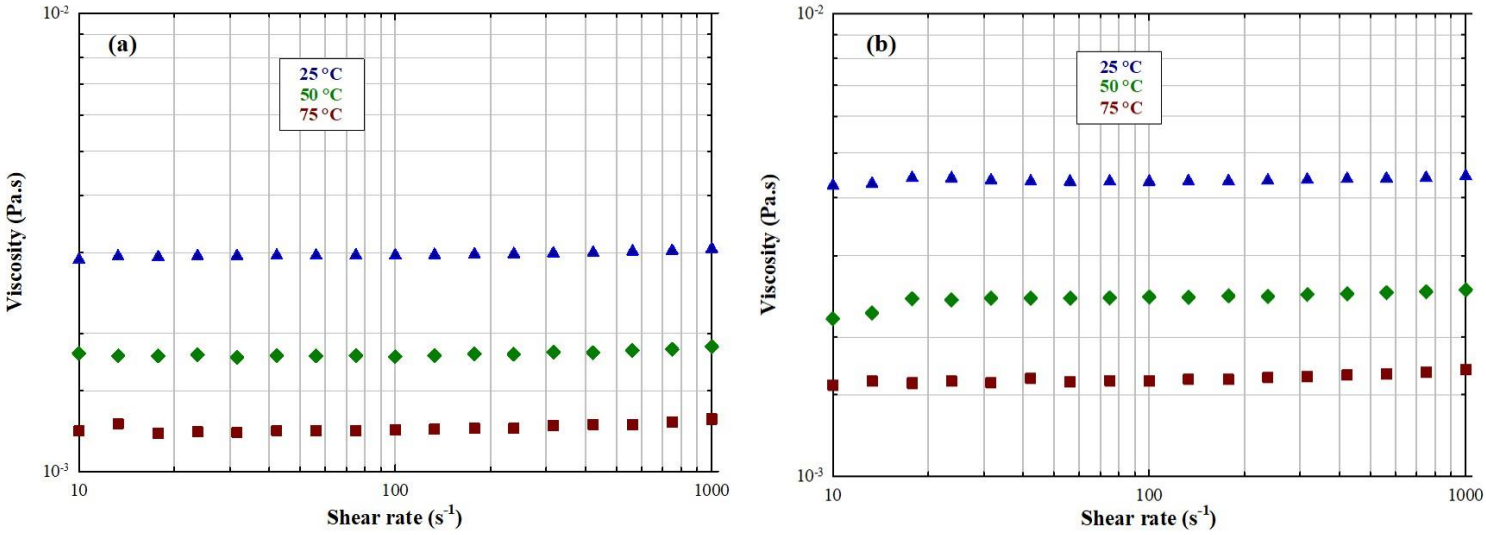

Figure 6.2 Variation of (a) Ketrul D100 and (b) Hydroseal G250 HL apparent viscosity with the shear rate at three different temperatures

Table 6.1 Physical properties of Ketrul D100 and Hydroseal G250 HL at different temperatures

	Apparent viscosity μ_{app} (mPa.s)		**Surface tension σ (mN/m)**		**Density (kg/m^3)**	
	KD100	HG250 HL	KD100	HG250 HL	KD100	HG250 HL
25˚C	2.9	4.35	28.1	27.2	815	815
50˚C	1.8	2.4	25.3	25.9		
75˚C	1.2	1.6	23.8	23.8		

The surface tension of the two hydrocarbons was measured at different temperatures by the pendant drop method using a dynamic TBU 90E tensiometer. The surface tension values for the two liquids are summarized in Table 6.1. At different temperatures, the liquids have almost the same surface tension. Also, they have almost the same density at ambient temperature. Therefore, the two hydrocarbons were strategically chosen to explore the response to the pressure increase of two liquids with almost the same properties but with different viscosities.

6.2.3 Numerical simulation and setup

The Two-Fluid Model[156, 157] was used to predict the gas-liquid hydrodynamics in the bubble column reactor investigated in this work. The governing equations can be written as follows:

$$\frac{\partial(\varepsilon_k \rho_k)}{\partial t} + \nabla \cdot (\varepsilon_k \rho_k \boldsymbol{u}_k) = 0 \tag{6.2}$$

$$\frac{\partial(\varepsilon_k \rho_k \boldsymbol{u}_k)}{\partial t} + \nabla \cdot (\varepsilon_k \rho_k \boldsymbol{u}_k \boldsymbol{u}_k) = -\varepsilon_k \nabla p + \nabla \cdot (\varepsilon_k \boldsymbol{\tau}_k) + \varepsilon_k \rho_k \boldsymbol{g} + \boldsymbol{M}_k^{\text{int}} \tag{6.3}$$

where ε represents the volume fraction of the gas or liquid phase and the sum of ε of each phase equals a unity, k represents the gas or liquid phase, ρ is the density, $\boldsymbol{u}$ is the velocity vector, p is the pressure, $\boldsymbol{g}$ is the gravitational acceleration vector, τ_k is the effective stress tensor and $\boldsymbol{M}^{\text{int}}$ represents interphase interaction between the gas and liquid phase. For the liquid phase, the effective stress tensor can be written as follows:

$$\boldsymbol{\tau}_l = \mu_{l,lam}\left[\nabla \boldsymbol{u}_l + (\nabla \boldsymbol{u}_l)^T\right] - \tfrac{2}{3}\mu_{l,lam}(\nabla \cdot \boldsymbol{u}_l)\boldsymbol{I} + \boldsymbol{\tau}_{l,turb} \tag{6.4}$$

where $\boldsymbol{\tau}_{l,turb}=-\rho_l \boldsymbol{R}_l$ is the Reynolds stress tensor, which can be modeled with the RSM model and $\mu_{l,lam}$ is the laminar viscosity. In this work, the closure law was proposed by Launder et al. [158] (LRR). For more details of the LRR model, readers are referred to Shu et al. [159]

Due to the fact that the presence of bubbles dramatically changes the liquid turbulence characters, the impact of the bubble-induced turbulence model is taken account into RSM of the liquid phase. Two source terms, S_R and $S\varepsilon$, are added into the RSM model, one for the Reynolds stress transport equation (S_R) and one for the turbulent dissipation rate ($S\varepsilon$). The source term for the Reynolds stress transport equation is written as follows:

$$\boldsymbol{S}_R = \begin{bmatrix} 0.5 & 0 & 0 \\ 0 & 0.5 & 0 \\ 0 & 0 & 1 \end{bmatrix} \frac{3C_D}{4d} \rho_l \left| \boldsymbol{u}_{slip} \right|^3 \tag{6.5}$$

where C_D is the drag force coefficient, d is the bubble diameter, and $\boldsymbol{u}_{slip}$ is the slip velocity between the gas and liquid phase.

The source term for the turbulent dissipation rate, $S\varepsilon$, can be generally written as

$$S_\varepsilon = C_{\varepsilon,BIT} \frac{S_R}{\tau} \tag{6.6}$$

where $C_{\varepsilon,\mathrm{BIT}}$ is a model constant and τ is the characteristic time-scale. In this work, $C_{\varepsilon,\mathrm{BIT}}$ is set as 1.44 and τ used in this work is proposed by Shu et al. [159] as

$$\tau = \frac{d}{2\left|\boldsymbol{u}_{slip}\right| \alpha_g^{n_0}} \tag{6.7}$$

where n_0 is a model constant and set as 0.75.

In this work, the IshiiZuber drag model[160] with the swarm effects corrections proposed by Simonnet et al.[161] and the turbulent dispersion model proposed by Burns et al.[162] with a Schmidt number of 1.25 were adopted for all simulation cases. For simplicity, the flows operated in both the homogeneous and heterogeneous flows are regarded as mono-dispersed and the bubble diameter used in the simulation follows the recommendation of Wilkinson et al.[70]

The governing equations were solved on the OpenFOAM 7 run on Compute Canada. The flow domain is discretized by 10,000 cells as shown in Figure 6.3. The liquid properties used in simulation were identical to those of Hydroseal G250 HL and the initial liquid level was 100 cm. The gas inlet was assumed to be uniform and the volume fraction of gas at the inlet was set as 1. A degassing boundary condition was used for the outlet. A no-slip boundary condition was imposed for the wall. The vanLeer scheme was used for the convection term discretization of the volume fraction and the limited Linear V scheme was used for the convection term discretization of velocity.

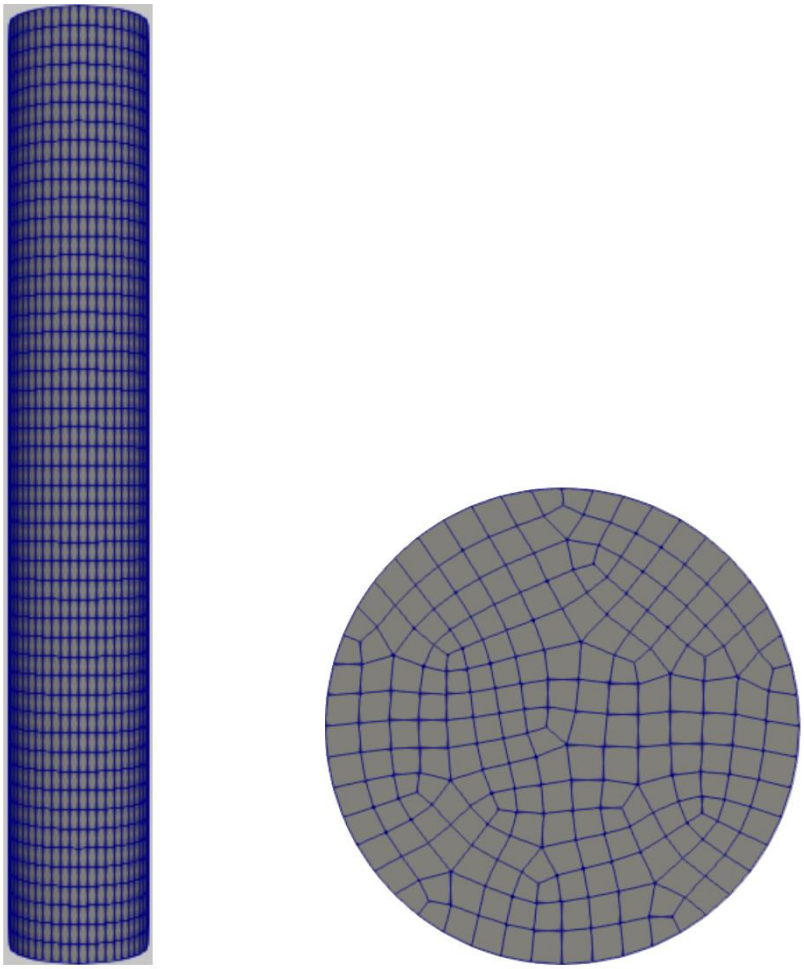

Figure 6.3 Geometry and grid information for CFD simulation.

6.3 Results and discussion

6.3.1 Effect of pressure on the total gas holdup

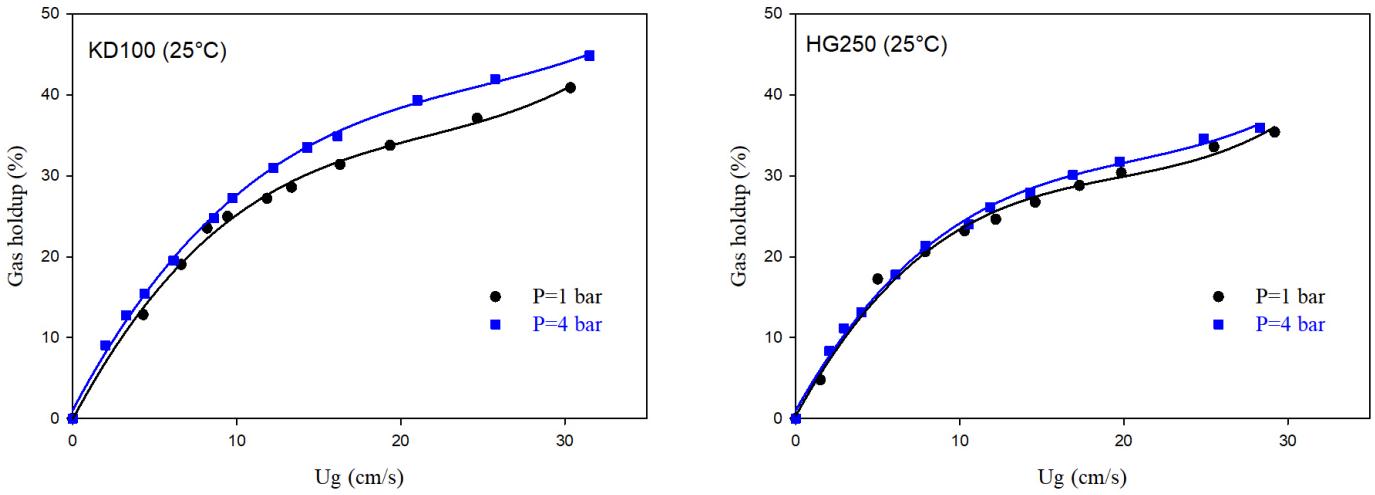

Figure 6.4 Effect of pressure on the total gas holdup for KD100 and HG250 at ambient temperature

Figure 6.4 shows the effect of increasing pressure on the total gas holdup at ambient temperature for the low-viscosity Ketrul D100 and the moderate-viscosity Hydroseal G250 HL obtained by DPT3. As a first observation, the gas holdup increased in tandem with pressure, which agrees with the finding of other works[68, 123, 153]. Thus, increasing pressure increases gas density and then gas-phase momentum, which increases the bubble breakup rate of large bubbles to small bubbles[123]. The second observation is that the effect of pressure was more significant in the heterogeneous regime (i.e., at high superficial gas velocities) where the coalescence and breakup phenomena occur. However, the increasing pressure effect was more significant for the low-viscosity hydrocarbon (KD100) if compared to the moderate-viscosity liquid (HG250). In fact, under the same operating conditions, the number of large bubbles in a moderate-viscosity liquid is higher than in the low-viscosity one[139]. Besagni et al.[149] reported that, at high superficial gas velocity, the large bubbles in moderate-viscosity liquids have a lower breaking probability into small bubbles than low-viscosity liquids. Consequently, the difference between the effect of pressure on the total gas holdup of the two liquids can be explained.

In order to prove that the effect of pressure is highly related to the viscosity range of the used liquid, the total gas holdup was measured by DPT3 for Hydroseal G250 HL at T=50˚C. The rheological measurements showed that, by increasing the temperature, the viscosity of Hydroseal G250 HL decreased from 4.35 mPa.s to 2.4 mPa.s (Table 6.1). Therefore, at 50˚C, the Hydroseal G250 HL could be considered as a low-viscosity liquid. Figure 6.5 shows the results at 1 and 4 bars, respectively. As expected, the effect of pressure on increasing gas holdup was more pronounced at 50˚C as the liquid viscosity shifted to the low-viscosity range. Also, since the Hydroseal G250 HL viscosity at 50˚C (2.4 mPa.s) is lower than the viscosity of Ketrul D100 at 25˚C (2.9 mPa.s), the effect of pressure on increasing gas holdup in the heterogeneous regime was even more pronounced (Figure 6.5).

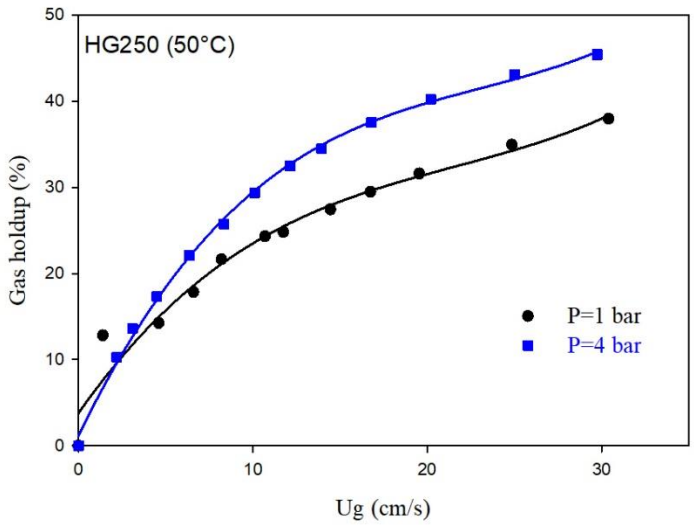

Figure 6.5 Effect of pressure on the total gas holdup of Hydroseal G250 HL at T=50˚C

6.3.2 Effect of pressure on the regime transition velocity

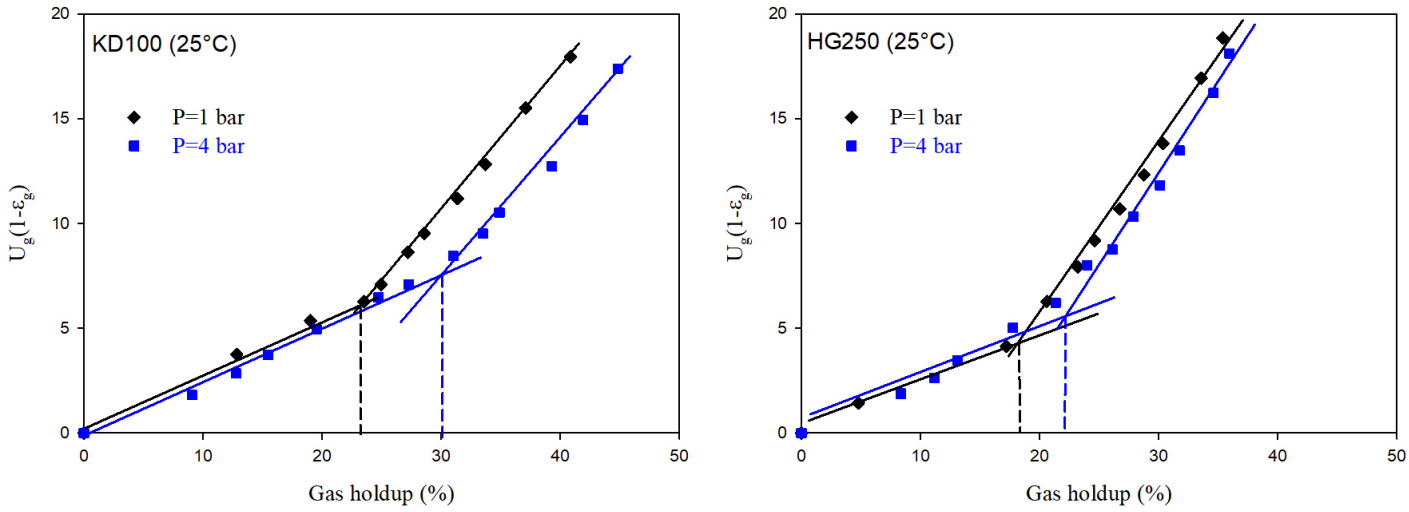

Figure 6.6 Identification of regime transition by Wallis' drift flux approach for KD100 and HG250 at ambient temperature

It is generally known that bubble columns can operate mainly in three different regimes, namely, the homogeneous, transition and heterogeneous regimes. The homogeneous regime prevails at low superficial gas velocities. The generated bubbles are small, spherical, monodisperse and rise vertically. When increasing gas velocity, the stability of the system decreases and the first large bubbles are formed due to bubbles clustering. The appearance of different bubble classes characterizes this regime. The heterogeneous regime prevails when the superficial gas velocity is very high or when the orifices of the distributor generate large bubbles (coarse spargers). It is characterized by an intense interaction between gas bubbles, which gives rise to coalescence and breakup phenomena. Consequently, bubbles have a large size distribution. Also, a gas holdup parabolic radial profile, as well as large macro-scale liquid circulation, is observed. However, Besagni et al.[149] stated that the above description of the three regimes is oversimplified. Hence, if large orifice spargers are used, large bubbles can be formed even at low superficial gas velocities, and the gas distribution quality is poor. Therefore, some authors came up with the definition of the *pure homogeneous regime* where discrete monodispersed bubbles are formed without any coalescence and *the pseudo homogeneous regime* where large and small bubbles coexist even at low U_g. The *pure homogeneous regime* prevails when using *fine distributors* (d_o< 1mm), whereas the *pseudo homogeneous regime* prevails when using coarse distributors (d_o > 1mm)[163]. Since

the orifices of the perforated plate distributor used in this work were 1mm in diameter, it is assumed that a *pure homogenous regime* was present at low superficial gas velocities in our experimental work. By increasing Ug, the transition from the homogenous to the heterogeneous regime occurs due to the appearance of large eddies and liquid macro-structures as a result of the onset of bubble coalescence. The generated large bubbles have a negative lift force that makes them move toward the center of the column, promoting the large liquid macrocirculation. It should be mentioned that the lift force is a force acting perpendicularly to the rising bubbles in the direction of decreasing liquid velocity. Large bubbles are characterized by a negative lift force and small bubbles by a positive one. Finally, the heterogeneous regime is fully developed at high superficial gas velocity.

The drift flux method proposed by Wallis[42] is commonly used to identify the superficial gas velocity at which the transition from the homogeneous to the heterogeneous regime occurs[18, 40, 84, 153]. The drift flux is the volumetric gas flux through a surface moving with the average velocity of the gas-liquid mixture. For a bubble column operating in a semi-batch mode ($U_l = 0$), the drift flux has the following expression:

$$j_{gl} = U_g\left(1 - \varepsilon_g\right) \tag{6.8}$$

The transition is identified by a change in the slope of the drift flux versus the gas holdup plot. Figure 6.6 shows the effect of increasing pressure on the regime transition velocity for both Ketrul D100 and Hydroseal G250HL. The values of the regime transition velocity and transition gas holdup are summarized in Table 6.2. For both liquids, increasing pressure from 1 to 4 bars stabilized the homogeneous regime by increasing the transition velocity ($U_{g,trans}$ increased from 8.2 cm/s to 12.2 cm/s for Ketrul D100 and, from 5 cm/s to 8 cm/s for Hydroseal G250HL when increasing the pressure from 1 to 4 bars). This result supports most of the previous works where the authors reported that an increased number of small bubbles with narrow size distribution are generated due to the increase of pressure[68, 71, 123]. The second observation is that, for the same operating conditions (same pressure), increasing liquid viscosity destabilizes the homogeneous regime at lower gas velocities ($U_{g,trans}$ decreased from 8.2 cm/s to 5 cm/s at 1 bar and from 12.2 cm/s to 8 cm/s at 4 bars). At low viscosities, the coalescence phenomenon is indeed limited. Then, the number of small bubbles increases, which stabilizes the homogeneous regime and increases the regime transition velocity. Inversely, moderate-viscosity liquids are more prone to coalescence,

destabilizing the homogeneous regime earlier, and decreasing the regime transition velocity. This finding agrees with Olivieri et al.[146]. They reported a stabilization of the homogenous regime for liquid viscosities up to 4.25 mPa.s and a destabilization of the flow regime for higher viscosities.

Table 6.2 Regime transition velocity and gas holdup at regime transition for different hydrocarbons

Liquid	**Operating pressure (bar)**	$U_{g,trans}$ **(cm/s)**	$\varepsilon_{g,trans}$ **(%)**
Ketrul D100	1	8.2	23
	4	12.2	31
Hydroseal G250HL	1	5	17
	4	8	22

The third most crucial finding is that the stabilizing effect of increasing pressure was more pronounced for the low-viscosity liquid if compared to the moderate-viscosity liquid. This finding is in agreement with the above-mentioned result on the increasing effect of pressure on the total gas holdup difference between the two liquids. Again, the bubble breaking probability is higher for the low-viscosity liquid, which increases the number of small bubbles. Therefore, the homogenous regime is more stabilized, and more gas momentum (higher superficial gas velocity) is required to shift the regime toward a coalescence-induced regime.

Following the same procedure as the total gas holdup data, in Figure 6.7 we plotted the drift flux as a function of superficial gas velocity for the Hydroseal G250 HL at 50˚C and 1 and 4 bars in order to explore the stabilizing effect of pressure on the drift flux for a low-viscosity liquid.

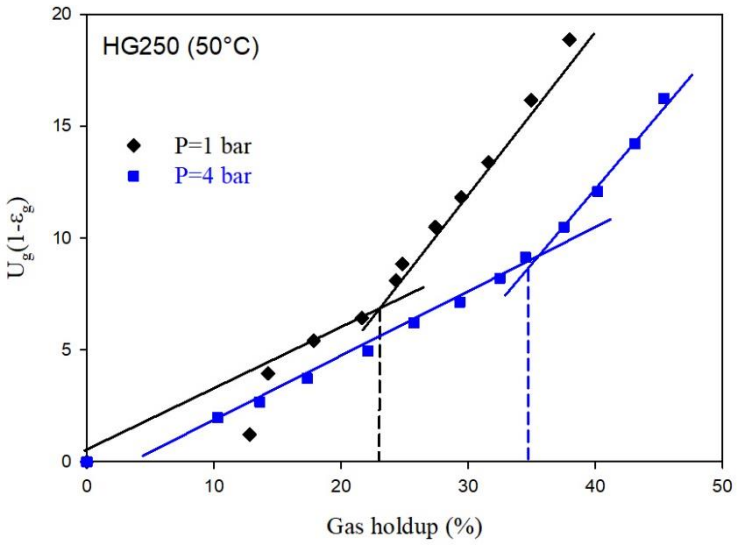

Figure 6.7 Identification of regime transition by Wallis' drift flux approach for HG250 at T=50˚C

As expected, by increasing the temperature, which decreases viscosity, the stabilizing effect of pressure on the homogeneous regime was more pronounced than at ambient temperature. By increasing pressure, $U_{g,trans}$ increased from 8.2 cm/s to 13.9 cm/s for HG250 (50˚C) and from 5 cm/s to 8 cm/s for HG250 (25˚C).

These findings confirm that, regardless of the increasing effect of pressure on the total gas holdup and the homogeneous regime stabilization, the response of the system might be different depending on the liquid viscosity range.

6.3.3 Effect of pressure on the axial gas holdup distribution

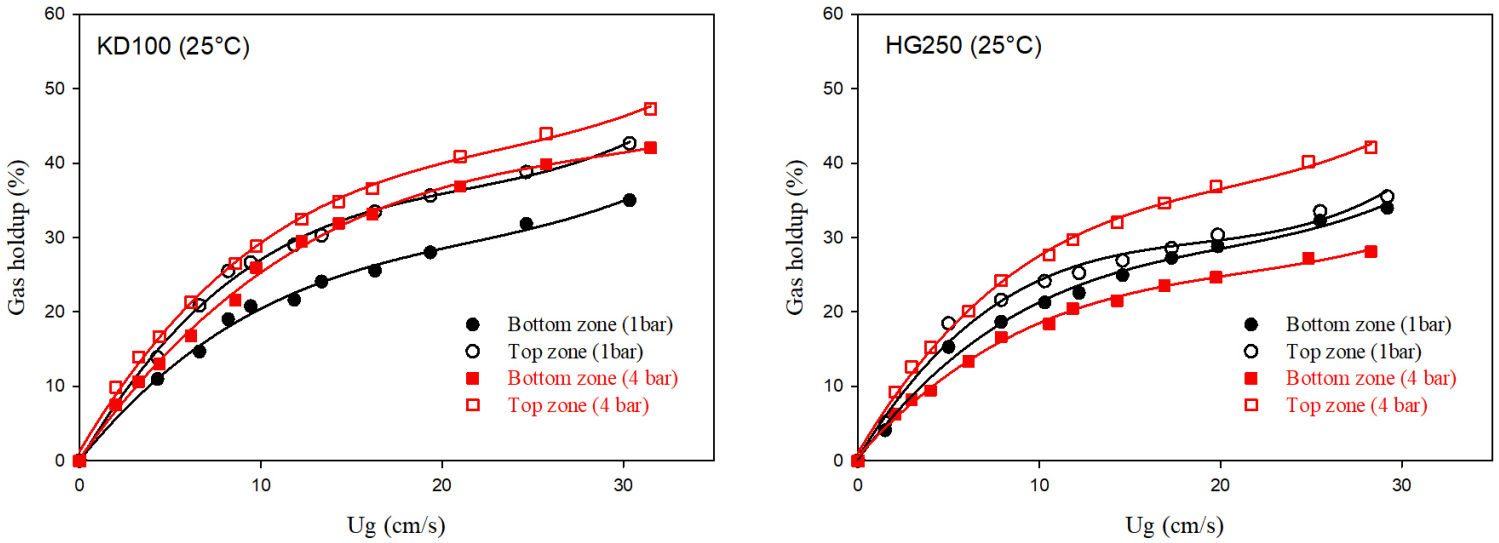

Figure 6.8 Effect of increasing pressure on the gas holdup axial distribution for KD100 and HG250 at ambient temperature

The essence of this work is to study the effect of increasing pressure on gas holdup distribution in the two equal-volume bottom and top zones of the gas-liquid bubble column. Figure 6.8 shows this effect by increasing the pressure from 1 to 4 bars for both Ketrul D100 and Hydroseal G250 HL. First, it is observed that the gas holdup of the top zone is always higher than the gas holdup of the bottom zone for both pressures and liquids. This finding is in agreement with the results of Jin et al.[151] and Kumar et al.[150] In another work, Esmaeili et al.[153] reported that, for an air-water system at 10 bars and the same bubble column setup as this work, the top zone gas holdup was higher than the bottom zone gas holdup. They attributed this effect to the expansion of gas bubbles when rising toward the liquid surface. Therefore, the macro liquid circulation is more developed in the top zone, which increases the residence time of small bubbles and thus increases the gas holdup. In another explanation of this effect, Kumar et al.[150] stated that the bubbles generated within the gas distributor zone are probably larger, and they gradually break up as they rise up through the reactor. An increase in the gas holdup with the increase of axial distance is then related to the smaller bubbles in the top zone.

The second observation is that, for Ketrul D100, increasing pressure increased both the bottom and top gas holdups (Figure 6.8 (KD100 (25˚C)). However, the increasing effect of pressure was more

pronounced in the bottom zone compared to the top zone. In fact, the top zone may contain smaller bubbles, as reported by Kumar et al.[150] and Esmaeili et al.[153]. Therefore, the effect of increasing pressure on enhancing the bubble breakup phenomenon in the top zone is diminished as the bubbles are already a smaller size. In contrast, the larger bubbles in the bottom zone may be more prone to breakup, which makes the effect of increasing pressure more pronounced in the bottom zone. The slight increase of the top gas holdup, as well as the significant increase of the bottom gas holdup in response to increasing pressure, narrows the difference between the two holdups (Figure 6.8 (KD100 (25˚C)). As a consequence, increasing pressure for the low-viscosity Ketrul D100 shifted the system to a more uniform gas holdup axial distribution.

For the moderate-viscosity Hydroseal G250 HL, a different effect of increasing pressure on the gas holdup axial distribution was observed. Increasing pressure from 1 to 4 bars decreased the bottom gas holdup and increased the top gas holdup. Therefore, this effect widened the difference between the two holdups and shifted the system to a less uniform gas holdup axial distribution (Figure 6.8 (HG250 (25˚C)). To verify the accuracy of the data, the total gas holdup $\varepsilon_{gtotal,2\ transducers}$ was calculated by the holdup measurements of the top and bottom zones ($\varepsilon_{g,DPT1}$ and $\varepsilon_{g,DPT2}$) and the comparison of $\varepsilon_{gtotal,2\ transducers}$ to $\varepsilon_{gtotal,DPT3}$, which is the total gas holdup obtained by the measurements of the DPT3 pressure transducer for the whole column. As the bottom and top zones have an equal volume, a simple calculation leads to the following equation:

$$\varepsilon_{gtotal,2\ transducers} = \frac{\varepsilon_{g,DPT1}+\varepsilon_{g,DPT2}}{2} \tag{6.9}$$

Figure 6.9 shows the results for Hydroseal G250 HL at 1 and 4 bar pressures. It should be mentioned that this comparison was made for both liquids and all operating conditions. As can be seen, the total gas holdups obtained from two different sources are almost the same. Therefore, we can rely on the data obtained in Figure 6.8 (HG250 (25˚C).

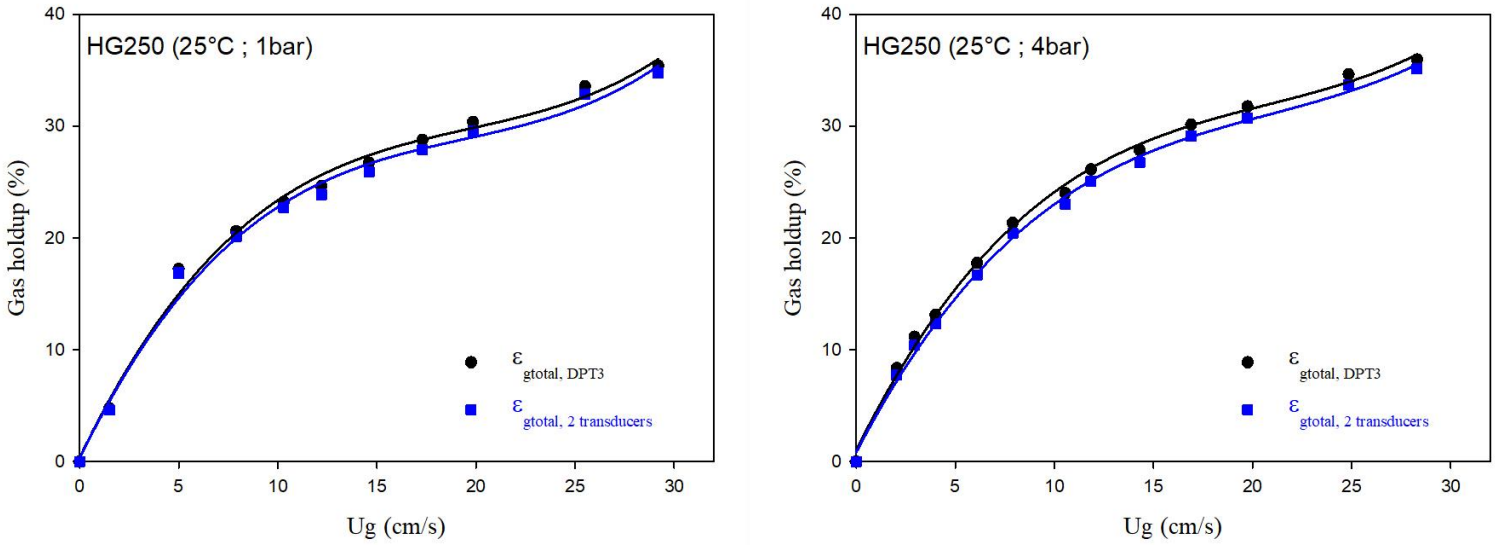

Figure 6.9 The total gas holdup measured by DPT3 and DPT1, DPT2 for HG250 at two different pressures

The literature was searched to find an explanation for the decreasing effect of pressure on the bottom gas holdup in the case of the moderate-viscosity Hydroseal G250 HL. Jordan et al.[164] investigated the effect of increasing gas density (corresponding to increasing pressure) on the large bubble holdup in a bubble column operating with four low-viscosity Ethanol (96%), 1-Butanol, Toluene and Decalin liquids (of 1.24, 2.94, 0.58 and 2.66 mPa.s viscosity respectively). Regardless of the range of the viscosity of these liquids, they observed that increasing gas density had almost no effect on large bubble holdup. This finding was in agreement with the work of Krishna and Ellenberger[165], who reported that increasing pressure had practically no influence on the holdup of the large bubbles. In another work, Behkish et al.[71] reported that for the low-viscosity Isopar-M liquid hydrocarbon (2.7 mPa.s at 25˚C), the large bubble holdup remained constant by increasing the system pressure. The first conclusion from the above-mentioned three papers is that for the whole height of the column, large bubble holdup is not affected by increasing pressure. Therefore, the following explanation is proposed for the decreasing effect of pressure on the bottom gas holdup observed for Hydroseal G250 HL: the large bubbles generated in the bottom zone of a bubble column filled with a moderate-viscosity liquid are bigger than the ones generated in the same zone filled with a low-viscosity liquid. Yan et al.[139] used computational fluid dynamics coupled with the population balance model to simulate the effect of increasing liquid viscosity on

the hydrodynamics of bubble columns. They found that by increasing liquid viscosity, the large bubbles were more stable, and the energy required for their breakup was higher. In other words, the turbulent eddies induced by increasing gas density can not break the large bubbles. On the other hand, bubble coalescence in a gas-liquid system can occur due to three main mechanisms. The first is coalescence due to turbulent eddies. The second is coalescence resulting from different bubble rise velocities. The third is coalescence caused by wake entrainment[166]. Wang et al.[166] stated that only the first mechanism was generally considered in previous studies for simplification purposes[49]. However, they reported that, at high superficial gas velocities, the wake entrainment-induced coalescence mechanism is more significant and responsible for the formation of large bubbles. In addition, the different rise velocity mechanism should be considered if the bubble rise velocity is sensitive to bubble size. The bottom zone also contains, in addition to large bubbles, a certain number of small bubbles. Increasing the system pressure decreases the size of these small bubbles more by breaking them up. As a result, their rise velocity decreases and they remain longer in the bottom zone. The smaller size of small bubbles caused by increasing the pressure renders them more prone to be entrained in the wake of the big bubbles at high superficial velocities. Furthermore, they become easier to catch by the large rising bubbles as their rise velocity decreases. Consequently, the coalescence rate between the non-pressure responsive large bubble and the small bubbles is increased by increasing the system pressure from 1 to 4 bars in the case of the low-moderate viscosity HG250 HL.

Finally, we performed the same experiments at 50˚C for Hydroseal HG250 HL to prove that the effect of pressure in shifting the gas-liquid system to a less uniform gas holdup axial distribution is specific to moderate-viscosity liquids. Figure 6.10 shows the results in terms of axial gas holdup vs. gas superficial velocity. As can be seen, increasing the pressure from 1 to 4 bars for Hydroseal G250 HL at 50˚C increased the bottom and top gas holdup in the same manner as Ketrul D100 at 25˚C as the two liquids have a low-viscosity under those respective conditions. Therefore, we can conclude that increasing pressure might shift the gas-liquid system toward a more uniform gas holdup axial distribution in the case of low-viscosity liquids, While the opposite might be observed in the case of moderate-viscosity liquids.

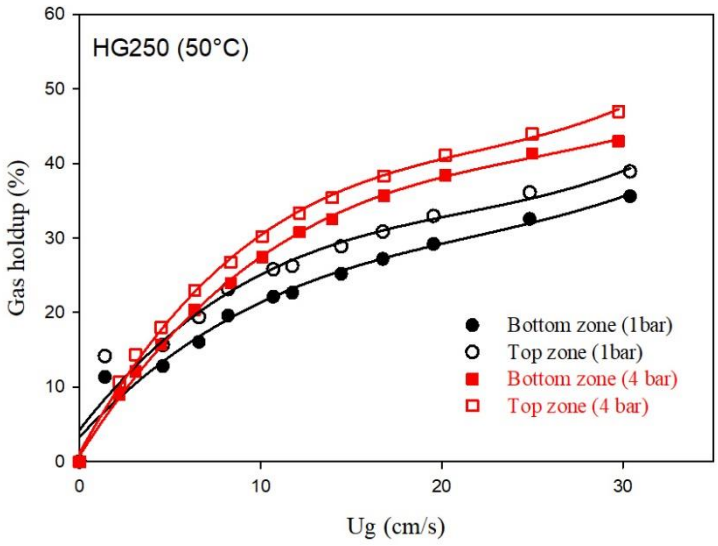

Figure 6.10 Effect of pressure on the axial gas holdup of HG250 at T=50˚C

6.3.4 CFD simulation of overall gas hold-up

Experimental validation is also important for the development of numerical simulation. Reliable experimental data can be used as a benchmark to test whether the numerical simulation is robust or not. Numerical simulation work has been initiated to corroborate the experimental results and provide a strong theoretical background regarding the observed increasing pressure effects. In this context, Figure 6.11 shows a comparison between the simulated and the experimental total gas holdup for the air-Hydroseal G250 HL system at ambient pressure. Since good agreement was obtained, the proposed monodispersed TFM model could be used to describe the bubble behaviour in such conditions. Interestingly, the simulation results predicted well the overall gas holdup in both the homogeneous and heterogeneous regimes. Work is in progress by other authors to generate CFD simulation data, especially for the two different effects of increasing the axial gas holdup distribution depending on the range of the liquid viscosity.

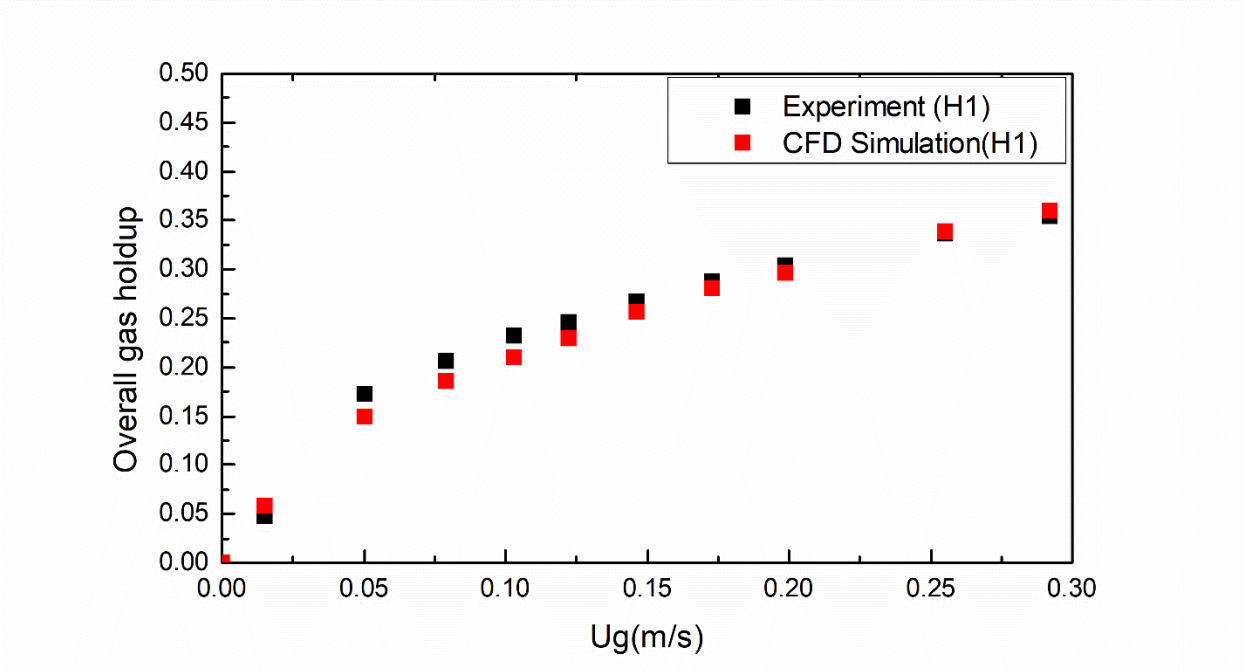

Figure 6.11 Comparison between predicted overall gas holdup and experimental measurement.

6.4 Conclusion

In this research work, we clarified the effect of pressure on some hydrodynamic aspects of a pilot-scale bubble column operating with low and moderate viscosity liquids. The experimental results showed that the total gas holdup increased by increasing pressure in the heterogeneous regime and the effect was more pronounced for the low-moderate viscosity liquid. At high superficial gas velocities, the large bubbles in the moderate viscosity liquid are indeed less prone to bubble breakup compared to the low viscosity liquid. Also, increasing the system pressure stabilized the homogeneous regime by increasing the transition velocity and this stabilizing effect is more significant in the case of low viscosity liquids. This result was in agreement with the total gas holdup findings. As the breaking probability is high, the low viscosity liquid contains a larger number of small bubbles, which requires more gas momentum to shift the system towards the heterogeneous regime. In the third part of the study, we investigated the effect of increasing pressure on the gas holdup axial distribution. It was found that, for the low viscosity liquid, increasing pressure increased both the bottom and top zone gas holdups. This increasing effect was

more favourable in the top zone containing smaller bubbles. In this range of viscosity, it was observed that increasing pressure shifted the system to a more uniform gas holdup distribution.

In contrast, increasing the pressure resulted in a decrease in the bottom zone gas holdup and an increase in the top zone gas holdup for the moderate viscosity liquid. In the bottom zone, increasing pressure enhanced the bubble coalescence phenomenon at high superficial gas velocity by promoting wake entrainment and different rise velocity mechanisms. As a consequence, the gas holdup axial distribution for a moderate viscosity liquid became less uniform in response to increasing pressure.

Furthermore, conducting experiments with similar fluids can be an appropriate tool to mimic the operating conditions in an industrial process. As shown in this work, varying the system temperature had a direct effect on the liquid viscosity and affected its response to pressure change.

However, more experimental work should be performed at higher pressures to investigate other potential effects of increasing pressure on the gas holdup axial distribution in bubble columns. Using more advanced measurement techniques to determine the bubble size distribution in the different zones under such conditions is crucial to clarify more bubble behaviour across the height of the reactor.

6.5 Acknowledgements

The authors thank TOTAL American Services, Inc. and the Natural Science and Engineering Research Council of Canada (NSERC) for their financial support.

CHAPTER 7 GENERAL DISCUSSION

The hydrodynamics and mass transfer are key factors for the design and scale-up of two-phase and three-phase bubble column reactors. These two important aspects are significantly affected by the properties of each of the three phases (gas-liquid-solid). Solid particles'presence in multiphase reactors is highly important as they are used as catalysts for several chemical reactions. Therefore, when suspended in a gas-liquid medium, they alter the bubble behaviour as well as the gas-liquid mass transfer. This impact should be studied carefully and understood based on the physical phenomena brought by the particles. Moreover, the effect of increasing pressure on the hydrodynamics of a gas-liquid system operating with liquids of different viscosities should be explored prior to add solid particles at these elevated pressures. The objective of this work was to narrow the number and the range of the parameters studied in order to investigate the physical mechanisms that describe their potential effect on hydrodynamics and mass transfer.

In the first step of this work, a three-phase bubble column operating at ambient pressure and temperature was constructed to perform the experimental work and to study the influence of solid properties on the global hydrodynamics. The approach was to conduct the experimental work with non-porous spherical hydrophilic glass bead particles with small solid concentration increments (0%-1%-3%-5% v/v) not to miss any potential phenomenon that could occur when adding particles. Besides, the size of the particles was changed from 35μm to 156μm, as many industrial catalysts have the same size magnitude. A differential pressure transducer was utilized to measure the total gas holdup by the manometric method. The simultaneous effect of particle size and solid concentration on the global hydrodynamics of SBCR was first explored in Chapter 3. It was found that increasing solid concentration decreased gas holdup for all particle sizes and destabilized the homogeneous regime earlier. This effect was in agreement with most of the findings in the literature. However, most of the researchers attributed it to bubble coalescence enhancement due to the increase of the apparent viscosity and considered the slurry as a pseudo homogeneous phase. The decreasing effect of solid concentration was to be found more pronounced at larger particle sizes (156μm). Also, at very low concentrations (1 and 3% v/v), the effect of particle size on gas holdup was not significant. At 5%v/v, increasing particle size decreased the total gas holdup, and this effect was more pronounced at high superficial gas velocities where the coalescence and breakup phenomena occur. These two findings indicated that the effect of solid concentration and

particle size on the global hydrodynamics could not be separated. In order to understand more this simultaneous effect, the applicability of the two-phase approach to the experimental data of this work was investigated. Thus, the experimental gas holdup was compared to the gas holdup estimated by the two-phase approach and obtained by applying a dimensional analysis on different gas-liquid systems. Interestingly, it was observed that the two-phase approach overestimated the experimental gas holdup by a mean absolute percentage error of 34%. Moreover, this error increased by increasing solid concentration and particle size. This step enabled to prove that solid particles have an additional effect on bubble flow besides their effect on changing liquid viscosity. The next step was then to have more insight and quantify this additional impact. In this context, it was decided to compare the bubble column process to the froth flotation process in which solid particles are also suspended in a gas-liquid medium. Among the three subprocesses that control the performance of a flotation cell (collision – attachment – bubble-particle stability), only the collision subprocess was considered while the other two were not. As experimental work in this study was conducted with hydrophilic particles, no attachment between the bubbles and the particles was expected. Also, the bubble-particle stability subprocess was not applicable as bubble columns are operating at relatively high gas velocities. Consequently, the additional effect of solid particles was chosen to be quantified by the collision efficiency parameter E_c. The latter is the percentage of particles that will collide with the bubble on the basis of a certain number of particles present in the system. The calculated collision efficiency E_c was interestingly found to be dependent on particle size and independent of solid concentration. A new correcting factor called the hindering factor (HF) $[(1 - E_c) \times (1 - C_v)]^{5.43}$ was developed to quantify the deviation between the gas holdup estimated by the two-phase approach and the experimental gas holdup. This factor includes a particle size depending term $[(1 - E_c)]^{5.43}$ and a concentration depending term $[(1 - C_v)]^{5.43}$. Finally, the simultaneous effect of particle size and solid was clarified based on the following statement: Increasing particle size and concentration increases the hindering factor. As a result, particles tend to hinder bubbles from rising, which increases the probability of contact between bubbles and then enhances bubble coalescence. The hindering effect was also proven by the results of the dynamic gas disengagement technique (DGD). When applying this correcting factor to the gas holdup estimated by the two-phase approach, the mean absolute percentage error between the experimental gas holdup and the corrected gas holdup decreased to 10.4%. In the last part of this

first objective, the applicability of the proposed correction was verified for other works' experimental data. The correlation could predict the data by an average error of 21.5%.

The effect of solid particles on the volumetric gas-liquid mass transfer coefficient $k_l a_l$ was investigated in Chapter 4. Following the same approach of narrowing the range of the parameters studied, the aim of this part was to provide reliable experimental data and determine the physical mechanism that governs mass transfer at the gas-liquid interface in the presence of solid particles. The mass transfer coefficient $k_l a_l$ measurement was performed with the dynamic oxygen absorption technique using the saturation method. A Visiferm DO325 optical probe was used to measure the dissolved oxygen (DO) concentration in the liquid phase. Experiments were carried out for three solid concentrations (1% - 3% - 5% v/v) and two particle sizes (71µm – 156 µm). It was observed that there was no dependency between the glass bead volume fraction and the $k_l a_l$ for the two sizes. It should be mentioned that the presence of solid particles in a gas-liquid system was found to enhance gas-liquid mass transfer if compared to a solid-free system. Four mechanisms were proposed in the literature to describe this enhancement phenomenon, namely *the hydrodynamic effect, the shuttle effect (solid porosity), the coalescence inhibition effect*, and *the reaction enhancement effect*. There are many discrepancies with respect to the effect of the presence of solid particles on the volumetric mass transfer coefficient. The first step was to discard *the shuttle* and *reaction enhancement* mechanisms by performing experiments with inert non-porous hydrophilic glass beads. The objective was to determine which of the two remaining mechanisms (*hydrodynamic* or *coalescence inhibition*) describes the solid impact within the range of operating conditions relevant to this research. The air-water surface area a_l was calculated based on the bubble Sauter mean diameter d_{32}. The latter was estimated based on the signal decomposition method that uses the coherence of pressure fluctuation in different zones of the bubble column. It was found that increasing solid concentration caused a decrease in a_l for both particle sizes due to enhanced bubble coalescence. Furthermore, an increase in particle size resulted in a decrease in $a_{l,}$ starting from a 3% volume fraction in the heterogeneous regime. This finding represented another way to confirm the finding reported in the first objective, namely the effect of increasing particle size at higher concentrations in hindering bubbles from rising and then enhancing the coalescence phenomenon. Consequently, the *coalescence inhibition* mechanism was also discarded for the range of operating conditions used in this work. Based on the measured $k_l a_l$ and the estimated a_l,

the effect of increasing superficial gas velocity as well as solid concentration on k_l for the two particle sizes was explored. The presence of particles in the bulk liquid affects its viscosity and decreases the gas-liquid interfacial area a_l. On the other hand, the presence of solids in the liquid film increases the liquid side mass transfer coefficient k_l. These two opposite effects of decreasing a_l and increasing k_l by solid concentration suppress any effect of the solid on $k_l a_l$. The last step of this second objective was to verify the applicability of the two-phase approach on predicting the experimental $k_l a_l$. By applying the most relevant correlations developed for gas-liquid systems, it was found that the two-phase approach couldn't predict well the low variability of the experimental three-phase $k_l a_l$. The two-phase approach considers only the change in liquid properties and doesn't consider the additional effect of solid particles on bubble behavior and liquid film turbulence. This finding could indicate that changing solid particle properties has less effect on $k_l a_l$ compared to a liquid system with the same properties.

Prior to the study on the effect of pressure on hydrodynamics in SBCR, the first step was to investigate this effect in a solid-free system. Chapter 6 was devoted to evaluating the total gas holdup, its axial distribution and the operating flow regime transition points in a pilot-scale bubble column operating with low and moderate viscosity hydrocarbons. The experimental results showed that the total gas holdup increased by increasing pressure at the heterogeneous regime, and this effect was more pronounced for the low-moderate viscosity liquid. Indeed, at high superficial gas velocities, the large bubbles in the moderate-viscosity liquid are less prone to bubble breakup if compared to the low-viscosity liquid. Also, increasing the system pressure stabilized the homogeneous regime by increasing the transition velocity, and this stabilizing effect is more significant in the case of low viscosity liquids. In the third part of this study, the effect of increasing pressure on the gas holdup axial distribution was investigated. It was found that, for the low-viscosity liquid, increasing pressure increased both the bottom and top zone gas holdups. In this range of viscosity, it was observed then that increasing pressure shifted the system to a more uniform gas holdup distribution. In contrast, increasing the pressure resulted in a decrease in the bottom zone gas holdup and an increase in the top zone gas holdup for the moderate-viscosity liquid. In the bottom zone, increasing pressure enhanced the bubble coalescence phenomenon at high superficial gas velocity by favoriting the wake entrainment and different rise velocity

mechanisms. As a consequence, the gas holdup axial distribution for a moderate-viscosity liquid became less uniform as a response to pressure increasing.

CHAPTER 8 CONCLUSIONS AND RECOMMANDATIONS

8.1 Concluding remarks

The effect of two solid properties on the hydrodynamics and gas-liquid mass transfer of slurry bubble column reactors was investigated. Two pilot-scale bubble column facilities were utilized to perform experiments within a wide range of operating conditions. Extensive experimental work was carried out to provide reliable global hydrodynamics and mass transfer data. A new approach based on a novel correcting factor was introduced to elucidate the simultaneous effect of particle size and concentration. A hindering factor was derived based on the collision efficiency parameter that is affected by particle size and solid concentration. The mechanism behind this effect of inert hydrophilic non-porous particles on the gas-liquid mass transfer was determined. Furthermore, prior to exploring the effect of solids at elevated pressure, series of experiments were conducted to evaluate the effect of increasing pressure on total and axial gas holdups as well as on the flow regime transition in a bubble column operating with low and moderate viscosity hydrocarbons.

8.2 Original contributions

This research work provides great insight and a considerable amount of information regarding the hydrodynamics and mass transfer of bubble column reactors operating with and without the presence of solid particles. The findings of this study will instigate a scientific debate on the effect of solid particles on bubble behaviour when suspended in a gas-liquid medium. It was demonstrated that the simplified design and scale-up procedure based on considering the slurry phase as a pseudo homogeneous liquid phase must be amended. Design could be biased if the models developed to predict hydrodynamic parameters, and applicable for gas-liquid systems, are utilized for three-phase systems. One main contribution of this study is to invite researchers working in this field to be aware of the additional effect of solid particles on bubble behaviour. This effect should be taken into account as it could either improve or deteriorate the reactor's performance. The specific novel aspects of this research work are as follows:

1. Extensive experimental work at a wide range of operating conditions and in large-scale bubble column setups prior to elucidating the effect of solid and liquid properties on the hydrodynamics and mass transfer.

2. The proposition of a new three-phase approach based on correcting the two-phase approach to describe the additional effect of solid particles. This novel approach could inspire researchers in this field and provide a new route to interpret the impact of solid particles in multiphase reactors, which has not yet been considered elsewhere.

3. The development of a new correcting factor for predicting total gas holdup by considering some of the solid properties and validating its use by experimental data from the literature.

4. An investigation on the impact of certain specific solid properties on the gas-liquid mass transfer and the physical mechanism behind.

5. An exploration of the effect of increasing pressure on the hydrodynamics of bubble columns operating with hydrocarbons of different viscosity ranges.

8.3 Future work and recommendations

To reach an optimal design, scale-up and operation of slurry bubble column reactors, it is important to have complete knowledge off the effect of different variables and design parameters on the bubble behaviour. Based on the findings of this work, the scientific approach that should be followed for the subsequent studies is to develop phenomenological models that include different operating variables and design parameters gradually. In other words, conducting experimental work to study the effect of all these influential parameters in slurry bubble column reactors at one time is tedious. Then, the accuracy of the developed models is not satisfactory. Therefore, the following scientific approach is recommended:

8.3.1 Scientific approach

- In order to develop a reliable phenomenological model, it is important to narrow the number, and the range of parameters studied and to link the effect of each parameter to a physical phenomenon that also affects the bubble behaviour. The next step is to improve this model by:
    - Widening the range of variability of the parameter

- Adding another parameter to the study

As an example, if the effect of solid concentration on gas holdup is studied, it is interesting to study this effect at a low range of variability depending on the application (Low concentration:0-10%v/v; High concentration: 25-40%v/v) and develop a correlation that describes accurately the physical phenomena related to this range. Thereafter, another parameter such as particle size can be added but also in a narrow range to not omit the real happening physical phenomenon.

- To link the effect of an operating variable to an easy calculated physical parameter that defines the system (loss modulus, dynamic modulus, collision efficiency, attachment efficiency, etc.)

Considering the above-mentioned points, some avenues for future research are recommended:

8.3.2 Specific recommendations related to the findings of this work

❖ *First objective*

- The error of the two-phase approach correction by the hindering factor was larger at low superficial gas velocities because the solid is not well dispersed at these velocities, and the solid concentration is not equal to the initial volume fraction. Therefore, the correction factor can be improved if the local solid concentration at low velocities is measured.
- The power a used in the hindering factor HF should be the subject of further studies. The parameter from the phase properties, operating conditions or reactor design that affects the error with respect to the two approaches more should be pinpointed. This parameter will then be directly linked to a .
- More experimental work with different solid properties (density – wettability – porosity) and relatively high concentrations is required to understand better how the solid affects bubble column hydrodynamics.

❖ *Second objective*

More experimental work with different solid properties (i.e. porous, reactive, hydrophobic) is required to investigate the occurring of *the shuttle effect* and the *reaction enhancement* mechanisms.

❖ *Third objective*

More experimental work should be performed at higher pressures to investigate other potential effects of increasing pressure on the gas holdup axial distribution in bubble columns. Advanced measurement techniques (Laser techniques, X-ray and γ-ray tomography, high pressure and high temperature withstanding fiber optic probes) could be used to determine the bubble size distribution in the different zones under such conditions is crucial to clarify more the bubble behaviour all over the height of the reactor.

8.3.3 General Recommendations

- Solid properties can significantly change the liquid phase properties and also bubble behaviour. However, this effect is not well covered in the literature. In this regard, further studies on the impact of solid properties such as degree of lyophobicity, porosity, size, shape on the different hydrodynamic aspects of the bubble column and developing models that consider each of these properties would be of great interest.

- It is of great importance to work with the real particles that are used in the chemical processes held in slurry bubble column reactors. An example is to study the effect of the Co/TiO_2 catalyst used in Fischer-Tropsch synthesis on the hydrodynamics of slurry bubble column reactors.

- Reactions held in slurry bubble column reactors can result in the formation of some immiscible liquids. An example is the hydroprocessing that combines thermal cracking at elevated temperature (440C) and hydrogenation at elevated temperature (12 MPa) to convert heavier liquid feed to lighter fractions. Upgrading heavy liquid feed can lead to the formation of immiscible liquid phases that can affect bubble behaviour. Biodiesel and glycerol liquids can be one of the examples of immiscible liquids.

- Investigating the above-mentioned parameters requires an accurate measurement of local hydrodynamic parameters such as local solid concentration, solid holdup profile, local gas holdup and axial and radial gas holdup profiles. Therefore, using reliable and non-intrusive measurement techniques such as radioactive particle tracking (RPT), Gamma-ray

densitometry, X-ray, and Gamma-ray tomography could provide valuable information about the effect of solid particles on the hydrodynamics of SBCR.

- The presence of internals used as heat exchangers to control the column temperature and their impacts on hydrodynamics would also be interesting to explore further.
- The effect of the gas distributor design should be considered in further studies on the effect of solid particles on the hydrodynamics. The presence of particles in the distributor zone might have a significant impact on the bubble detachment process from the sparger orifices.

- The flow dynamics of the liquid phase and its interaction with solid particles in terms of mixing quality, flow pattern, recirculation, axial dispersion should be deeply investigated.

- The effect of non-Newtonian and viscoelastic behaviour of the liquid phase on the reactor performance.

REFERENCES

1. Kara, S., et al., *Hydrodynamics and axial mixing in a three-phase bubble column.* Industrial & Engineering Chemistry Process Design and Development, 1982. **21**(4): p. 584-594.
2. Krishna, R., et al., *Gas hold-up in bubble columns: Operation with concentrated slurries versus high viscosity liquid.* The Canadian Journal of Chemical Engineering, 2000. **78**(3): p. 442-448.
3. Pfaltzgraff, L. and J. Clark, *Green chemistry, biorefineries and second generation strategies for re-use of waste: an overview*, in *Advances in Biorefineries*. 2014, Elsevier. p. 3-33.
4. *Evolution of the Chemical Industry and Importance of Multiphase Reactors*, in *Design of Multiphase Reactors*. p. 1-29.
5. *Multiphase Reactors*, in *Design of Multiphase Reactors*. p. 47-86.
6. Tatterson, G.B., *Fluid mixing and gas dispersion in agitated tanks*. 1991: McGraw-Hill New York.
7. Chen, P.-C., *Absorption of carbon dioxide in a bubble-column scrubber*, in *Greenhouse Gases-Capturing, Utilization and Reduction*. 2012, InTech. p. 95-112.
8. Navaza, J.M., D. Gómez-Díaz, and M.D. La Rubia, *Removal process of CO2 using MDEA aqueous solutions in a bubble column reactor.* Chemical Engineering Journal, 2009. **146**(2): p. 184-188.
9. Gruenewald, M. and A. Radnjanski, *Gas–liquid contactors in liquid absorbent-based PCC*, in *Absorption-Based Post-combustion Capture of Carbon Dioxide*. 2016, Elsevier. p. 341-363.
10. Majumder, S.K., *1 - Introduction*, in *Hydrodynamics and Transport Processes of Inverse Bubbly Flow*, S.K. Majumder, Editor. 2016, Elsevier: Amsterdam. p. 1-24.
11. Rollbusch, P., et al., *Bubble columns operated under industrially relevant conditions – Current understanding of design parameters.* Chemical Engineering Science, 2015. **126**: p. 660-678.
12. Kantarci, N., F. Borak, and K.O. Ulgen, *Bubble column reactors.* Process Biochemistry, 2005. **40**(7): p. 2263-2283.
13. King, D., et al., *Chemical reactor technology for environmentally safe reactors and products.* Ravella Eds., NATO ASI Series, 1992. **225**: p. 17-50.

14. Fan, L., *Gas-Liquid-Solid Fluidization Engineering, Butterworths.* Stonehair, MA, 1989.
15. Cui, Z., *Hydrodynamics in a bubble column at elevated pressures and turbulence energy distribution in bubbling gas-liquid and gas-liquid-solid flow systems*. 2005, The Ohio State University.
16. Gunjal, P.R. and V.V. Ranade, *Chapter 7 - Catalytic Reaction Engineering*, in *Industrial Catalytic Processes for Fine and Specialty Chemicals*, S.S. Joshi and V.V. Ranade, Editors. 2016, Elsevier: Amsterdam. p. 263-314.
17. Basha Omar, M., et al., *Fischer–Tropsch Synthesis in Slurry Bubble Column Reactors: Experimental Investigations and Modeling – A Review*, in *International Journal of Chemical Reactor Engineering*. 2015. p. 201.
18. Shaikh, A. and M.H. Al-Dahhan, *A review on flow regime transition in bubble columns.* International Journal of Chemical Reactor Engineering, 2007. **5**(1).
19. Esmaeili Khalil Saraei, A., *Hydrodynamics of Bubble Column Reactors Operating with Non-Newtonian Liquids*. 2015, École Polytechnique de Montréal.
20. Ferreira, A., et al., *8 - Nonmechanically Agitated Bioreactors*, in *Current Developments in Biotechnology and Bioengineering*, C. Larroche, et al., Editors. 2017, Elsevier. p. 217-233.
21. Deckwer, W.-D. and A. Schumpe, *Improved tools for bubble column reactor design and scale-up.* Chemical Engineering Science, 1993. **48**(5): p. 889-911.
22. Behkish, A., *Hydrodynamic and mass transfer parameters in large-scale slurry bubble column reactors*. 2005, University of Pittsburgh.
23. Yang, G., B. Du, and L. Fan, *Bubble formation and dynamics in gas–liquid–solid fluidization—a review.* Chemical Engineering Science, 2007. **62**(1): p. 2-27.
24. Luo, X., et al., *Single bubble formation in high pressure liquid—solid suspensions.* Powder technology, 1998. **100**(2): p. 103-112.
25. Ramakrishnan, S., R. Kumar, and N.R. Kuloor, *Studies in bubble formation—I bubble formation under constant flow conditions.* Chemical Engineering Science, 1969. **24**(4): p. 731-747.
26. Jean, R.-H. and L.-S. Fan, *Rise velocity and gas—liquid mass transfer of a single large bubble in liquids and liquid—solid fluidized beds.* Chemical engineering science, 1990. **45**(4): p. 1057-1070.

27. Zhang, J. and L.-S. Fan, *On the rise velocity of an interactive bubble in liquids.* Chemical Engineering Journal, 2003. **92**(1): p. 169-176.
28. Chhabra, R.P., *Bubbles, drops, and particles in non-Newtonian fluids*. 2006: CRC press.
29. Prince, M.J. and H.W. Blanch, *Bubble coalescence and break-up in air-sparged bubble columns.* AIChE Journal, 1990. **36**(10): p. 1485-1499.
30. Chen, Y.-M. and F. Liang-Shin, *Bubble breakage mechanisms due to collision with a particle in liquid medium.* Chemical engineering science, 1989. **44**(1): p. 117-132.
31. Clift, R., J.R. Grace, and M.E. Weber, *Bubbles, drops, and particles*. 2005: Courier Corporation.
32. Hinze, J., *Fundamentals of the hydrodynamic mechanism of splitting in dispersion processes.* AIChE Journal, 1955. **1**(3): p. 289-295.
33. Fan, L.-S., et al., *Some aspects of high-pressure phenomena of bubbles in liquids and liquid–solid suspensions.* Chemical engineering science, 1999. **54**(21): p. 4681-4709.
34. JOACHIM, H., *Flotation as a heterocoagulation process: possibilities of calculating the probability of flotation.* Coagulation and Flocculation: Theory and Applications, 1993. **126**: p. 321.
35. Tsabet, È. and L. Fradette, *Semiempirical Approach for Predicting the Mean Size of Solid-Stabilized Emulsions.* Industrial & Engineering Chemistry Research, 2015. **54**(46): p. 11661-11677.
36. Chen, P., *Modeling the fluid dynamics of bubble column flows*. 2004, Washington University in St. Louis.
37. Abdulrahman, M.W., *Experimental studies of the transition velocity in a slurry bubble column at high gas temperature of a helium–water–alumina system.* Experimental Thermal and Fluid Science, 2016. **74**: p. 404-410.
38. Mena, P., et al., *Effect of solids on homogeneous–heterogeneous flow regime transition in bubble columns.* Chemical Engineering Science, 2005. **60**(22): p. 6013-6026.
39. Bouaifi, M., et al., *A comparative study of gas hold-up, bubble size, interfacial area and mass transfer coefficients in stirred gas–liquid reactors and bubble columns.* Chemical engineering and processing: Process intensification, 2001. **40**(2): p. 97-111.

40. Esmaeili, A., C. Guy, and J. Chaouki, *The effects of liquid phase rheology on the hydrodynamics of a gas–liquid bubble column reactor.* Chemical Engineering Science, 2015. **129**: p. 193-207.
41. Ruzicka, M., et al., *Effect of viscosity on homogeneous–heterogeneous flow regime transition in bubble columns.* Chemical Engineering Journal, 2003. **96**(1): p. 15-22.
42. Wallis, G.B., *One-dimensional two-phase flow.* 1969.
43. Chilekar, V.P., et al., *Influence of elevated pressure and particle lyophobicity on hydrodynamics and gas-liquid mass transfer in slurry bubble columns.* AIChE Journal, 2009: p. NA-NA.
44. Mota, A., A.A. Vicente, and J. Teixeira, *Effect of spent grains on flow regime transition in bubble column.* Chemical Engineering Science, 2011. **66**(14): p. 3350-3357.
45. Kluytmans, J.H., et al., *Gas holdup in a slurry bubble column: influence of electrolyte and carbon particles.* Industrial & engineering chemistry research, 2001. **40**(23): p. 5326-5333.
46. Ruthiya, K.C., et al., *Influence of particles and electrolyte on gas hold-up and mass transfer in a slurry bubble column.* International Journal of Chemical Reactor Engineering, 2006. **4**(1).
47. Cheng, N.-S. and A.W.-K. Law, *Exponential formula for computing effective viscosity.* Powder Technology, 2003. **129**(1): p. 156-160.
48. Tsuchiya, K., et al., *Suspension viscosity and bubble rise velocity in liquid-solid fluidized beds.* Chemical Engineering Science, 1997. **52**(18): p. 3053-3066.
49. Schäfer, R., C. Merten, and G. Eigenberger, *Bubble size distributions in a bubble column reactor under industrial conditions.* Experimental Thermal and Fluid Science, 2002. **26**(6): p. 595-604.
50. Chaumat, H., A.M. Billet, and H. Delmas, *Hydrodynamics and mass transfer in bubble column: Influence of liquid phase surface tension.* Chemical Engineering Science, 2007. **62**(24): p. 7378-7390.
51. Camarasa, E., et al., *Influence of coalescence behaviour of the liquid and of gas sparging on hydrodynamics and bubble characteristics in a bubble column.* Chemical Engineering and Processing: Process Intensification, 1999. **38**(4): p. 329-344.
52. Liang-Shih, F. and K. Tsuchiya, *Bubble wake dynamics in liquids and liquid-solid suspensions*. 2013: Butterworth-Heinemann.

53. Van der Zon, M., et al., *Coalescence of freely moving bubbles in water by the action of suspended hydrophobic particles.* Chemical engineering science, 2002. **57**(22): p. 4845-4853.
54. Jamialahmadi, M. and H. Müller-Steinhagen, *Effect of solid particles on gas hold-up in bubble columns.* The Canadian Journal of Chemical Engineering, 1991. **69**(1): p. 390-393.
55. Bukur, D.B., S.A. Patel, and J.G. Daly, *Gas holdup and solids dispersion in a three-phase slurry bubble column.* AIChE journal, 1990. **36**(11): p. 1731-1735.
56. Omota, F., *Adhesion of catalyst particles to gas bubbles.* 2005.
57. Ojima, S., K. Hayashi, and A. Tomiyama, *Effects of hydrophilic particles on bubbly flow in slurry bubble column.* International Journal of Multiphase Flow, 2014. **58**: p. 154-167.
58. Ojima, S., et al., *Effects of particle diameter on bubble coalescence in a slurry bubble column.* Journal of Chemical Engineering of Japan, 2015. **48**(3): p. 181-189.
59. De Swart, J., R. Van Vliet, and R. Krishna, *Size, structure and dynamics of "large" bubbles in a two-dimensional slurry bubble column.* Chemical Engineering Science, 1996. **51**(20): p. 4619-4629.
60. Lewis, W. and W. Whitman, *Principles of gas absorption.* Industrial & Engineering Chemistry, 1924. **16**(12): p. 1215-1220.
61. Bird, R., W. Stewart, and E. Lightfoot, *Diffusivity and the mechanisms of mass transport.* Transport phenomena, 1960: p. 513-542.
62. Calderbank, P. and M. Moo-Young, *The continuous phase heat and mass-transfer properties of dispersions.* chemical Engineering science, 1961. **16**(1): p. 39-54.
63. Hughmark, G., *Holdup and mass transfer in bubble columns.* Industrial & Engineering Chemistry Process Design and Development, 1967. **6**(2): p. 218-220.
64. Akita, K. and F. Yoshida, *Bubble size, interfacial area, and liquid-phase mass transfer coefficient in bubble columns.* Industrial & Engineering Chemistry Process Design and Development, 1974. **13**(1): p. 84-91.
65. Schügerl, K., J. Lücke, and U. Oels, *Bubble column bioreactors*. 1977: Springer.
66. Mena, P., et al., *Effect of some solid properties on gas–liquid mass transfer in a bubble column.* Chemical Engineering and Processing: Process Intensification, 2011. **50**(2): p. 181-188.

67. Hashemi, S., A. Macchi, and P. Servio, *Gas–liquid mass transfer in a slurry bubble column operated at gas hydrate forming conditions.* Chemical engineering science, 2009. **64**(16): p. 3709-3716.

68. Sehabiague, L., et al., *Assessing the performance of an industrial SBCR for Fischer–Tropsch synthesis: Experimental and modeling.* AIChE Journal, 2015. **61**(11): p. 3838-3857.

69. Sehabiague, L. and B.I. Morsi, *Hydrodynamic and Mass Transfer Characteristics in a Large-Scale Slurry Bubble Column Reactor for Gas Mixtures in Actual Fischer–Tropsch Cuts.* International Journal of Chemical Reactor Engineering, 2013. **11**(1): p. 1-20.

70. Wilkinson, P.M., H. Haringa, and L.L. Van Dierendonck, *Mass transfer and bubble size in a bubble column under pressure.* Chemical Engineering Science, 1994. **49**(9): p. 1417-1427.

71. Behkish, A., et al., *Gas holdup and bubble size behavior in a large-scale slurry bubble column reactor operating with an organic liquid under elevated pressures and temperatures.* Chemical Engineering Journal, 2007. **128**(2-3): p. 69-84.

72. Vandu, C.O., K. Koop, and R. Krishna, *Volumetric mass transfer coefficient in a slurry bubble column operating in the heterogeneous flow regime.* Chemical Engineering Science, 2004. **59**(22-23): p. 5417-5423.

73. Krishna, R., et al., *Gas holdup in slurry bubble columns: effect of column diameter and slurry concentrations.* AIChE Journal, 1997. **43**(2): p. 311-316.

74. Deckwer, W.-D., et al., *Hydrodynamic properties of the Fischer-Tropsch slurry process.* Industrial & Engineering Chemistry Process Design and Development, 1980. **19**(4): p. 699-708.

75. Letzel, M.H., et al., *Effect of gas density on large-bubble holdup in bubble column reactors.* AIChE journal, 1998. **44**(10): p. 2333-2336.

76. Chilekar, V., et al., *Bubble size estimation in slurry bubble columns from pressure fluctuations.* AIChE journal, 2005. **51**(7): p. 1924-1937.

77. Shabanian, J. and J. Chaouki, *Hydrodynamics of a gas–solid fluidized bed with thermally induced interparticle forces.* Chemical Engineering Journal, 2015. **259**: p. 135-152.

78. Li, H. and A. Prakash, *Influence of slurry concentrations on bubble population and their rise velocities in a three-phase slurry bubble column.* Powder Technology, 2000. **113**(1): p. 158-167.
79. Mena, P., et al., *Measurement of gas phase characteristics using a monofibre optical probe in a three-phase flow.* Chemical Engineering Science, 2008. **63**(16): p. 4100-4115.
80. Gruber, M.C., S. Radl, and J.G. Khinast, *Effect of bubble–particle interaction models on flow predictions in three-phase bubble columns.* Chemical engineering science, 2016. **146**: p. 226-243.
81. Li, Y.D., S.M. Lu, and Q.P. Guan. *A review of theoretical research on partial parameters in three-phase slurry bubble column reactor*. in *Advanced Materials Research*. 2014. Trans Tech Publ.
82. Sehabiague, L., et al., *Assessing the performance of an industrial SBCR for F ischer–T ropsch synthesis: Experimental and modeling.* AIChE Journal, 2015. **61**(11): p. 3838-3857.
83. Carbonell, M.M. and R. Guirardello, *Modelling of a slurry bubble column reactor applied to the hydroconversion of heavy oils.* Chemical engineering science, 1997. **52**(21-22): p. 4179-4185.
84. Shaikh, A. and M. Al-Dahhan, *Scale-up of Bubble Column Reactors: A Review of Current State-of-the-Art.* Industrial & Engineering Chemistry Research, 2013. **52**(24): p. 8091-8108.
85. Basha, O.M., et al., *Fischer–Tropsch synthesis in slurry bubble column reactors: experimental investigations and modeling–a review.* International Journal of Chemical Reactor Engineering, 2015. **13**(3): p. 201-288.
86. Rabha, S., M. Schubert, and U. Hampel, *Regime transition in viscous and pseudo viscous systems: A comparative study.* AIChE Journal, 2014. **60**(8): p. 3079-3090.
87. Rabha, S., M. Schubert, and U. Hampel, *Intrinsic flow behavior in a slurry bubble column: a study on the effect of particle size.* Chemical Engineering Science, 2013. **93**: p. 401-411.
88. Rabha, S., et al., *Bubble size and radial gas hold-up distributions in a slurry bubble column using ultrafast electron beam X-ray tomography.* AIChE journal, 2013. **59**(5): p. 1709-1722.
89. Sasaki, S., et al., *Effects of Particle Concentration and Slurry Height on Gas Holdup in a Slurry Bubble Column.* Journal of Chemical Engineering of Japan, 2016. **49**(9): p. 824-830.

90. Wu, C., K. Suddard, and M.H. Al-dahhan, *Bubble dynamics investigation in a slurry bubble column.* AIChE Journal, 2008. **54**(5): p. 1203-1212.

91. Gandhi, B., A. Prakash, and M. Bergougnou, *Hydrodynamic behavior of slurry bubble column at high solids concentrations.* Powder Technology, 1999. **103**(2): p. 80-94.

92. Garcia-Ochoa, J., et al., *Hydrodynamics and mass transfer in a suspended solid bubble column with polydispersed high density particles.* Chemical engineering science, 1997. **52**(21-22): p. 3827-3834.

93. Kim, Y., A. Tsutsumi, and K. Yoshida, *Effect of particle size on gas holdup in three-phase reactors.* Sadhana, 1987. **10**(1-2): p. 261-268.

94. Li, H., et al., *Effects of micron-sized particles on hydrodynamics and local heat transfer in a slurry bubble column.* Powder Technology, 2003. **133**(1-3): p. 171-184.

95. Esmaeili, A., C. Guy, and J. Chaouki, *Local hydrodynamic parameters of bubble column reactors operating with non-Newtonian liquids: Experiments and models development.* AIChE Journal, 2016. **62**(4): p. 1382-1396.

96. Brian, B. and J. Chen, *Surface tension of solid-liquid slurries.* AIChE journal, 1987. **33**(2): p. 316-318.

97. Saxena, S. and Z. Chen, *Hydrodynamics and heat transfer of baffled and unbaffled slurry bubble columns.* Reviews in Chemical Engineering, 1994. **10**(3-4): p. 193-400.

98. Dai, Z., D. Fornasiero, and J. Ralston, *Particle–bubble collision models—a review.* Advances in Colloid and Interface Science, 2000. **85**(2-3): p. 231-256.

99. Schulze, H., *Hydrodynamics of bubble-mineral particle collisions.* Mineral Procesing and Extractive Metallurgy Review, 1989. **5**(1-4): p. 43-76.

100. Liu, T. and M. Schwarz, *CFD-based multiscale modelling of bubble–particle collision efficiency in a turbulent flotation cell.* Chemical Engineering Science, 2009. **64**(24): p. 5287-5301.

101. Michael, D. and P. Norey, *Particle collision efficiencies for a sphere.* Journal of Fluid Mechanics, 1969. **37**(3): p. 565-575.

102. Firouzi, M., A.V. Nguyen, and S.H. Hashemabadi, *The effect of microhydrodynamics on bubble–particle collision interaction.* Minerals Engineering, 2011. **24**(9): p. 973-986.

103. Mokhtari, M. and J. Chaouki, *New technique for simultaneous measurement of the local solid and gas holdup by using optical fiber probes in the slurry bubble column.* Chemical Engineering Journal, 2019. **358**: p. 831-841.

104. Kito, M., K. Tabei, and K. Murata, *Gas and liquid holdups in mobile beds under the countercurrent flow of air and liquid.* Industrial & Engineering Chemistry Process Design and Development, 1978. **17**(4): p. 568-571.

105. Koide, K., et al., *Gas holdup and volumetric liquid-phase mass transfer coefficient in solid-suspended bubble columns.* Journal of chemical engineering of Japan, 1984. **17**(5): p. 459-466.

106. Reilly, I., et al., *A correlation for gas holdup in turbulent coalescing bubble columns.* The canadian journal of chemical engineering, 1986. **64**(5): p. 705-717.

107. Chen, C.-M. and L.-P. Leu, *Hydrodynamics and mass transfer in three-phase magnetic fluidized beds.* Powder Technology, 2001. **117**(3): p. 198-206.

108. Sehabiague, L. and B.I. Morsi, *Hydrodynamic and mass transfer characteristics in a large-scale slurry bubble column reactor for gas mixtures in actual Fischer–Tropsch cuts.* International Journal of Chemical Reactor Engineering, 2013. **11**(1): p. 83-102.

109. Götz, M., et al., *Novel gas holdup correlation for slurry bubble column reactors operated in the homogeneous regime.* Chemical Engineering Journal, 2017. **308**: p. 1209-1224.

110. Li, H. and A. Prakash, *Heat transfer and hydrodynamics in a three-phase slurry bubble column.* Industrial & engineering chemistry research, 1997. **36**(11): p. 4688-4694.

111. Shah, Y., et al., *Design parameters estimations for bubble column reactors.* AIChE Journal, 1982. **28**(3): p. 353-379.

112. Higbie, R., *The rate of absorption of a pure gas into a still liquid during short periods of exposure.* Trans. AIChE, 1935. **31**: p. 365-389.

113. Danckwerts, P., *Significance of liquid-film coefficients in gas absorption.* Industrial & Engineering Chemistry, 1951. **43**(6): p. 1460-1467.

114. Alper, E. and S. Öztürk, *The effect of activated carbon loading on oxygen absorption into aqueous sodium sulphide solutions in a slurry reactor.* The Chemical Engineering Journal, 1986. **32**(2): p. 127-130.

115. Alper, E., B. Wichtendahl, and W.-D. Deckwer, *Gas absorption mechanism in catalytic slurry reactors.* Chemical Engineering Science, 1980. **35**(1-2): p. 217-222.

116. Ruthiya, K.C., B.F. Kuster, and J.C. Schouten, *Gas-liquid Mass Transfer Enhancement in a Surface Aeration Stirred Slurry Reactors.* The Canadian Journal of Chemical Engineering, 2003. **81**(3-4): p. 632-639.
117. Kluytmans, J., et al., *Mass transfer in sparged and stirred reactors: influence of carbon particles and electrolyte.* Chemical Engineering Science, 2003. **58**(20): p. 4719-4728.
118. Ruthiya, K., et al., *Mechanisms of physical and reaction enhancement of mass transfer in a gas inducing stirred slurry reactor*. Chemical Engineering Journal, 2003. **96**(1-3): p. 55-69.
119. Behkish, A., et al., *Mass transfer characteristics in a large-scale slurry bubble column reactor with organic liquid mixtures.* Chemical Engineering Science, 2002. **57**(16): p. 3307-3324.
120. Vandu, C.O. and R. Krishna, *Volumetric mass transfer coefficients in slurry bubble columns operating in the churn-turbulent flow regime.* Chemical Engineering and Processing: Process Intensification, 2004. **43**(8): p. 987-995.
121. Zaidi, A., et al., *Mass transfer in the liquid phase Fischer-Tropsch synthesis.* Ger. Chem. Engng, 1979. **2**: p. 94.
122. Lakhdissi, E.M., et al., *Simultaneous effect of particle size and solid concentration on the hydrodynamics of slurry bubble column reactors.* AIChE Journal, 2020. **66**(2): p. e16813.
123. Letzel, H., et al., *Gas holdup and mass transfer in bubble column reactors operated at elevated pressure.* Chemical Engineering Science, 1999. **54**(13): p. 2237-2246.
124. Abbasi, M., et al., *A novel approach for simultaneous hydrodynamic characterization of gas–liquid and gas–solid systems.* Chemical Engineering Science, 2013. **100**: p. 74-82.
125. Ruthiya, K.C., et al., *Detecting regime transitions in slurry bubble columns using pressure time series.* AIChE journal, 2005. **51**(7): p. 1951-1965.
126. Sonolikar, R. and T.R. Rao, *Effective interfacial area in magnetically stabilized slurry bubble column.* Chemical engineering science, 1996. **51**(11): p. 2701-2707.
127. Chen, Z., et al., *Oxygen mass transfer coefficient in bubble column slurry reactor with ultrafine suspended particles and neural network prediction.* The Canadian Journal of Chemical Engineering, 2013. **91**(3): p. 532-541.
128. Zheng, C., et al., *Mass transfer in different flow regimes of three-phase fluidized beds.* Chemical engineering science, 1995. **50**(10): p. 1571-1578.

129. Kim, J.O. and S.D. Kim, *Gas-Liquid mass transfer in a three-phase fluidized bed with floating bubble breakers.* The Canadian Journal of Chemical Engineering, 1990. **68**(3): p. 368-375.

130. Koide, K., et al., *Gas holdup and volumetric liquid-phase mass transfer coefficient in a gel-particle suspended bubble column with draught tube.* Journal of chemical engineering of Japan, 1992. **25**(1): p. 11-16.

131. Akita, K. and F. Yoshida, *Gas Holdup and Volumetric Mass Transfer Coefficient in Bubble Columns. Effects of Liquid Properties.* Industrial & Engineering Chemistry Process Design and Development, 1973. **12**(1): p. 76-80.

132. Hikita, H., et al., *The volumetric liquid-phase mass transfer coefficient in bubble columns.* The chemical engineering journal, 1981. **22**(1): p. 61-69.

133. Shah, Y., et al., *Design parameters estimations for bubble column reactors.* AIChE Journal, 1982. **28**(3): p. 353-379.

134. Vandu, C. and R. Krishna, *Influence of scale on the volumetric mass transfer coefficients in bubble columns.* Chemical Engineering and Processing: Process Intensification, 2004. **43**(4): p. 575-579.

135. Letzel, H., et al., *Gas holdup and mass transfer in bubble column reactors operated at elevated pressure.* Chemical Engineering Science, 1999. **54**(13-14): p. 2237-2246.

136. Öztürk, S., A. Schumpe, and W.D. Deckwer, *Organic liquids in a bubble column: holdups and mass transfer coefficients.* AIChE journal, 1987. **33**(9): p. 1473-1480.

137. Clark, J. and D. Macquarrie, *Handbook of green chemistry and technology. 2002*. Oxford: Blackwell Science Ltd.

138. Shu, S., et al., *Multiscale multiphase phenomena in bubble column reactors: A review.* Renewable energy, 2019. **141**: p. 613-631.

139. Yan, P., et al., *Numerical simulation of bubble characteristics in bubble columns with different liquid viscosities and surface tensions using a CFD-PBM coupled model.* Chemical Engineering Research and Design, 2020. **154**: p. 47-59.

140. Wilkinson, P.M., A.P. Spek, and L.L. van Dierendonck, *Design parameters estimation for scale-up of high-pressure bubble columns.* AIChE Journal, 1992. **38**(4): p. 544-554.

141. Kuncová, G. and J. Zahradník, *Gas holdup and bubble frequency in a bubble column reactor containing viscous saccharose solutions.* Chemical Engineering and Processing: Process Intensification, 1995. **34**(1): p. 25-34.

142. Hwang, S.-J. and Y.-L. Cheng, *Gas holdup and liquid velocity in three-phase internal-loop airlift reactors.* Chemical Engineering Science, 1997. **52**(21-22): p. 3949-3960.

143. Yang, J.H., et al., *Two regime transitions to pseudo-homogeneous and heterogeneous bubble flow for various liquid viscosities.* Chemical Engineering and Processing: Process Intensification, 2010. **49**(10): p. 1044-1050.

144. Khare, A. and J. Joshi, *Effect of fine particles on gas hold-up in three-phase sparged reactors.* The Chemical Engineering Journal, 1990. **44**(1): p. 11-25.

145. Ruzicka, M., et al., *Effect of viscosity on homogeneous–heterogeneous flow regime transition in bubble columns.* Chemical Engineering Journal, 2003. **96**(1-3): p. 15-22.

146. Olivieri, G., et al., *Effects of viscosity and relaxation time on the hydrodynamics of gas–liquid systems.* Chemical engineering science, 2011. **66**(14): p. 3392-3399.

147. Godbole, S., M. Honath, and Y. Shah, *Holdup structure in highly viscous Newtonian and non-Newtonian liquids in bubble columns.* Chemical Engineering Communications, 1982. **16**(1-6): p. 119-134.

148. Eissa, S.H. and K. Schügerl, *Holdup and backmixing investigations in cocurrent and countercurrent bubble columns.* Chemical Engineering Science, 1975. **30**(10): p. 1251-1256.

149. Besagni, G., et al., *The dual effect of viscosity on bubble column hydrodynamics.* Chemical Engineering Science, 2017. **158**: p. 509-538.

150. Kumar, S.B., D. Moslemian, and M.P. Duduković, *Gas-holdup measurements in bubble columns using computed tomography.* AIChE Journal, 1997. **43**(6): p. 1414-1425.

151. Jin, H., et al., *The axial distribution of holdups in an industrial-scale bubble column with evaluated pressure using γ-ray attenuation approach.* Chemical Engineering Journal, 2005. **115**(1-2): p. 45-50.

152. Chen, J., et al., *Gas holdup distributions in large-diameter bubble columns measured by computed tomography.* Flow Measurement and instrumentation, 1998. **9**(2): p. 91-101.

153. Esmaeili, A., et al., *Effect of elevated pressure on the hydrodynamic aspects of a pilot-scale bubble column reactor operating with non-Newtonian liquids.* Chemical Engineering Journal, 2016. **288**: p. 377-389.

154. Nishikawa, M., H. Kato, and K. Hashimoto, *Heat transfer in aerated tower filled with non-Newtonian liquid.* Industrial & engineering chemistry process design and development, 1977. **16**(1): p. 133-137.

155. McCabe, W.L., J.C. Smith, and P. Harriott, *Unit operations of chemical engineering*. Vol. 5. 1993: McGraw-hill New York.

156. Demol, R., et al., *Mass transfer in the homogeneous flow regime of a bubble column.* Chemical Engineering and Processing-Process Intensification, 2019. **144**: p. 107647.

157. Shu, S., J. Zhang, and N. Yang, *GPU-accelerated transient lattice Boltzmann simulation of bubble column reactors.* Chemical Engineering Science, 2020. **214**: p. 115436.

158. Launder, B.E., G.J. Reece, and W. Rodi, *Progress in the development of a Reynolds-stress turbulence closure.* Journal of fluid mechanics, 1975. **68**(3): p. 537-566.

159. Shu, S., Bahraoui,Naoufel, Bertrand, François and Chaouki, Jamal, *A bubble-induced turbulence model for gas-liquid bubbly flows in airlift columns, pipes and bubble columns.* Chemical Engineering Science, 2020.

160. Ishii, M. and N. Zuber, *Drag coefficient and relative velocity in bubbly, droplet or particulate flows.* AIChE journal, 1979. **25**(5): p. 843-855.

161. Simonnet, M., et al., *Experimental determination of the drag coefficient in a swarm of bubbles.* Chemical Engineering Science, 2007. **62**(3): p. 858-866.

162. Burns, A.D., et al. *The Favre averaged drag model for turbulent dispersion in Eulerian multi-phase flows*. in *5th international conference on multiphase flow, ICMF*. 2004. ICMF.

163. Mudde, R., W. Harteveld, and H. Van den Akker, *Uniform flow in bubble columns.* Industrial & Engineering Chemistry Research, 2009. **48**(1): p. 148-158.

164. Jordan, U., A.K. Saxena, and A. Schumpe, *Dynamic Gas Disengagement in a High-Pressure Bubble Column.* The Canadian Journal of Chemical Engineering, 2003. **81**(3-4): p. 491-498.

165. Krishna, R. and J. Ellenberger, *Gas holdup in bubble column reactors operating in the churn-turbulent flow regime.* AIChE journal, 1996. **42**(9): p. 2627-2634.

166. Wang, T., J. Wang, and Y. Jin, *Theoretical prediction of flow regime transition in bubble columns by the population balance model.* Chemical Engineering Science, 2005. **60**(22): p. 6199-6209.